

**Coordination of synaptonemal complex
formation and pachytene checkpoint
signaling in meiosis**

Dissertation der
Fakultät für Biologie der
Ludwig-Maximilians-Universität
München

vorgelegt von
Diplom-Biologe
Christian Stefan Eichinger

4. Mai 2009

Hiermit erkläre ich, dass ich die vorliegende Dissertation selbständig und ohne unerlaubte Hilfe angefertigt habe. Ich habe weder anderweitig versucht, eine Dissertation einzureichen oder eine Doktorprüfung durchzuführen, noch habe ich diese Dissertation oder Teile derselben einer anderen Prüfungskommission vorgelegt.

Christian Eichinger

München, den 4. Mai 2009

Promotionsgesuch eingereicht: 4. Mai 2009

Tag der mündlichen Prüfung: 14. Juli 2009

Erster Gutachter: Prof. Dr. Stefan Jentsch

Zweiter Gutachter: Prof. Dr. Peter Becker

Die vorliegende Arbeit wurde zwischen April 2005 und April 2009 unter der Anleitung von Prof. Dr. Stefan Jentsch am Max-Planck-Institut für Biochemie in Martinsried durchgeführt.

Wesentliche Teile dieser Arbeit sind in der folgenden Publikation veröffentlicht:

Christian S. Eichinger & Stefan Jentsch. Synaptonemal complex formation and pachytene checkpoint signaling are coordinated through Red1—9-1-1 interaction (submitted to Nature Cell Biology, 2009).

I SUMMARY.....	1
II INTRODUCTION.....	2
II.1 Ubiquitin and ubiquitin-like modifiers.....	2
II.1.1 The ubiquitin and SUMO conjugation system.....	3
II.1.2 Functions of ubiquitin and SUMO.....	6
II.2 Meiosis.....	11
II.2.1 Major processes in meiosis.....	11
II.2.2 Role of SUMO in meiosis.....	14
II.3 DNA damage response.....	15
II.3.1 DNA repair pathways.....	15
II.3.2 DNA damage checkpoints.....	16
II.3.3 The 9-1-1 checkpoint complex.....	16
II.3.4 Meiotic recombination and surveillance mechanisms.....	18
II.4 Aim.....	24
III RESULTS.....	25
III.1 Red1 is modified by SUMO during meiosis.....	25
III.1.1 Purification of meiotic SUMO substrates in <i>S. cerevisiae</i>	25
III.1.2 The SUMO substrate Red1.....	25
III.1.3 The SUMO acceptor lysines in Red1.....	26
III.1.4 The SUMO substrate Sycp3 in <i>Homo sapiens</i>	28
III.2 Red1 SUMOylation recruits Zip1 for timely establishment of SCs.....	29
III.2.1 Red1 and Zip1 interact in a SUMO-dependent manner.....	29
III.2.2 Red1 SUMO-deficient mutant shows delayed zipping.....	31
III.3 Red1 binds 9-1-1 for pachytene checkpoint activation and normal SC formation..	35
III.3.1 Domain mapping and identification of specific point mutants.....	35
III.3.2 Function of Red1 interaction with the 9-1-1 complex.....	37
III.4 Regulation of Red1 SUMOylation and expression.....	41
III.4.1 Regulation of Red1 SUMOylation.....	41
III.4.2 Regulation of Red1 expression.....	44
III.5 SUMOylation of the 9-1-1 complex.....	46
III.5.1 Each 9-1-1 subunit is modified with SUMO.....	46
III.5.2 Regulation of 9-1-1 SUMOylation.....	48
III.5.3 Towards a function for the SUMOylation of 9-1-1.....	49
III. 6 Psy2 links the SC to pachytene checkpoint exit.....	51
III. 6.1 Interaction between Zip1 and Psy2.....	51
III. 6.2 Psy2 functions in meiotic checkpoint control.....	54
IV DISCUSSION	60
IV.1 Red1 SUMOylation is important for timely zipping.....	67

IV.2 Red1 binds 9-1-1 for pachytene checkpoint activation and normal SC formation..	67
IV.3 Intimate connection between pachytene checkpoint and SC formation.....	70
<u>V MATERIAL AND METHODS.....</u>	<u>74</u>
V.1 Computational analyses.....	74
V.2 Microbiological and genetic techniques	74
V.2.1 <i>Escherichia coli</i> techniques.....	74
V.2.2 <i>Saccharomyces cerevisiae</i> techniques.....	76
V.3 Cell biological techniques.....	82
V.3.1 Tissue culture.....	82
V.3.2 Live-cell microscopy.....	83
V.4 Molecular biology techniques.....	83
V.4.1 Isolation of DNA.....	84
V.4.2 Polymerase chain reaction (PCR).....	85
V.4.3 Cloning of plasmids constructs.....	88
V.5 Biochemical techniques.....	89
V.5.1 Gel electrophoresis and immunoblot techniques.....	89
V.5.2 Preparation of cell extracts.....	92
V.5.3 Protein purification and binding experiments.....	93
<u>VI REFERENCES.....</u>	<u>96</u>
<u>ABBREVIATIONS.....</u>	
<u>ACKNOWLEDGEMENTS.....</u>	
<u>CURRICULUM VITAE.....</u>	

I SUMMARY

Genome integrity is challenged by numerous endogenous and exogenous DNA damages which are potentially harmful for an organism. In order to preserve the genetic information, errors in the DNA have to be rapidly recognized and repaired. Therefore, cells are equipped with two highly interconnected mechanisms: DNA damage checkpoints that alert and signal the presence of DNA mistakes and DNA repair pathways which – depending on the nature of the defect – make use of the appropriate set of proteins to overcome the lesion.

For the transmission of genetic material to the next generation of a diploid organism, haploid gametes are formed by two subsequent cell divisions: meiosis I and II. During meiosis I, genetic material of the parents is exchanged and divided to two daughter cells. This process is followed by meiosis II, where the genetically identical sister chromatids are separated and divided into two daughter cells. Any mistake in this highly orchestrated series of events may lead to aneuploidy and therefore to severe defects or lethality of the progeny.

Before cell division in meiosis I, homologous recombination functions in the mixing of parental genetic material as well as in the correct recognition of homologous sequences, which is an essential prerequisite for the faithful transmission of exactly one of each chromosome to each daughter cell. Curiously, this essential process is initiated by the formation of double-strand breaks (DSBs) at multiple sites throughout the genome, which are lethal for a cell if not repaired. In order to control the processing and repair of DSBs during meiosis I, the pachytene checkpoint plays a crucial role. Another major event during prophase of meiosis I is the formation of synaptonemal complexes (SCs). These large protein structures serve as a scaffold for the tight pairing of homologous chromosomes and ensure proper crossover (CO) formation.

This study shows that the axial element protein Red1 is an essential component and coordinator of two major meiotic events: SC formation and the activation of the pachytene checkpoint. First, Red1 is modified by the small ubiquitin-like modifier SUMO to foster the recruitment of the SUMO-interacting motif (SIM)-containing central element protein Zip1 and thereby ensures timely establishment of mature SCs. Second, Red1 binds two subunits of the conserved, PCNA-related 9-1-1 checkpoint complex via two distinct, subunit-selective motifs. Remarkably, association of Red1 with 9-1-1 is not only essential for checkpoint activation but also for SC formation. Thus, Red1, besides its structural role in the SC, crucially connects pachytene checkpoint signaling to SUMO-stimulated SC formation.

II INTRODUCTION

II.1 Ubiquitin and ubiquitin-like modifiers

Posttranslational modification of proteins is a key mechanism for the regulation of various cellular processes. Such covalent alterations of proteins occur in a rapid and reversible manner and can be attached to either single or several amino acid residues. Due to conjugation and de-conjugation of these posttranslational marks, proteins may change their activity, localization, stability or interaction with other proteins or nucleic acids. Besides phosphorylation, methylation, acetylation, or glycosylation, ubiquitylation and the modification with ubiquitin-like (UBL) modifiers are further regulators for proteins in a broad field of biology, like DNA repair and replication, gene transcription, cell signalling and cell cycle. The broad range of functions implies the importance for studying these modifications for the understanding of basic biological principles and molecular mechanisms of diseases.

Despite low sequence homology, members of the UBL protein family are highly conserved among species on a structural level (**Fig. 1**). Characteristic for all members is the so-called *ubiquitin-fold*, a rather small globular protein domain. Ubiquitin itself exists of 76 amino acids, only three of which differ between the human and yeast orthologs. Its best-known function is marking proteins for degradation by the 26S proteasome.

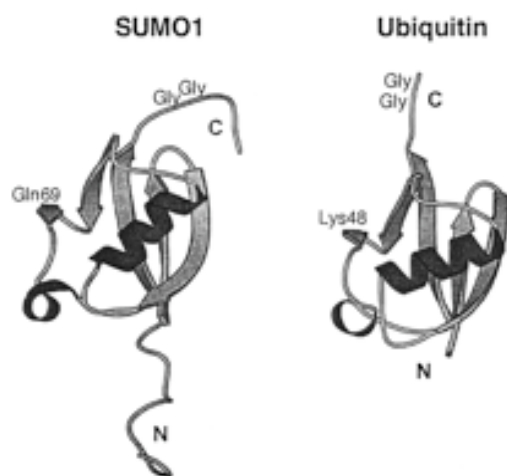


Figure 1: Structure of ubiquitin and the human SUMO1. Despite low homology in sequence both proteins show high structural similarity and a conserved globular domain, which is typical for members of the ubiquitin-like modifier family (Melchior, 2000).

Apart from ubiquitin and SUMO, which regulate a huge number of processes, the UBL family also contains the modifiers Rub1 (NEDD8), Atg12,

Atg8, Urm1, ISG15, FAT10 and FUB1 each of which seem to be limited to fewer substrates and therefore to a more specific range of functions (Muller et al., 2001; Schwartz and Hochstrasser, 2003; Welchman et al., 2005).

II.1.1 The ubiquitin and SUMO conjugation system

Protein modification by covalent attachment with **ubiquitin** occurs in all eukaryotic cells. Substrates are usually modified on lysine residues by covalent linkage to the C-terminal glycine residue of ubiquitin, thereby forming a branched isopeptide-linked protein complex. This reaction is ATP-dependent and requires the sequential activities of at least three enzymes (**Fig. 2**): the ubiquitin-activating enzyme (E1 or Uba1), a ubiquitin-conjugating enzyme (E2 or Ubc) and a ubiquitin ligase (E3). In a first step, ubiquitin gets covalently linked to a cysteine in the active centre of the E1 via a thioester bond. Secondly, ubiquitin is transferred to the cysteine in the active centre of an E2 thereby again forming a thioester bond. Finally, the E3 links ubiquitin to the lysine of the substrate. In case of RING E3 ligases, ubiquitin is directly transferred to the protein, while in case of HECT E3 ligases the ligation to the substrate follows an intermediate coupling of ubiquitin to a cysteine within the ligase via a thioester bond. While there is only one E1 involved in the ubiquitin-conjugation system, several E2 and a large number of E3 enzymes are known to ensure the modification of a certain protein or pool of substrates. The modification with ubiquitin is a reversible process and can be cleaved off from the substrate by a number of de-ubiquitylating enzymes (DUB; Amerik and Hochstrasser, 2004). The same enzymes are needed for generating ubiquitin from a precursor protein by hydrolytic cleavage.

Apart from the best-known function of ubiquitin in labelling proteins for degradation, non-proteolytic functions of ubiquitin have been described during the last years. The crucial parameter that differentiates between proteolytic and non-proteolytic function is the type of ubiquitin modification (Pickart, 2000). Namely, ubiquitin can be attached to the substrate either as a single molecule (monoubiquitylation) or as a chain of ubiquitins that are linked via isopeptide bonds (polyubiquitylation). Ubiquitin harbors 7 lysine (K) residues all of which can apparently be used for multiubiquitin chain formation. While multiubiquitin chains linked via K48 and K29 promote proteasomal degradation,

monoubiquitylation and polyubiquitylation by K63 chains mediate non-proteolytic functions.

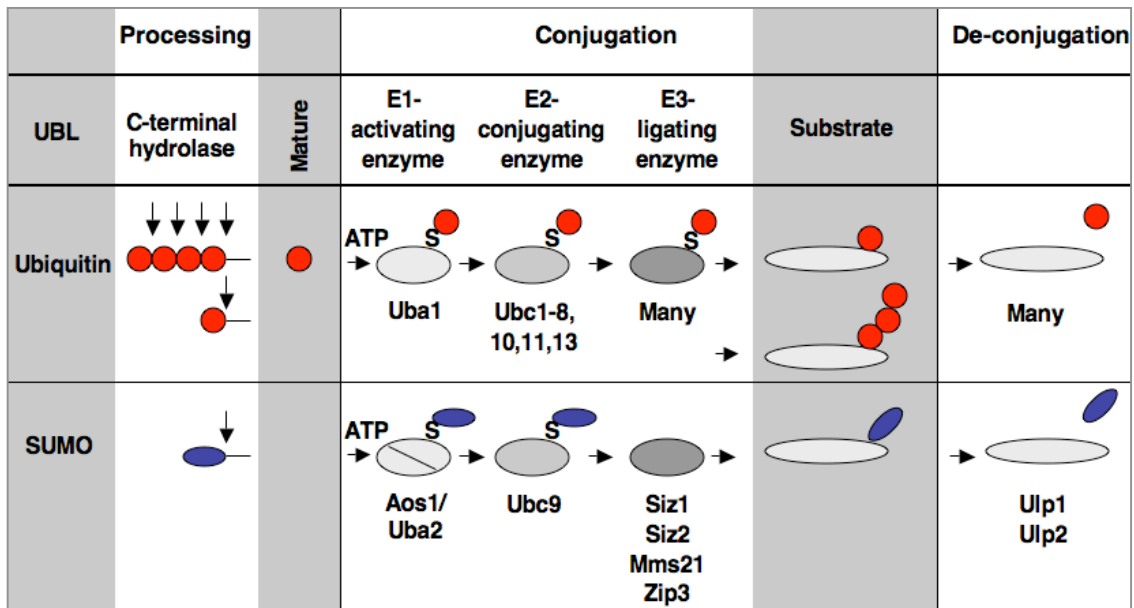


Figure 2: Conjugation of ubiquitin and SUMO to its substrates in *S. cerevisiae*. Conjugation of Ubiquitin and SUMO to their target proteins involves at least three classes of enzymes. A processing step is necessary to generate the mature modifier. Subsequently, the ATP-dependent reaction is carried out by a cascade of activating, conjugating and ligating enzymes, finally leading to a modified substrate. Modification by ubiquitin and SUMO is transient and can be removed from substrates by a set of de-conjugation enzymes. The “S” marks a thioester between the modifier and an enzyme (adapted from Muller et al., 2001).

Apart from ubiquitin, eukaryotes express various protein modifiers that are related to ubiquitin and form conjugates with proteins in a similar manner. The best characterized is **SUMO**, which shows 18% sequence identity to ubiquitin (Hay, 2005). While only one gene exists for SUMO (SMT3) in *S. cerevisiae*, one can distinguish four isoforms in humans (SUMO-1, -2, -3, -4). In yeast, SUMO conjugation to proteins is carried out by a different set of enzymes. First, the SUMO precursor is processed by SUMO specific proteases (Ulp1 and Ulp2 in yeast) to reveal the C-terminal di-glycine motif that is activated by the E1 enzyme (Aos1/Uba2 in yeast). After transesterification onto the E2 conjugating enzyme (Ubc9), the protein target is selected and with the help of an E3 ligase, SUMO is ligated to the substrate (**Fig. 2**). Similar to ubiquitylation, the modification of proteins with SUMO is a reversible process, which again depends on the proteases Ulp1 and Ulp2. In contrast to ubiquitin E2 enzymes, Ubc9 can also bind substrates directly and therefore does not always need an E3 for SUMOylation of a substrate. SUMO E3 ligases rather function in

stimulating the conjugation and can be classified into three categories: SP-RING family ligases as well as RanBP2 and PC2 (Johnson, 2004). Until now, the SUMO E3 ligases Siz1, Siz2, Mms21 and Zip3 (**Fig. 2**) as well as the SUMO-stimulated ubiquitin ligase complex Slx5-Slx8 have been reported in yeast and play very diverse roles (for details **see II.1.2**).

In the human system, SUMO conjugation requires the E1 activating enzyme and the E2 conjugating enzyme, and in some cases E3 SUMO ligases. The best characterized ligases in humans are four members of the PIAS (protein inhibitor of activated STAT) group, PIAS1, PIAS2 (PIASx), PIAS3 and PIAS4, and the Ran binding protein 2 (RanBP2) (Palvimo, 2007; Pichler et al., 2002; Schmidt and Muller, 2003). SUMO can be removed from its target protein by the action of so far six known members of a family of SUMO-specific isopeptidases termed SENP1-3 and SENP5-7 (Hay, 2007; Mukhopadhyay and Dasso, 2007), making this modification often transient.

SUMOylation often takes place on a lysine residue embedded in the core consensus motif ψ KxE. The limited specificity of this motif on the SUMOylation process is overcome by E3 ligases, which add specificity to the conjugation of SUMO to a substrate. However, it is possible that proteins are SUMOylated at non-consensus sites and also consensus motifs are not necessarily modified by SUMO. Additionally, it became clear that the modification can occur on several sites within a protein and that several acceptor lysines have redundant functions. More recently, clusters of acidic residues located downstream from the core SUMO modification sites were described to further define functional SUMO targets (Yang et al., 2006). It can be assumed that several factors regulate the efficient modification of a protein at a specific site and time. One described function for SUMOylated proteins is the recruitment of factors harbouring a specific domain for SUMO interaction, termed SUMO-interacting motif (SIM; Kerscher, 2007). SIMs contain a cluster of hydrophobic and negatively charged residues and can be minimized to the following consensus sequence: K-x₃₋₅-(I/V)-(I/L)-(I/L)-x₃-(D/E/Q/N)-(D/E)-(D/E) (Hannich et al., 2005). Notably, SIMs are themselves subject to regulation and modification. It has been shown recently that serine residues juxtaposing the hydrophobic part of a SIM can be phosphorylated by the kinase CK2 and this phosphorylation is instrumental for the non-covalent interaction with SUMO (Stehmeier and Muller, 2009).

Similar to ubiquitin, SUMO is able to form poly-modifier chains. This has been shown for yeast SUMO (Smt3) as well as for the human SUMO-2 and SUMO-3 (Bylebyl et al., 2003; Tatham et al., 2001). In yeast, SUMO chain formation is apparently not essential in mitotic cells (Bylebyl et al., 2003), however there are first hints towards a significant function during meiosis (Cheng et al., 2006). In *S. cerevisiae*, the cysteine proteases Ulp1 and Ulp2 carry out the de-conjugation of SUMO from substrates (Li and Hochstrasser, 1999; Li and Hochstrasser, 2000; Li and Hochstrasser, 2003). While Ulp1 is located at the nuclear pore, Ulp2 localizes to the nucleus. Ulp1 is essential in yeast and necessary for the processing of the SUMO precursor protein to reveal the di-glycine motif for subsequent conjugation. Ulp2 seems to play a major role in meiosis as its deletion results in abnormal sporulation (Li and Hochstrasser, 2000). Recently, it was reported that Ulp2 is required for cell division following termination of the DNA damage checkpoint, although the exact mechanism is not understood yet (Felberbaum and Hochstrasser, 2008).

II.1.2 Functions of ubiquitin and SUMO

The roles of ubiquitin are very broad, ranging from **ubiquitin-dependent protein degradation** to DNA metabolism, cell signalling, nuclear transport and many other functions. In contrast to ubiquitylation, SUMOylation does not seem to promote protein degradation, but is rather involved in altering the function and intracellular localization of proteins, presumably by regulating protein-protein interactions.

The best-known function of ubiquitin is labelling proteins for degradation by the proteasome system. The substrates for degradation can be either malformed, non-functional proteins or factors that are regulated via its expression levels e.g. during the cell cycle or upon DNA damage or stress responses. In order to ensure faithful degradation, several adaptor proteins that deliver polyubiquitylated substrates to the 26S proteasome were described: Rpn10, an ubiquitin-interacting motif (UIM)-containing subunit of the proteasomal 19S cap (Deveraux et al., 1994) as well as the homologous proteins Rad23 and Dsk2, both containing UBA domains and loosely associating with the proteasome (Richly et al., 2005). Examples for **non-proteolytic functions of ubiquitin** are the monoubiquitylation of the cytosolic

domains of plasma membrane proteins which signals endocytosis (Haglund et al., 2003) or the monoubiquitylation of the histone H2B by the Rad6 pathway which triggers Dot1-dependent methylation of histone H3, and subsequently mediates gene silencing and checkpoint activation (Giannattasio et al., 2005; Sun and Allis, 2002). More recently, the ubiquitin ligase Rnf8 was reported to mediate focus accumulation of the p53-binding protein 1 (53BP1) and the breast cancer susceptibility protein BRCA1 at sites of DNA lesions thereby promoting DNA damage checkpoint activation. In detail, Rnf8 is recruited to damaged sites by phospho-dependent FHA domain-mediated binding to MDC1 and protects genome integrity by ubiquitylation of histone H2A and H2AX. This further leads to the licensing of DSB-flanking chromatin to concentrate repair factors close to the DNA lesion (Huen et al., 2007; Kolas et al., 2007; Mailand et al., 2007).

Further non-proteolytic functions of ubiquitin as well as for SUMO are described for the homotrimeric DNA sliding-clamp PCNA, a very central player in DNA metabolism (Moldovan et al., 2007). PCNA encircles double stranded DNA and functions as a processivity factor for DNA polymerases. It further plays a role as a platform for accessory factors involved in DNA replication and replication-linked mechanisms. Interestingly, **ubiquitylation and SUMOylation of PCNA** are closely linked and show specific functions in DNA repair (**Fig. 3**; (Hoege et al., 2002; Papouli et al., 2005; Pfander et al., 2005; Stelter and Ulrich, 2003). PCNA is modified at K164, a conserved lysine residue, found in nearly all eukaryotes, by three different types of modifications: monoubiquitylation, K63-linked polyubiquitylation, and SUMOylation. Mono- and polyubiquitylation of PCNA require Rad6, an ubiquitin-conjugating enzyme, which plays a key role in postreplicative repair, and Rad18, a RING-finger type ubiquitin ligase and DNA-binding protein. K63-linked polyubiquitylation also requires Rad5 and Ubc13/Mms2 in addition to Rad6 and Rad18. Rad6 and Rad18 are necessary for both branches of postreplicative DNA repair, the *error-prone* DNA repair pathway involving translesion polymerases as well as the *error-free* DNA repair pathway, which presumably includes recombination-like mechanisms. In contrast, the ubiquitin-conjugating enzyme Ubc13/Mms2 and the ubiquitin ligase Rad5 are required for the *error-free* pathway only. In yeast, Rad6-mediated monoubiquitylation of PCNA activates translesion DNA synthesis by the

damage-tolerant polymerases eta and zeta. SUMOylation of PCNA requires the SUMO-conjugating enzyme Ubc9 and the SUMO ligase Siz1 and prevents recombination during S-phase by recruiting the helicase Srs2. In contrast to SUMOylation, which is restricted to the S-phase, ubiquitylation occurs exclusively upon DNA damage. In case of the NF κ B inhibitor I κ B, SUMOylation prevents ubiquitin/proteasome-dependent degradation thus again showing that ubiquitylation and SUMOylation can function antagonistically (Desterro et al., 1998).

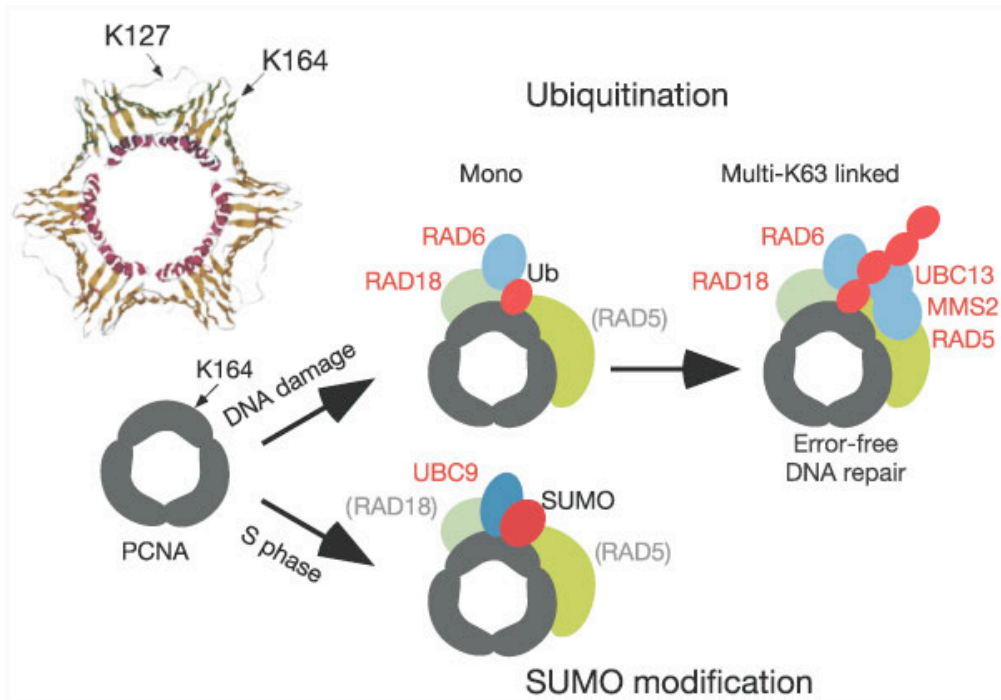


Figure 3: Posttranslational modifications of PCNA and its functions. PCNA is modified by at least three different modes of modification each of them playing a role in unique pathways: monoubiquitylation recruits translesion polymerases, poly-ubiquitylation signals an error-free DNA repair pathway and SUMOylation recruits the anti-recombinase Srs2 during S phase (Figure from Hoege et al., 2002).

Apart from PCNA and I κ B, a large number of SUMO substrates has been identified during the last years in yeast as well as higher eukaryotes (Denison et al., 2005; Hannich et al., 2005; Li et al., 2004; Makhnevych et al., 2009; Panse et al., 2004; Rosas-Acosta et al., 2005; Vertegaal et al., 2004; Wohlschlegel, 2009; Wohlschlegel et al., 2004; Wykoff and O'Shea, 2005; Zhao et al., 2004; Zhou et al., 2005). As the function of SUMOylation can be very diverse depending on the substrate, the following examples shall provide further principles of how SUMO acts.

Most of **SUMO functions** occur in the nucleus. In case of many transcription factors, SUMO modification leads to their repression, whereas ubiquitylation results in their activation (Gill, 2004; Muller et al., 2004). It has been proposed that SUMOylation leads to the recruitment of inhibitory factors like histone de-acetylases to the promoter of a gene (Girdwood et al., 2003). Another mechanism might be the recruitment of SUMOylated transcription factors to nuclear bodies, together with histone de-acetylases (Khan et al., 2001). PML-nuclear bodies are generally believed to concentrate SUMOylated substrates. PML-SUMO is thereby crucial for the assembly of these sub-nuclear structures by recruiting other proteins and facilitating their modification with SUMO (Ishov et al., 1999; Kamitani et al., 1998; Muller et al., 1998; Seeler et al., 2001).

Another major function of SUMO is connected with the transport of proteins between the nucleus and the cytoplasm. The most abundant SUMO substrate in mammalian cells is RanGAP1, the GTP-activating enzyme of the nuclear import factor Ran (Mahajan et al., 1997; Matunis et al., 1996). Its modification with SUMO leads to the association of RanGAP1-SUMO, the E3-ligase RanBP2 and Ubc9 (Mahajan et al., 1998; Matunis et al., 1998; Saitoh et al., 1998), a complex that subsequently localizes to the cytoplasmic side of the nuclear pore. Interestingly in that context, enzymes that carry out SUMO de-conjugation are located at the nuclear side of the nuclear pore (Takahashi et al., 2000; Zhang et al., 2002). More recently, RanBP2 has been shown to SUMOylate topoisomerase II alpha in mitosis and that this modification is required for its proper localization to inner centromeres. This leads to the resolution of sister centromeres and thereby suppresses tumorigenesis (Dawlaty et al., 2008).

Many proteins involved in DNA repair and genome maintenance have also been reported to be SUMOylated. A few examples are the human Werner and Bloom helicases, which negatively regulate recombination, the central base excision repair protein TDG as well as topoisomerases which change DNA topology (Bachant et al., 2002; Eladad et al., 2005; Hardeland et al., 2002; Ho et al., 2001; Kawabe et al., 2000; Mao et al., 2000a; Mao et al., 2000b). Moreover, the transcriptional response to DNA damage is clearly linked to the SUMO pathway as proteins like the human proteins p53, Mdm2 and PML are

SUMO-modified (Muller et al., 2000; Rodriguez et al., 1999; Sternsdorf et al., 1997). In a recently suggested model, the establishment of repair foci is enforced and stabilized by SUMO modification (Bergink and Jentsch, 2009). Very recently, SUMOylation has been shown to be involved in the recruitment of DSBs to the nuclear periphery which involves the modification of the histone variant Htz1 with SUMO (Kalocsay et al., 2009).

In case of the DNA repair enzyme TDG, the modification with SUMO leads to a significant conformational change. While TDG is strongly associated with hydrolysed products of TG or UG base mismatches in its unmodified form, its SUMOylation and subsequent conformational change allows the dissociation of the enzyme from the hydrolysed product (Baba et al., 2005; Hardeland et al., 2002; Steinacher and Schar, 2005). In contrast, the SUMO modification of PCNA probably does not result in a conformational change of the homotrimeric ring. Most likely, the conjugated SUMO moiety is rather exposed at the surface and easily accessible for recruited factors like the anti-recombinase Srs2.

In *S. cerevisiae*, SUMO functions can also be viewed from a different perspective by taking a look at the role of the so far known and potential **SUMO E3 ligases**. Siz1 is involved in the SUMOylation of septines which are proteins building up the filamentous, contractile ring at the bud neck (Johnson and Blobel, 1999). Moreover, Siz1 modifies PCNA with SUMO in order to recruit the helicase Srs2 (Hoege et al., 2002; Pfander et al., 2005). Siz2, another E3 ligase, has recently been shown to be the major SUMOylation enzyme for the recombination protein Rad52. In case of Rad52, SUMOylation acts pro-recombinogenic, plays a role in specific recombination reactions and protects those molecules from degradation, which are involved in the recombination process (Sacher et al., 2006). The SUMO E3 ligase Mms21 forms a complex including the structural-maintenance-of-chromosome proteins Smc5 and Smc6. Abolition of the SUMO E3 activity of Mms21 leads to a wide range of phenotypes such as DNA damage sensitivity, defects in nucleolar integrity and telomere clustering, silencing, and length regulation. The substrates for this SUMO ligase include a subunit of the octameric complex, Smc5, and the DNA repair protein Yku70 (Zhao and Blobel, 2005). Moreover, an *mms21* ligase mutant behaves similar to *ubc9* cells concerning the Rad51-dependent accumulation of cruciform (X) structures during replication of damaged

templates. It has been proposed recently that Ubc9 and Mms21 act in concert with Sgs1 to resolve the X structures formed during replication (Branzei et al., 2006; Branzei et al., 2008). Interestingly, Slx5 and Slx8 function in a complex and seem to be linked to both the SUMO and the ubiquitin conjugation machinery. Slx5-Slx8 has been shown to have ubiquitin ligase activity (rather than SUMO ligase activity), which is however stimulated by SUMOylated substrates (li et al., 2007a; li et al., 2007b; Mullen and Brill, 2008; Prudden et al., 2007; Uzunova et al., 2007; Xie et al., 2007). A recent report suggests a role in modulating the SUMOylation of DNA repair proteins and in negatively regulating Rad51-independent recombination (Burgess et al., 2007). Finally, Zip3 is a SUMO E3 ligase specifically expressed during meiosis (Cheng et al., 2006). Unique features of meiosis and the potential roles of SUMO in these processes will be addressed in the following paragraph.

II.2 Meiosis

II.2.1 Major processes in meiosis

Sexual organisms must halve the chromosome number in gametes to maintain the genome size. This is achieved through meiosis in which two rounds of chromosome segregation follow a single round of **pre-meiotic DNA replication** (Neale and Keeney, 2006). During meiosis I maternal and paternal copies of each chromosome are separated. Therefore chromosomes must pair with their correct partner and physically connect (by the exchange of chromosome arms) to correctly orient together at the meiotic spindle. The specific search for the homologous partner is achieved by the **introduction of DSBs** and the subsequent repair by **meiotic homologous recombination (Fig. 4)**. The paired chromosomes are tightly held together through the **establishment of the synaptonemal complex (SC)**, another specific feature of meiosis (**Fig. 4 and 5**). Importantly, these events occur in the prophase of meiosis I, consisting of leptotene, zygotene, pachytene and diakinesis. In summary, meiosis is thus distinguished from mitosis by two crucial events: the pairing of homologous chromosomes and high recombination levels. Both processes are essential for the proper segregation of chromosomes in meiosis I, and can be linked to the appearance of two proteinaceous structures in meiotic cells: the synaptonemal

complex and recombination nodules (RN). In order to carry out the meiotic program, a set of meiosis-specific proteins is expressed.

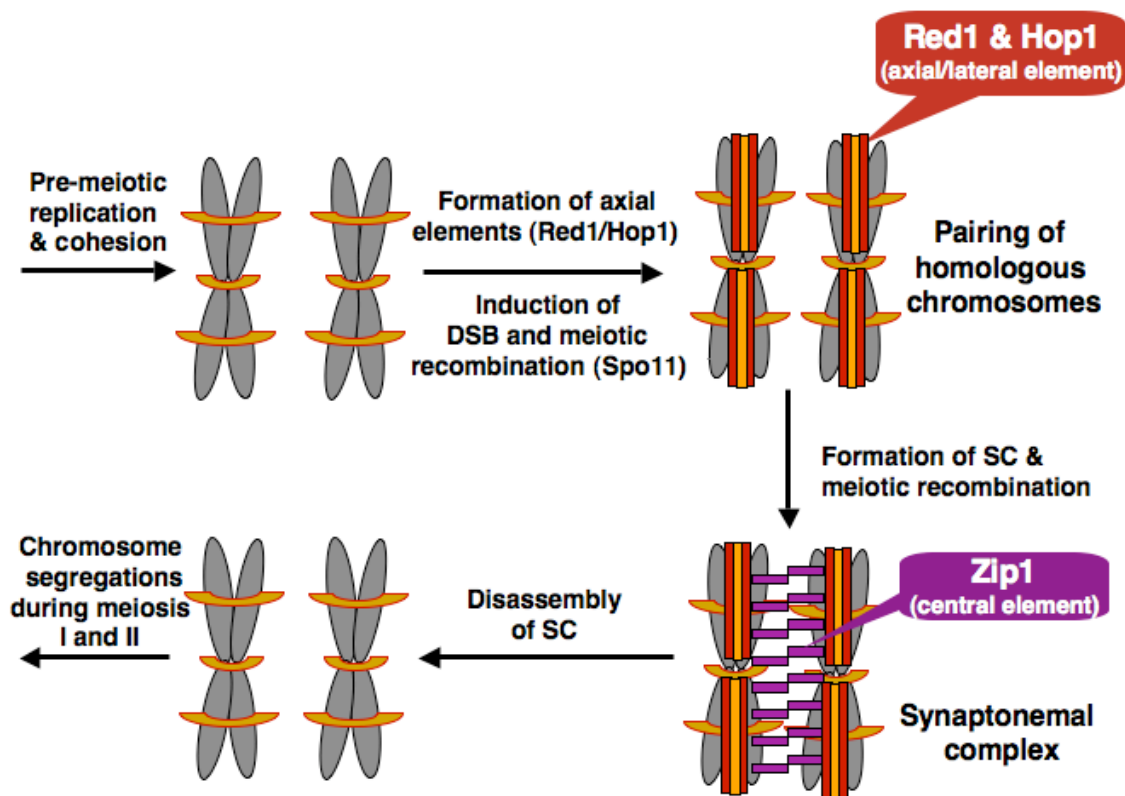


Figure 4: Unique features of early meiosis: Pre-meiotic replication, induction of DSB by the topoisomerase-like enzyme Spo11, meiotic recombination between homologous chromosomes and the formation of synaptonemal complexes (see text for details).

In the following, the most unique features connected to meiosis are discussed:

First, meiosis is introduced by a specific **pre-meiotic replication**. During and after pre-meiotic replication, cohesion (including the meiosis specific subunit Rec8) is established. Replication initiation requires CDK-S and probably partially depends on the Cdc7/Dbf4 activity. Both activities are also essential for DSB formation, thereby linking replication with the onset of homologous recombination and tightly regulating the time at which DSBs are formed (Murakami and Keeney, 2008). The lateral element protein Red1 localizes to chromatin very early during meiosis and regulates DSB formation by locally restricting Spo11's interaction to the core region of the hotspot (Prieler et al., 2005).

Second, **induction of DSBs** (150-200 per genome in *S. cerevisiae*) is achieved through the topoisomerase-like enzyme Spo11, which gets covalently linked to the formed 5' DNA ends at the break. After removal of Spo11, DSBs

are resected each giving rise to about 1 kb of ssDNA. To deal with DSBs induced during meiosis, their immediate and appropriate repair by homologous recombination is essential in order to prevent aneuploidy and keep the integrity of genomic information.

Third, **meiotic homologous recombination** (for detailed mechanism **see II.3.4**) occurs at high levels and has a strong preference for interhomologue recombination rather than intersister recombination. This preference assures the joining of homologues and involves several specific factors (Neale and Keeney, 2006): Dmc1, the meiosis-specific counterpart of Rad51 covers ssDNA formed at the breaks and promotes an interhomologue-only recombination pathway that is unique for meiosis. Moreover, the loss of the meiosis-specific heterodimeric complex Hop2-Mnd1 leads to non-homologous synapsis of chromosomes and persistence of DSBs, the clear mechanism behind this observation is however still unknown. Another pair of meiotic proteins, Mei5 and Sae3, interacts with Dmc1 and seems to promote Dmc1 filament formation.

Fourth, the structural basis of homologous chromosomes is the **synaptonemal complex**, a proteinaceous structure resembling railroad tracks that juxtaposes homologues and connects them along their entire length (**Fig. 5**; Page and Hawley, 2004). Each SC consists of two lateral elements connected by transverse filaments that lie perpendicular to the long axis of the complex. In *S. cerevisiae*, the meiosis specific proteins Red1 and Hop1 are major constituents of the lateral elements of the SC (Hollingsworth et al., 1990; Smith and Roeder, 1997), while the coiled-coil protein Zip1 is the major component of the central region of the SC. It has been suggested that Zip1 forms parallel dimers along its coiled-coil domain and that these interact via their N-terminal domains to form the central element while they are linked to the lateral elements via their C-termini (Dong and Roeder, 2000). Very interesting is the functional similarity between yeast and human meiotic functions, including the SC architecture. Red1 seems to play a similar role as the human proteins Sycp3 and Sycp2, while Zip1 shares homology with human Sycp1 (Liu et al., 1996; Offenberg et al., 1998; Schalk et al., 1998; Yuan et al., 2000). The processes described in this study for the yeast system might therefore very well hold true for the human system as well.

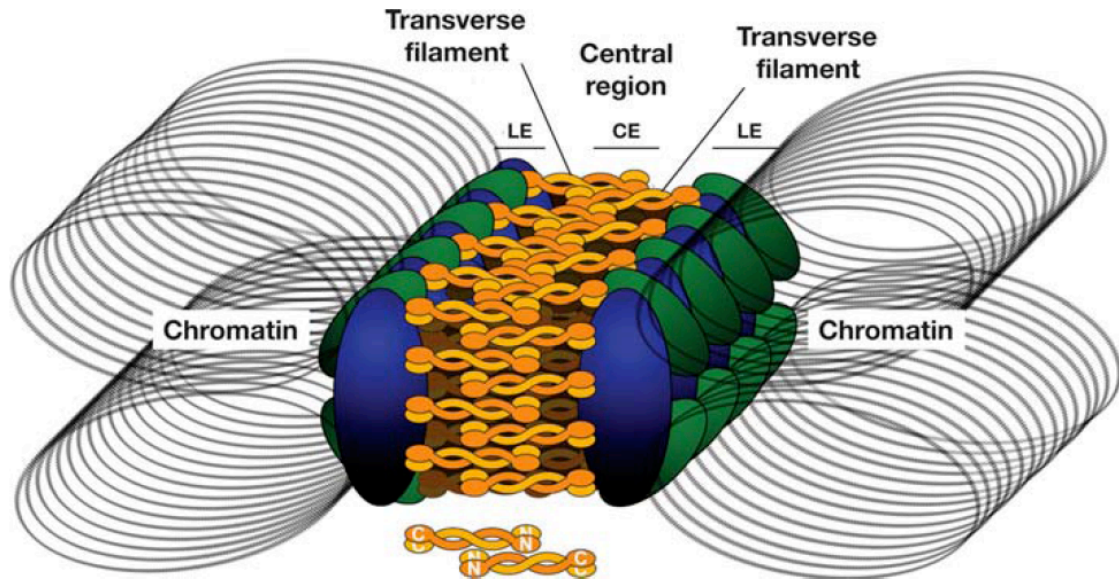


Figure 5: Structural model of the synaptonemal complex. Depicted is a segmental cross-section of the SC, showing the arrangement of lateral elements (LE), central elements (CE), transverse filaments and the central region. The orientation of Zip1 dimers is shown at the bottom (Figure from Page and Hawley, 2004).

II.2.2 Role of SUMO in meiosis

Recent reports suggest a crucial role for SUMO during meiosis by controlling Rad52 activity during recombination of homologous chromosomes (Sacher et al., 2006) as well as for the establishment of SCs (Cheng et al., 2006; Hooker and Roeder, 2006). For example, a functionally impaired *ubc9* allele leads to delayed SC formation and meiotic progression. Moreover, the meiosis-specific protein Zip3 was identified as a SUMO E3 ligase essential for normal zipping. Interestingly, two waves of SUMOylation were postulated during meiotic progression: Siz1/Siz2-dependent processes and subsequent Zip3-dependent mechanisms.

The structural protein and major central element protein Zip1 reveals an extended N-terminal region for dimerization and a SUMO-interacting motif in its very C-terminal region. Indeed, Zip1 might bind SUMOylated components of the SC (e.g. Red1 or Hop1) and thereby build up the ladder-like architecture of the SC which is visible by electron microscopy (Dong and Roeder, 2000). SCs from yeast and mammalian cells can be decorated with antibodies specific for SUMO or Ubc9 along their entire axis (Kovalenko et al., 1996; Tarsounas et al., 1997), suggesting that SC regulation by SUMO is a conserved feature among species.

Ubc9 is recruited to the SC by binding Zip3 (Hooker and Roeder, 2006), which itself localizes to the initiation sites of SCs and binds to early and late meiotic factors thereby linking DSB processing with synapsis (Agarwal and Roeder, 2000). Thus, the SUMO E3 ligase Zip3 might be involved in the modification of SC elements and SC-associated proteins. Interestingly, Zip3 seems to have specificity for the conjugation of poly-SUMO chains (shown *in vitro*) which apparently have effects on SC formation (Cheng et al., 2006). Moreover, the SUMO de-conjugating enzyme Ulp2 is necessary for normal sporulation (Li and Hochstrasser, 2000) and was suggested to have a more specific role in connection with poly-SUMO chain formation (Bylebyl et al., 2003). Taken together, SUMO plays a critical role in meiosis progression and SC formation, the underlying mechanisms are however unclear so far.

II.3 DNA damage response

In order to preserve genomic integrity, cells are equipped with a complex network of pathways, which are activated in response to DNA damage (**Fig. 6**). In a simplified view, mechanisms that repair the DNA lesion (*see II.3.1*) and DNA damage checkpoints that signal the presence of damaged sites (*see II.3.2*) can be distinguished. Many of the principal mechanisms are highly conserved between yeast and higher eukaryotes.

II.3.1 DNA repair pathways

DNA is constantly altered by endogenous and exogenous causes leading to mutations that are potentially harmful for the cell. In order to repair DNA damages, several pathways dealing with the altered sites have evolved: nucleotide-excision repair (NER), base-excision repair (BER), homologous recombination (HR) and non-homologous end joining (NHEJ), mismatch repair and telomere metabolism (reviewed in Hoeijmakers, 2001). Depending on the nature of the damage as well as the cellular context, the appropriate pathway is activated to assure genome maintenance.

II.3.2 DNA damage checkpoints

DNA damage checkpoints are closely linked to DNA repair mechanisms, but have a more specific role in sensing DNA damages and activating a cascade of

cellular pathways to deal with genomic mistakes (reviewed in Shiloh, 2003). Upon DNA damages, cell-cycle checkpoints lead to the sudden arrest of the cell cycle involving rapid changes in the gene expression profile as well as protein synthesis and degradation. A basic trigger in this response is the family of PI3K-related protein kinases including ATM and ATR/ATRIP (in *S. cerevisiae*: Tel1 and Mec1-Ddc2, respectively), which trigger a broad network of DNA damage response factors.

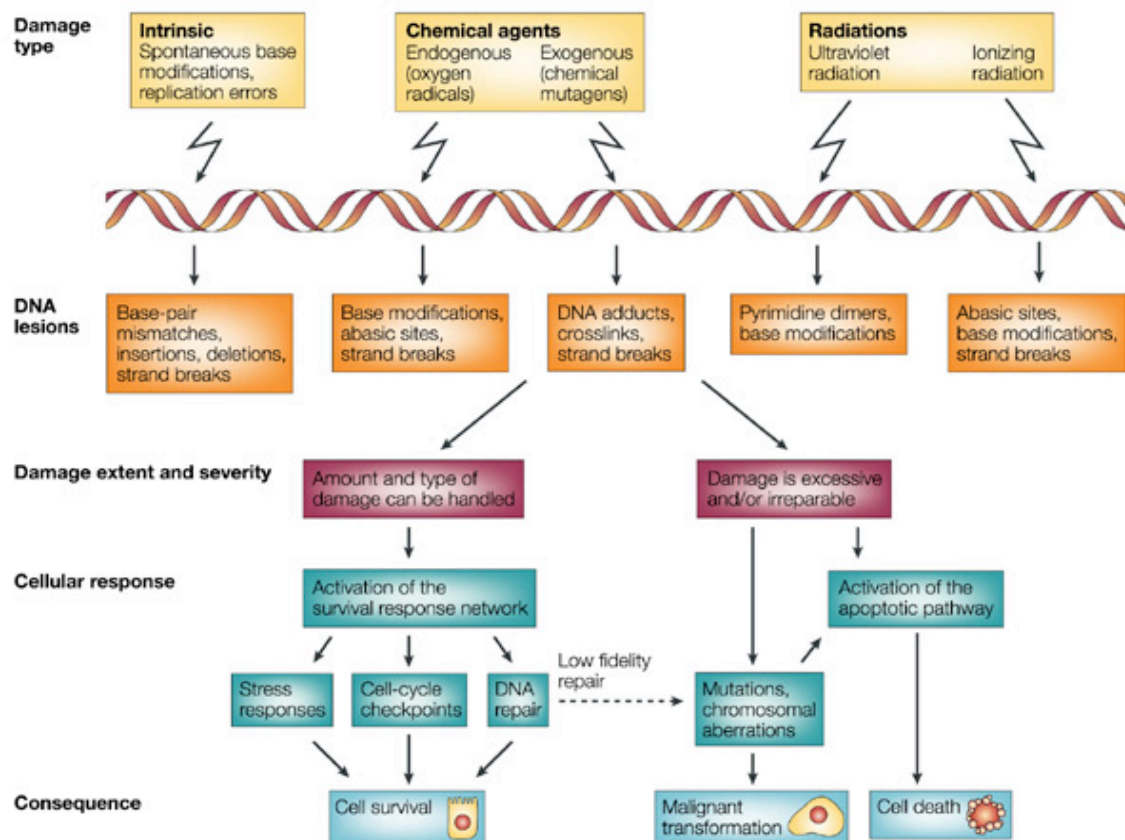


Figure 6: Cellular DNA damage response. Different types of damages lead to various kinds of DNA lesions. Cells activate a network of control and repair pathways depending on the nature and severity of DNA damage in order to assure survival. In higher eukaryotes, genomic alterations can lead to apoptosis or malignant transformations (Figure from Shiloh, 2003).

11.3.3 The 9-1-1 checkpoint complex

In eukaryotic organisms, the 9-1-1 complex plays a key role in checkpoint activation. Its three subunits (in *S. cerevisiae*: Ddc1, Mec3 and Rad17; in humans: Rad9, Hus1 and Rad1, therefore the term “9-1-1”) form a heterotrimeric, circular complex, which closely resembles the PCNA sliding clamp (Venclovas and Thelen, 2000). In analogy to the function of PCNA in

DNA replication, the 9-1-1 complex is thought to encircle DNA specifically at damaged sites, and serve as a platform for checkpoint and DNA repair proteins.

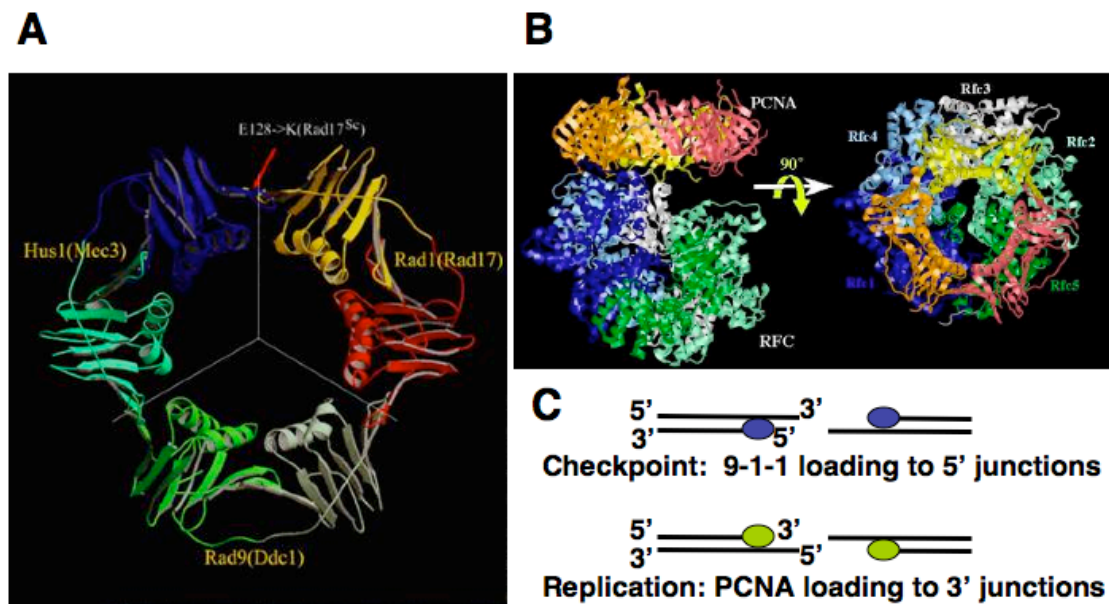


Figure 7: The 9-1-1 checkpoint complex. A: Hypothetic structure of the 9-1-1 complex. Depicted are the three subunits of the human 9-1-1 complex Rad9, Rad1 and Hus1 (in *S. cerevisiae* Ddc1, Rad17 and Mec3) based on alignments with PCNA (Venclovas et al., 2002; Venclovas and Thelen, 2000). **B: Loading of PCNA by the Rfc1-5 complex.** Other clamp-loader complexes (in which Rfc1 is replaced by Rad24, Elg1 or Ctf18) work in a very similar manner, but have distinct functions. Shown is the crystal structure of the PCNA ring together with the five-subunit loader complex Rfc1-5 (Bowman et al., 2004). **C: Differential loading of PCNA and the 9-1-1 complex.** PCNA recognizes 3' junctions, which are perfect templates for DNA replication, while 9-1-1 is specifically recruited to RPA-coated 5' junctions, which do not serve as substrates for replication but mark sites of DNA damage and trigger checkpoint signalling (Majka et al., 2006a).

In addition to its similarities with PCNA concerning structure and DNA binding, the principal loading mechanism of PCNA and the 9-1-1 sliding clamp is as well comparable (**Fig. 7**). The recruitment of the 9-1-1 complex to damaged DNA is mediated via a complex containing the Rad24 subunit. By replacing Rfc1, which is necessary for the DNA loading of PCNA, Rad24 functions in complex with Rfc2-5. Critical for the recruitment is the nature of junction. While PCNA is loaded on a 3'-junction (replication fork), 9-1-1 is recruited to replication protein A (RPA)-coated 5'-junction (DNA damage). Thus, as loading of each clamp requires RPA, the distinction is probably made through the DNA state and the action of the respective clamp-loader complex (Majka et al., 2006a), **Fig. 7**). After loading, the DNA-bound 9-1-1 sliding clamp

facilitates ATR-mediated phosphorylation and activation of Chk1, a protein kinase that regulates S-phase progression, G2/M arrest, and replication fork stabilization (Parrilla-Castellar et al., 2004). Moreover, a recent report shows an involvement of 9-1-1 and the cyclin-dependent kinase Cdc28 in the recruitment of Ddc2 (homologue to human ATRIP) depending on the nature of the damage and the cell cycle phase (Barlow et al., 2008). Interestingly, co-localization of Mec1-Ddc2 (homologue to human ATR/ATRIP) and 9-1-1 is sufficient for checkpoint activation even in the absence of DNA damage (Bonilla et al., 2008). In addition to its role in checkpoint activation, there is evidence that 9-1-1 also participates in DNA repair (Helt et al., 2005). In general, 9-1-1 plays a central role in the coordination of DNA damage checkpoint and repair functions by binding to sites of damaged DNA and serving as a recruitment platform. Similar to PCNA, post-translational modification of SUMO and ubiquitin might be crucial in the regulation of 9-1-1-mediated events in eukaryotic cells. Indeed, ubiquitylation of the Rad17 subunit by Rad6-Rad18 was proposed to promote DNA-damage-dependent transcriptional induction as well as checkpoint functions (Fu et al., 2008).

II.3.4 Meiotic recombination and surveillance mechanisms

Meiotic progression includes the controlled induction of DSBs and their repair by homologous recombination assuring the correct pairing and segregation of homologous chromosomes. The tight control of DSB repair and recombination intermediates by specific surveillance mechanisms is crucial for creating gametes with correct chromosome numbers. Indeed, in humans, up to 30% of spontaneous miscarriages seem to be the result of chromosome missegregation events (Hassold and Hunt, 2001). Only a few missegregation events are compatible with human life including Down (trisomy 21), Turner (monosomic for X) and Klinefelter (XXY male) syndromes.

Meiotic recombination is initiated through the topoisomerase-like enzyme Spo11 (**Fig. 8**). After its removal, DSBs are resected in the 5' to 3' direction to produce 3' single overhangs by the Mre11 complex (Keeney, 2001). Very recently the functioning of a set of nucleases involved in the resection of induced DSBs have been described in more detail (Gravel et al., 2008; Huertas et al., 2008; Zhu et al., 2008), which very likely also holds true for meiotic DSB

processing. Following resection, ssDNA tails are coated with the heterotrimeric RPA complex consisting of Rfa1, Rfa2 and Rfa3 (Alani et al., 1992; Krogh and Symington, 2004). RPA fulfils two functions: it stabilizes ssDNA by preventing secondary structures and serves as a component of the meiotic checkpoint pathway (Lisby et al., 2004; Lisby and Rothstein, 2004). Next, ssDNA tails are covered with Rad51 and its meiosis-specific counterpart Dmc1 to form nucleoprotein filaments. Rad51 and Dmc1 have overlapping, but nonidentical functions and are both essential for high meiotic recombination rates. Following assembly, the Rad51 and Dmc1 nucleoprotein filaments engage in the search for homologous repair templates and interact with corresponding DNA segments to initiate strand exchange. As mentioned before, meiotic recombination is characterized by a strong bias towards the alignment and connection of homologous chromosomes rather than sister chromatids (Schwacha and Kleckner, 1997).

In order to achieve recombination specifically between homologous chromosomes, cells are equipped with a set of meiosis-specific factors. The chromosome associated kinase Mek1 blocks recombination between sister chromatids (Niu et al., 2007; Niu et al., 2005; Wan et al., 2004), Hop2-Mnd1 prevents chromosome synapsis with nonhomologous partners (Leu et al., 1998) and the ZMM group of proteins, consisting of Zip1, Zip2 and Zip3 as well as the Mer3 helicase and the Msh3/Msh5 complex, are essential for stable invasion of homologous repair templates and the maturation of recombination intermediates into crossovers (Borner et al., 2004; Lynn et al., 2007).

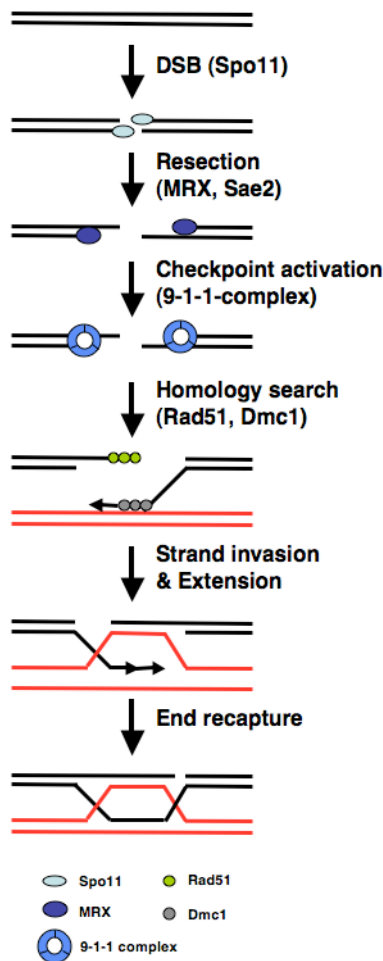


Figure 8: Meiotic recombination. Spo11 cleaves dsDNA, yielding a covalent Spo11-DNA complex. Resection of DSB gives rise to 3'-ssDNA overhangs. 5' junctions are recognized by the 9-1-1 checkpoint complex thereby activating DNA damage response. ssDNA overhangs are covered by Rad51 and the meiosis-specific Dmc1. These nucleofilaments are crucial for homology search and invasion of ssDNA to form asymmetric strand exchange intermediates.

CO pathway (shown): DNA synthesis is primed from the invading 3' end; the second DSB end is captured and primes DNA synthesis. Ligation yields a pair of Holliday junctions. Depending on the resolution of these structures, the final outcome can be either a crossover or a non-crossover product.

NCO pathway (not shown): Transient strand invasion and DNA synthesis probably occur, but are counteracted by helicases. Newly synthesized DNA anneals to complementary ssDNA on the other side of the break. Further DNA synthesis and ligation yield a mature non-crossover product.

The induction of DSBs by Spo11 and consequential intermediates of meiotic recombination are harmful for the cell if not resolved. It is therefore necessary to control ongoing recombination events and to avoid meiotic exit before resolution of all intermediate structures. This is carried out by the **pachytene checkpoint** which prevents meiotic cell cycle progression in response to unrepaired recombination intermediates and coordinates recombination-associated events and meiosis I progression (Hochwagen and Amon, 2006; Roeder and Bailis, 2000).

It has become clear that Ddc1, a subunit of the 9-1-1 complex is required for the pachytene checkpoint in *S. cerevisiae* (Hong and Roeder, 2002). Ddc1 localizes to chromosomes and becomes phosphorylated during meiotic prophase. These events depend on the formation and processing of DSBs consistent with the general idea that the 9-1-1 complex is loaded upon single-stranded DNA after several kinds of DNA damage. In a $\Delta dmc1$ background in which unresolved recombination events accumulate, Ddc1 phosphorylation and

foci formation are observed, both indicating an activated checkpoint. Apart from the 9-1-1-dependent pachytene checkpoint pathway, a genetically separable pathway involving the putative AAA-ATPase Pch2 has been identified (Wu and Burgess, 2006). This checkpoint requires Zip1 and probably monitors malformed SCs. Therefore, at least two ways of checkpoint induction can be distinguished: ssDNA intermediates activate a Rad17-Sae2-dependent pathway, whereas incomplete synapsis triggers a Pch2-Zip1-dependent pathway.

In a recent review, four major checkpoint pathways are postulated for meiosis. Notably, in this classification the recombination checkpoint represents the classical “pachytene checkpoint” (**Fig. 9**; Hochwagen and Amon, 2006). The **Meiotic DNA damage checkpoint** works similar to how cells undergoing mitosis react on DNA damage and evidence was provided that such a DNA damage checkpoint also functions during the meiotic cell cycle (Garvik et al., 1995; Lydall et al., 1996). The mitotic DNA damage checkpoint is triggered by signal activation through RPA-coated ssDNA resulting from the resection of DSBs (Garvik et al., 1995; Lydall, 2003; Zou and Elledge, 2003; Zou et al., 2003). Single-stranded DNA filaments are recognized by the checkpoint kinase Mec1 and by Rad24, which functions as a clamp-loader for the 9-1-1 complex. These events lead to the full activation of Mec1, which in turn activates the protein kinases Rad53 and Chk1 by phosphorylation (Rouse and Jackson, 2002). The activation process requires the adaptor protein Rad9 and leads to the phosphorylation of a variety of checkpoint targets that determine the cellular response to DNA damages. It is important to note that deleting Rad9 or Rad53 does not lead to a reduced spore viability indicating a minor role of this pathway during meiosis.

The definition of the **rad50S checkpoint** rises from a set of non-null alleles of *RAD50* and *SAE2/COM1* that are characterized by the accumulation of unresected DSBs covalently attached to Spo11 (Alani et al., 1990). Notably, as typical single-stranded recombination intermediates are not present in these backgrounds, it has been suggested that the MRX complex and the checkpoint kinase Tel1 function as the primary signal sensors of protein-linked DSBs. Like all other checkpoints described here, the *rad50S* checkpoint also requires the protein kinase Mec1 and the clamp-loader Rad24 (Usui et al., 2001; Usui et al., 2006). In contrast to the meiotic DNA damage checkpoint, *rad50S* checkpoint

function utilizes the meiosis-specific Rad53 paralogue kinase Mek1 as well as the axial element proteins Red1 and Hop1 (Usui et al., 2001; Usui et al., 2006; Woltering et al., 2000; Xu et al., 1997).

The **recombination checkpoint** (termed “**pachytene checkpoint**” in this study) has been investigated mainly in mutants lacking essential recombination factors, such as Dmc1 and Hop2, which are required for the initial strand invasion step during meiotic recombination. These mutants are capable of removing Spo11 from DSBs, but accumulate hyperresected DSBs, thereby causing a pronounced delay in meiotic G2/prophase (Bishop et al., 1992; Gerton and DeRisi, 2002). As the failure in homology search and the hyperresection of DSBs leads to an extensive accumulation of Rad51 coated ssDNA, it was suggested that Rad51 nucleoprotein filaments function as activation signals for the recombination checkpoint (Lydall et al., 1996; Shinohara et al., 1997). Similar functions were proposed for Dmc1 nucleoprotein filaments (Hochwagen and Amon, 2006). Like the before-mentioned DNA damage checkpoint and the *rad50S* checkpoint, signal transduction within the recombination checkpoint requires Mec1 as well as loading of the 9-1-1 complex (Hong and Roeder, 2002; Lydall et al., 1996). In addition, the recombination checkpoint strictly depends on the meiotic proteins Red1, Hop1 and Mek1 (Hochwagen et al., 2005; Xu et al., 1997), but does not depend on Rad9 or Tel1 (Lydall et al., 1996; Usui et al., 2001).

Meiotic recombination is highly dependent on the correct alignment of homologous chromosomes. The **Zip1 checkpoint** is defined by the finding that cells undergo a temperature-dependent delay in meiotic G2/prophase when SC components like Zip1, Zip2 or Zip3 are absent (Agarwal and Roeder, 2000; Borner et al., 2004; Chua and Roeder, 1998; Sym et al., 1993). Detailed insights were gained from analyzing *zip1* mutants, which exhibit a meiotic cell cycle delay requiring the meiotic proteins Red1, Hop1 and Mek1, as well as Mec1, Rad24 and the 9-1-1 complex (Roeder and Bailis, 2000). Additionally, the ATPase Pch2 seems to be specifically required for the *zip1* checkpoint (San-Segundo and Roeder, 1999; Wu and Burgess, 2006).

II.4 Aim

Previous studies showed the localization of Ubc9 and SUMO to synaptonemal complexes (SCs) in yeast and higher eukaryotes, however SUMO substrates connected to SC biology were not known and detailed molecular mechanisms unclear. In this study, we first tested whether major SC components are SUMO targets and found that the axial element protein Red1 is modified with SUMO specifically during early meiosis. Having established Red1 as a meiosis-specific SUMO substrate, the next aim was to identify acceptor lysines and to analyze the phenotypes of the respective mutant in order to understand the function of this conjugation. A second aim was to define the exact role of Red1 within the pachytene checkpoint pathway. Having found direct interaction of Red1 with two subunits of the 9-1-1 complex (Mec3, Ddc1), the next goal was to map the respective domains within Red1, generate specific binding mutants and analyse the phenotypes. The characterization of these Red1 mutants (lysine mutant and 9-1-1-binding mutants) will help to decipher Red1 functions in SC formation and pachytene checkpoint activation and thereby shed further light on the complex interplay between these pathways in meiosis.

III RESULTS

III.1 Red1 is modified by SUMO during meiosis

*III.1.1 Purification of meiotic SUMO substrates in *S. cerevisiae**

Several recent reports hint towards a role of SUMO during meiosis and more specifically in the establishment of SCs, however mechanistic details are not understood (Cheng et al., 2006; Hooker and Roeder, 2006). In order to find SUMO substrates specifically connected to these processes, we carried out ^{His}SUMO Ni-NTA pull-down assays (as described in Sacher et al., 2005) from synchronously growing cultures of SK1 strains and tested potential proteins for their modification with SUMO using substrate-specific antibodies. Diploid SK1 yeast strains were used for this purpose as they show very synchronous sporulation behaviour upon transfer into 2% potassium acetate media. All pull-down experiments were carried out under denaturing conditions in order to preserve transiently SUMO-modified species. To control for pull-down efficiency, ^{His}Pol30 (PCNA)-expressing cultures were mixed with the meiotic cultures before lysis and pull-down, and ^{His}Pol30 was detected by Western analysis using an anti-Pol30 antibody. SUMO constructs fused to seven histidines are expressed from an *ADH1* promoter and integrated into the *URA3* locus of wild-type SK1 strains.

III.1.2 The SUMO substrate Red1

By using the above-mentioned strategy, we identified endogenous Red1 as a SUMO substrate using an anti-Red1 peptide antibody raised in this study. Corresponding to the structural role of Red1 in SCs, Red1 levels strongly rose after sporulation induction when SCs are known to form (**Fig. 10A**). Concomitantly, also SUMOylated Red1 species accumulated (**Fig. 10A**), but, as expected for this reversible modification, only a fraction of Red1 was modified at steady state. The pattern of the SUMO conjugation suggests modification on either several lysines or with poly-SUMO chains. Correspondingly, we also detected two-hybrid interaction of Red1 with SUMO,

the SUMO-conjugating enzyme Ubc9, and the de-SUMOylation enzyme Ulp2 (Fig. 10B,C).

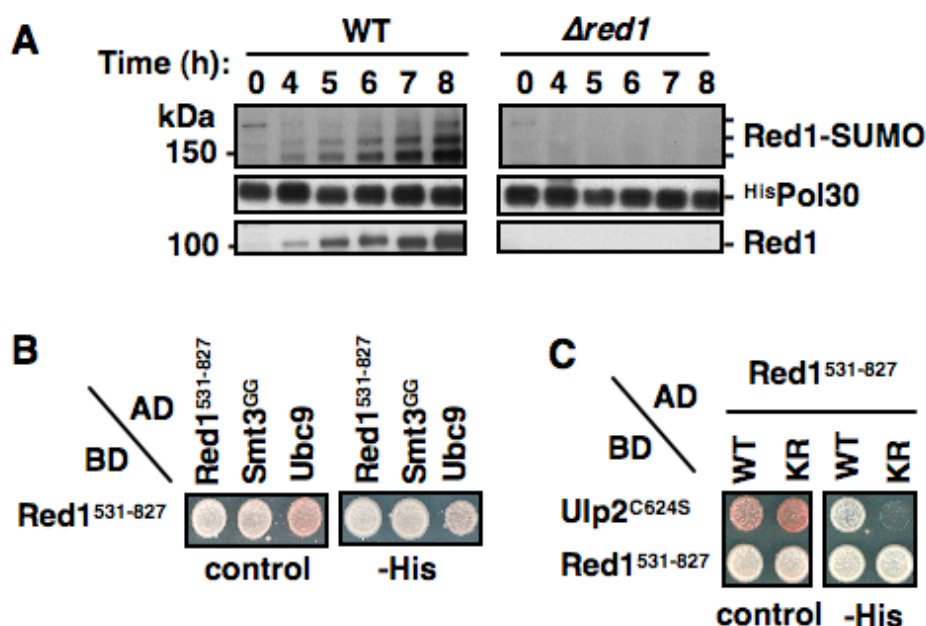


Figure 10: Red1 is modified by SUMO and interacts with components of the SUMO pathway. **A:** SUMOylation of endogenous Red1. Diploid homozygous SK1 WT or $\Delta red1$ cells were released into synchronous sporulation and cell extracts were harvested after the indicated times. His SUMO-conjugates monitored by Ni-NTA pull-down followed by Western blotting using an anti-Red1 antibody detect Red1 species carrying one, two, or more SUMO moieties. To control for pull-down efficiency, His Pol30-expressing cultures were mixed with the meiotic cultures before lysis and pull-down, and His Pol30 was detected by Western analysis using an anti-Pol30 antibody (lower panel: Red1 input levels). **B:** Red1 interacts with Red1, SUMO (Smt3), and Ubc9. **C:** Enzymatic inactive Ulp2 (Ulp2^{C624S}) specifically binds SUMOylation-proficient Red1, but not the SUMOylation-deficient Red1^{KR} variant. For these two-hybrid assays (**B**, **C**) cells were transformed with respective AD- and BD-fusions and spotted on selective media and were grown for 3 days at 30°C.

III.1.3 The SUMO acceptor lysines in Red1

In order to reveal a specific function for the SUMOylation of Red1, we searched for the acceptor lysine(s) to construct mutants deficient in the conjugation. We took advantage of a DF5 strain in which a Red1 fragment (residues 531-827; termed Red1⁵³¹⁻⁸²⁷) was fused to the binding domain (BD) of Gal4 on a yeast-two hybrid plasmid and in which a His SUMO variant is overexpressed under an *ADH1* promoter. In this system, Red1 is highly SUMOylated as shown by Ni-NTA pull-down (**Fig. 11A**). Taking advantage of this finding, we introduced lysine-to-arginine replacements in this region in order to identify the SUMO acceptor sites. A particular lysine-rich (K-rich)

region is located between residues 569-590 of Red1 (**Fig. 11C**), and indeed most *in vivo* SUMOylation sites lie within this domain. The most frequently used sites locate between residues 569-577 (KR1), but changing all lysine residues to arginine in the K-rich region reduced the SUMOylation level of the Red1 fusion further to less than 10% of the wild-type protein (**Fig. 11A**, lane KR). Importantly, when we introduced these changes into full-length Red1 expressed from its endogenous genetic locus (designated Red1^{KR}), Red1 was expressed to normal levels, but its SUMOylation was strongly reduced (**Fig. 11B**). Throughout this study we used the Red1^{KR} variant for analysis of phenotypes, as it shows the most significant reduction in SUMOylation.

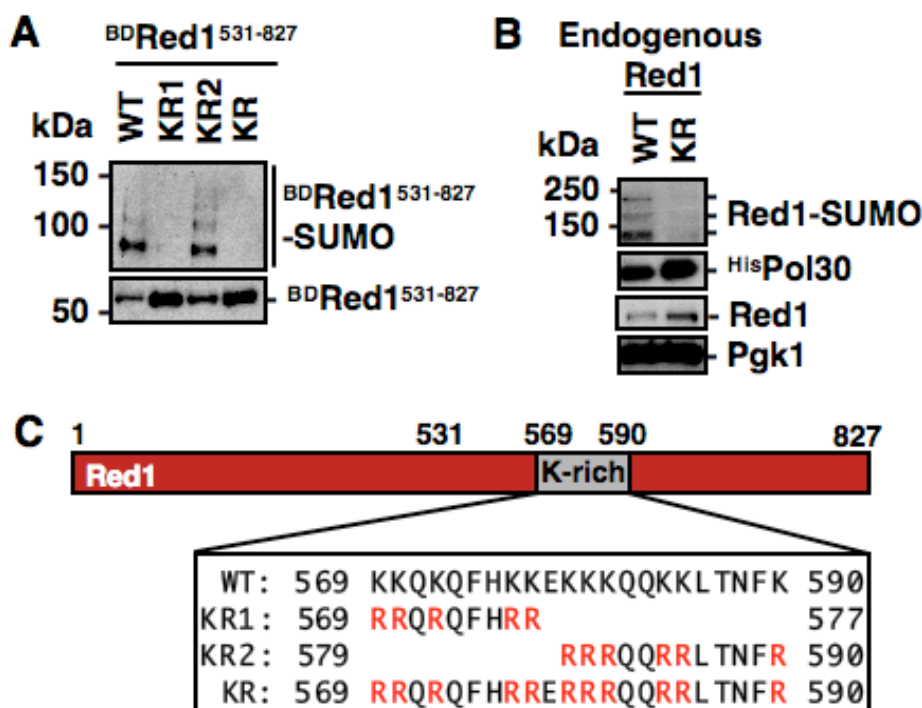


Figure 11: Identification of SUMO acceptor lysines in Red1. **A:** Identification of Red1 SUMO acceptor sites using cells expressing ^{His}SUMO and ^{BD}Red1⁵³¹⁻⁸²⁷, in which Red1 sequences were derived from WT Red1 or Red1 variants carrying lysine-to-arginine (K-R) exchanges (KR1, KR2, KR; see Fig. 11C). SUMO conjugates were isolated by Ni-NTA pull-down from lysates and detected by Western blotting using anti-BD monoclonal antibodies (Santa Cruz) (lower panel: Red1 input levels). **B:** SUMOylation of endogenous Red1^{KR}. Ni-NTA pull-down of SUMO conjugates from lysates of SK1 strains expressing Red1 WT or Red1^{KR} variant from the genome using *RED1* promoter and terminator elements. Western analysis was carried out using an anti-Red1 antibody, control of pull-down efficiency was done as in Fig. 10A (^{His}Pol30). Red1 input levels (third panel) and loading control (Pgk1; fourth panel) are shown. **C:** Diagram of Red1 indicating a lysine-rich region (K-rich; aa 569-590). Red1 variants harbouring K-R replacements of all lysines within regions aa 569-577 (designated KR1), aa 579-590 (KR2), and 569-590 (KR) are indicated.

III.1.4 The SUMO substrate Sycp3 in *Homo sapiens*

Synaptonemal complexes can be decorated with antibodies specific for SUMO or Ubc9 along their entire axis in yeast and mammalian cells (Kovalenko et al., 1996; Tarsounas et al., 1997), suggesting a conserved mechanism of SC regulation by SUMO in higher eukaryotes. Indeed, the mammalian SC protein Sycp3 (alias Scp3, Cor1), a possible functional analogue of yeast Red1 (Schalk et al., 1998; Yuan et al., 2000), binds Ubc9, and homodimerizes (**Fig. 12A**; Tarsounas et al., 1997) and is modified by SUMO2 (to a lesser extent also by SUMO1) in 293T cells (**Fig. 12B**). Notably, a second potential analogue of yeast Red1, the mammalian Sycp2 (alias Scp2), shares similarity with the Red1 K-rich region, despite no apparent homologies throughout the rest of the protein (**Fig. 12C**).

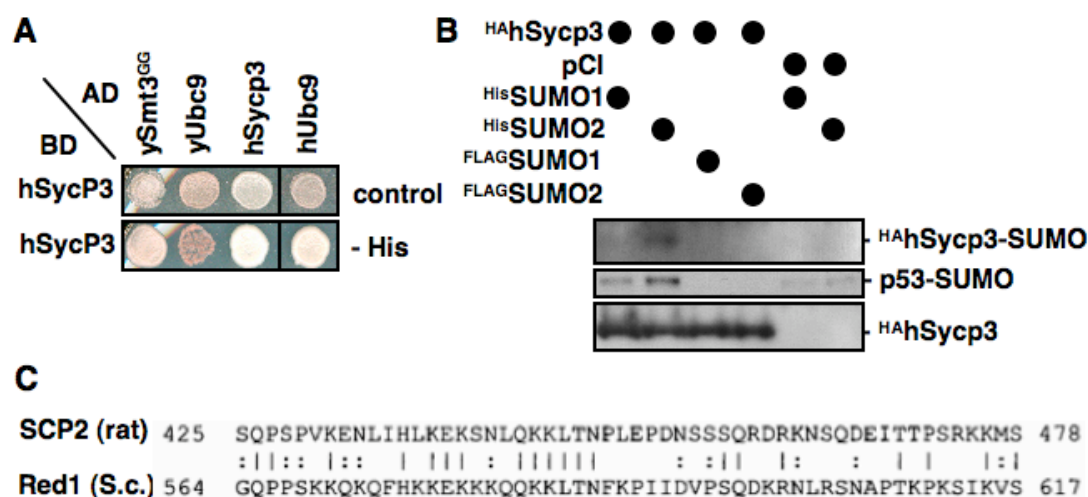


Figure 12: Human Sycp3 interacts with the SUMO pathway and is modified with SUMO. **A:** Sycp3 interacts with human Ubc9, another Sycp3 as well as with Ubc9 and Smt3 from yeast. “y” indicates yeast proteins, “h” stands for human proteins. **B:** HA-tagged human Sycp3 (^{HA}Sycp3; a putative Red1 homolog) and human ^{His}SUMO1 or ^{His}SUMO2 were overexpressed in HEK 293T cells. SUMO-conjugates were isolated by Ni-NTA pull-downs and modified species of Sycp3 were detected by Western blot analysis using a monoclonal anti-HA antibody (Clone 16B12, Convnance). Modification of Sycp3 occurred specifically with ^{His}SUMO2, barely with ^{His}SUMO1, but not in controls (expression of vector pCl or of ^{FLAG}SUMO1 and ^{FLAG}SUMO2, which lack His-tags). SUMOylation of endogenous p53 was detected by a monoclonal anti-p53 antibody (DO-1, Santa Cruz) and used as a positive control (lower panel: hSycp3 input levels). **C:** Alignment of Red1 and a functional analogue in rat, Scp2. Underlined is the K-rich region of Red1.

III.2 Red1 SUMOylation recruits Zip1 for the timely establishment of SCs

The axial element protein Red1 is SUMO-modified and this modification is specific for an early period during meiosis when SCs are initiated and mature. Given previous results showing that Zip1 harbours a SUMO-interacting motif (SIM) in its very C-terminus, which is essential for SC assembly (Cheng et al., 2006), we wanted to test the idea that Zip1 interacts specifically with SUMOylated Red1 and thereby plays a role in the zipping process.

III.2.1 Red1 and Zip1 interact in a SUMO-dependent manner

In order to prove this hypothesis, we first scored for the viability of spores as a measure for meiosis competence. For this, diploid SK1 strains were cultured overnight in complete medium (YPD) and transferred to a “pre-sporulation” medium (YP acetate) overnight, before initiating synchronous sporulation in 1,5% potassium acetate media. Tetrads were dissected (after 3 days) and spore viability was scored on YPD plates. Indeed, spore viability of the *red1^{KR}* mutant was significantly reduced to about 40% compared to WT cells (**Fig. 13A**). For comparison, the deletion of the major central element protein Zip1 and therefore the loss of functional SCs leads to a stronger reduction of spore viability of around 30% (**Fig. 13A**). Interfering with the SUMO E3 ligase Zip3 is known to cause delayed and incomplete SC formation (Agarwal and Roeder, 2000) and shows even stronger defects of only 10% spore survival in this assay (**Fig. 13A**).

Next, using two-hybrid assays, we directly tested the binding of a C-terminal part of Zip1’s C-terminal domain that harbours a SIM and found that this fragment specifically binds the SUMOylated version of Red1 but not the SUMO-deficient Red1^{KR} mutant, while the Red1-Red1 dimerization was not affected (**Fig. 13B**). This suggests that Red1-SUMOylation may indeed be critical for Zip1-Red1 interaction and thus for SC maturation.

Moreover, again using two-hybrid assays, we showed that Zip1 dimerizes via its N-terminal domains and strongly interacts with SUMO (**Fig. 13C**; Cheng et al., 2006). Interestingly, full-length Zip1 (which contains the

extended N-terminus for dimerization) shows strongest interaction with SUMO suggesting that Zip1 dimers/oligomers bind SUMO more efficiently. Altogether, these results strongly argue for a SUMO-mediated recruitment of Zip1 by SUMO-modified Red1 and allow the attractive model of SUMO functioning as the “zipping glue” that fosters the assembly of lateral and central elements to mature SCs (**Fig. 13D**).

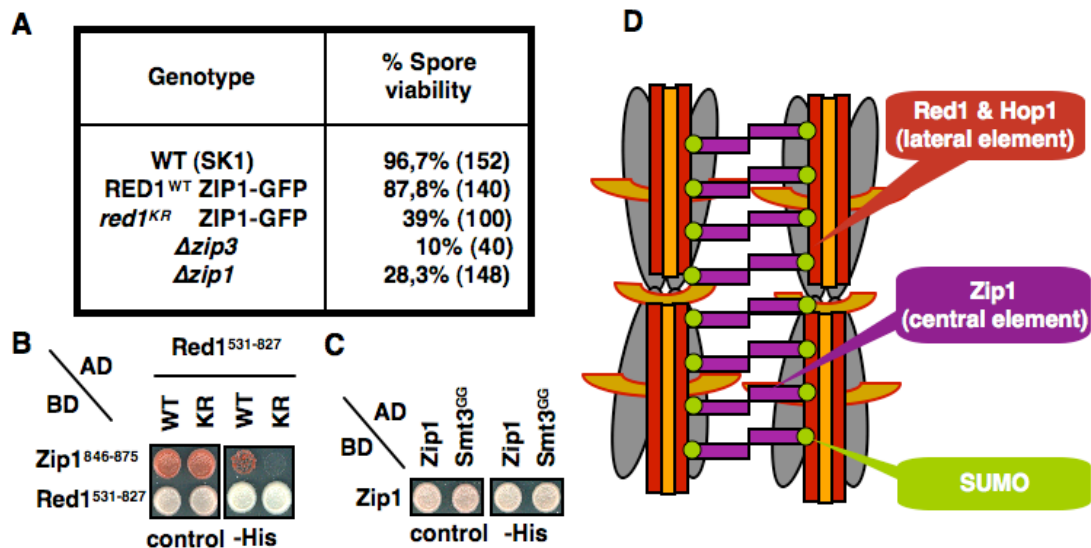


Figure 13: SUMO as the “zipping glue”. **A: Red1 lysine mutant (*red1^{KR}*) is defective in spore viability.** Spore viabilities of WT cells (SK1 strain) were compared with GFP-Zip1-expressing cells that express Red1 WT or *red1^{KR}* under the *RED1* promoter. Also shown are spore viabilities of $\Delta zip3$ and $\Delta zip1$ mutants. Strains were released into sporulation in 1,5% potassium acetate solution for 3 days before tetrad dissection, and spore viability was scored on YPD plates after 3 days. Indicated are the percentages of viable spores and the total number of spores counted (brackets). **B: Zip1 specifically binds SUMOylated Red1.** The SUMO-interacting motif (SIM)-containing C-terminal region of Zip1 specifically binds SUMOylation-proficient WT Red1, but not Red1^{KR}. Two-hybrid interactions of a C-terminal fragment of Zip1 (aa 846-875) with a Red1 fragment (aa 531-827) derived from WT Red1 or Red1^{KR} were identified on selective media (-His). Fusions with activating domain (AD) or DNA-binding domain (BD) are indicated. **C: Zip1 binds SUMO and another Zip1.** Two-hybrid assay was done as in Fig. 13B using the respective AD and BD fusions. **D: Model for SC assembly.** Association of the central element protein Zip1 to the lateral element is fostered by SUMO modification of Red1 (and maybe Hop1) through recognition by a SIM in Zip1’s C-terminal domain.

III.2.2 Red1 SUMO-deficient mutant shows delayed zipping

According to the model that Zip1-Red1 interaction is modulated by SUMO modification of Red1, we expect changes in either the maturation of SCs or the timing of SC appearance.

To address the role of SUMOylated Red1 more directly, we microscopically monitored the different stages of SC assembly by using strains that express a GFP-tagged Zip1 variant. In detail, two copies of either the wild-type version or the lysine-mutant of Red1 under the endogenous promoter were integrated into diploid $\Delta red1 \Delta zip1$ strains, which were additionally transformed with a GFP-tagged Zip1 version as the only source of Zip1 (**Fig. 14A**). Because GFP-tagging to either end of Zip1 inactivates the protein, we rather used a variant that harbours GFP embedded within the protein's central coiled-coil region (Scherthan et al., 2007). Judged by the spore viability of this strain, this Zip1 variant is almost as functional as the WT protein (**Fig. 13A**) and the expression levels of Red1 WT and $red1^{KR}$ strain were comparable (**Fig. 14B**). In order to categorize and quantify SC formation, we distinguished four different states, which subsequently occur during early meiosis I. The GFP signal was monitored by spinning disk microscopy, which allowed accurate counting of cells by the rapid acquisition of several stacks of a pool of cells (**Fig. 14C**). In Red1 wild-type cells, full SCs are formed already two hours after sporulation induction (**Fig. 14D**). By contrast, although the $red1^{KR}$ strain is capable in forming full SCs, their formation is significantly delayed by several hours (**Fig. 14D**). This finding is in accordance with the highly reduced but not totally absent SUMOylation of Red1 in $red1^{KR}$ strain even after 6 or 8 hours and suggests that SUMO-modified Red1 may initiate and foster SC assembly, thereby securing timely SC formation. Unlike Zip1-SIM mutants (termed Zip1-SIM^{3N} and Zip1-SIM^{3R}), which show rather severe defects (**Fig. 14E**; Cheng et al., 2006), the SUMO-deficient Red1 variant leads to a milder phenotype.

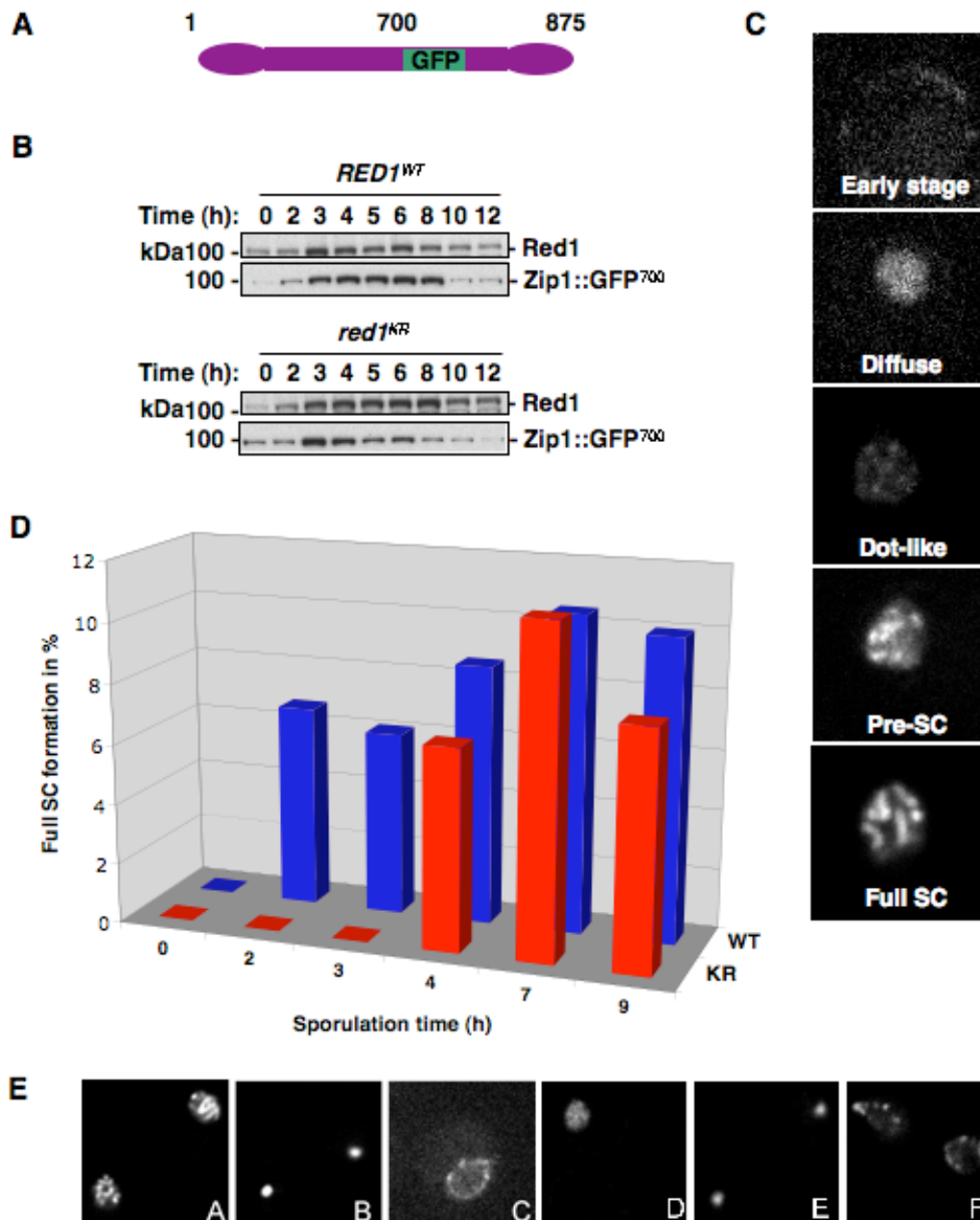


Figure 14: Red1 SUMOylation is important for the timely establishment of SC.

A: Zip1 was fused with a GFP tag within its coiled-coil domains. **B:** Red1 expression in strains carrying Red1 WT or lysine mutant under the *RED1* promoter. **C:** Maturation of SCs shown by monitoring the GFP-tagged Zip1 signal using spinning disk microscopy. **D:** Red1 lysine mutant shows defects in the timely establishment of mature SCs. SC formation in WT and *red1* lysine mutant (identical strains as Fig. 14B). SCs were visualized using GFP-tagged Zip1 and spinning disk microscopy. Maturation of SCs was categorized in the indicated classes (early stage, diffuse, dot-like, pre-SCs and full SCs). In the quantified assay only full SCs were counted. Cells were released into synchronous sporulation and samples observed after the indicated times. For each time-point more than 100 cells were analyzed. **E:** Zip1-SIM mutants are defective in the establishment of SCs (pictures were taken after 9 hours in sporulation media). A: *RED1^{WT} ZIP1^{WT}-GFP*, B: *RED1^{WT} zip1^{3N}-GFP*, C: *RED1^{WT} zip1^{3R}-GFP*, D: *red1^{KR} ZIP1^{WT}-GFP*, E: *red1^{KR} zip1^{3N}-GFP*, F: *red1^{KR} zip1^{3R}-GFP*. All strains are $\Delta red1 \Delta zip1$ background.

Further SUMO functions linked to the SC?

Apart from Red1's interaction with the SUMO pathway, its SUMO modification within the K-rich region and the specific phenotype in the timely establishment of SCs, several pieces of data speak for additional interactions of SC proteins with the SUMO machinery.

First, we found that Red1 contains a SIM at aa 455-473 and that specific mutations can abolish the interaction with SUMO (**Fig. 15A**). However, the respective mutants did not show significant effects on spore viability or the quality of SCs (data not shown). Second, Red1 SUMOylation seems to involve chain formation as the pattern of SUMO-modified ^{BD}Red1⁵³¹⁻⁸²⁷ fusions is shifted towards lower migrating species when replacing the wild-type version of ^{His}SUMO with a ^{His}SUMO variant that has the first three lysines mutated to arginins ^{His}SUMO^{KKK} as the only source of SUMO in the cell (**Fig. 15B**). Third, also the second major axial element protein Hop1 interacts with Ubc9 and SUMO in a two-hybrid assay (**Fig. 15C, D**). Whether this is due to an interaction of SUMO with a SIM domain or due to conjugation to a lysine residue remains to be shown. As Hop1 also interacts with the C-terminal region of Red1, it is possible that also the Hop1-Red1 association is stimulated via a SUMO-SIM binding interface (**Fig. 15D**). Fourth, using the purified GST-tagged C-terminus of Zip1 (aa 824-875), we could further show that a very short fragment of Zip1 harbouring the SIM region might pull-down endogenous Red1 from sporulating cells (data not shown). Whether this Red1 species is (specifically) modified by SUMO was not clear in this experimental setup. Moreover, using the same assay, we could pull-down substrates modified by several SUMO moieties or SUMO chains (data not shown), suggesting that perhaps additional SUMO-modified meiotic proteins bind Zip1.

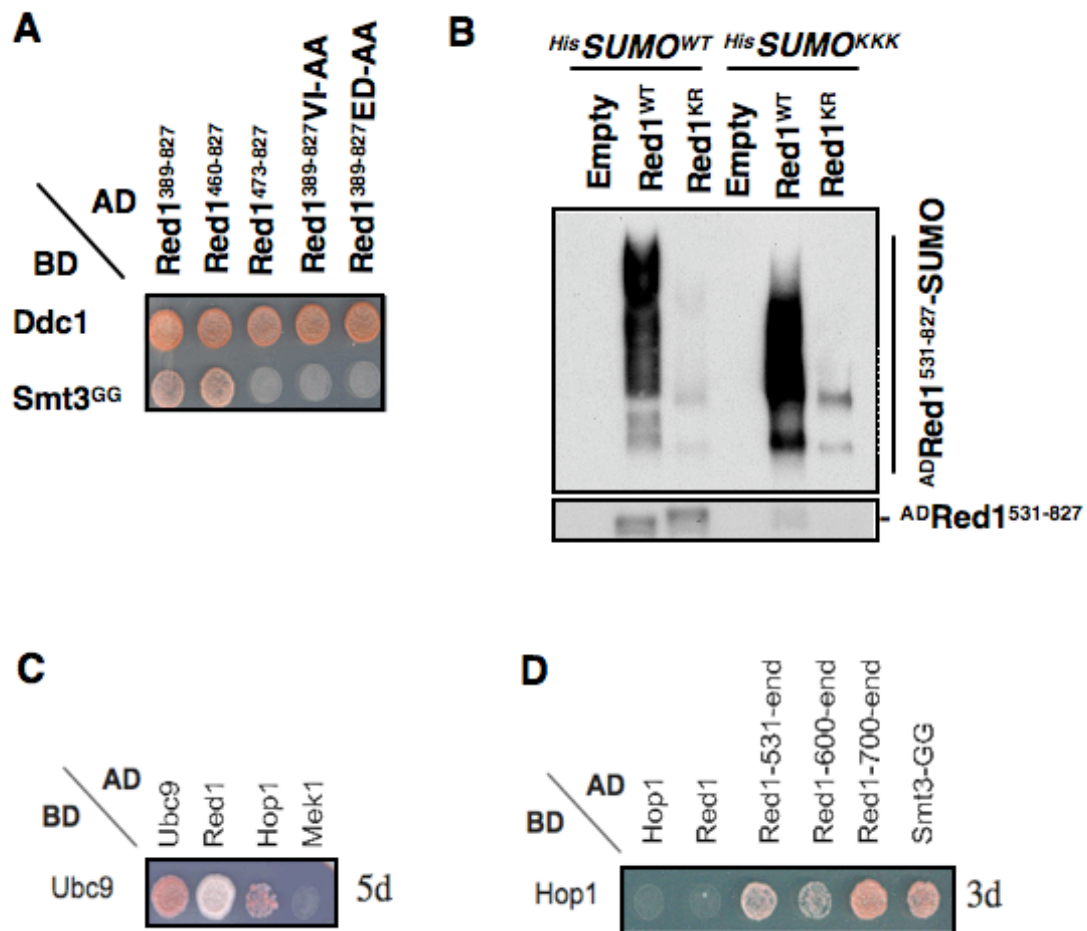


Figure 15: Lateral element Hop1 binds SUMO and the C-terminus of Red1. A: Red1 binds SUMO by a SUMO-interacting motif at aa 455-473. **B:** Red1 is a substrate for poly-SUMO chain formation. Ni-NTA pull-down experiments were done as in Fig. 10A using DF5 yeast extracts with integrated ^{His}SUMO (WT or KKK variant). ^{AD}Red1⁵³¹⁻⁸²⁷ was expressed under an *ADH1* promoter (lower panel: input levels). **C,** **D:** Hop1 interacts with SUMO, Ubc9 as well as a C-terminal fragment of Red1. For the two-hybrid assays (**A, C, D**) cells were transformed with respective AD- and BD-fusions and spotted on selective media and were grown for 3 days at 30°C.

III.3 Red1 binds 9-1-1 for pachytene checkpoint activation and normal SC formation

III.3.1 Domain mapping and identification of specific point mutants

Apart from its function in the pairing of homologous chromosomes and the formation of SCs, Red1 has been connected to the pachytene checkpoint. Previous work has shown that 9-1-1 stabilizes the association of the checkpoint kinase Mek1 with chromosomes and that 9-1-1 is required for Mek1-dependent phosphorylation of Red1 (Hong and Roeder, 2002). In addition, loading of functional 9-1-1 and the major checkpoint kinase Mec1 are essential for correct formation of SCs (Grushcow et al., 1999). To explore this connection further, we tested whether Red1 and 9-1-1 physically interact.

In fact, even though we could not detect significant interaction by immunoprecipitation experiments, we observed strong interaction of Red1 with 9-1-1 in two-hybrid assays (**Fig. 16A**). Surprisingly, we found that the C-terminal domain of Red1 (Red1⁵³¹⁻⁸²⁷) binds two subunits of the heterotrimeric complex, Mec3 and Ddc1 (**Fig. 16A**). Next, in order to define the exact binding domains within Red1, we cloned several Red1 fragments into AD vectors and tested the binding to BD-fusions of either Mec3 or Ddc1. Using a two-hybrid assay, we mapped the 9-1-1-binding sites to two distinct regions. Whereas Mec3 binds between residues 531-551 of Red1, Ddc1 binds between residues 729-751 of Red1 (**Fig. 16A**). Interestingly, this assay also revealed Red1 oligomerization involving Red1's C-terminal tail (residues 703-827; **Fig. 16A**), suggesting that the C-terminal region of Red1 is involved in most of the protein's functions. Thus, we can conclude that Red1 binds two subunits of the 9-1-1 complex and raises the possibility that Red1 exists in at least two conformations, a free as well as a 9-1-1-bound (perhaps bended) form (**Fig. 16A**).

was completely lost, but Ddc1 binding was unaltered (**Fig. 16C**). Conversely, changing Q⁷⁴⁰ and I⁷⁴³ (or I⁷⁴³ alone) to alanine abolished binding of Ddc1, but not of Mec3 (**Fig. 16D**). However, because Q⁷⁴⁰ was not required for Ddc1 interaction, and both 9-1-1-binding elements do not bind PCNA (**Fig. 16A**), the sites may be PIP-box related, but are evidently no *bona fide* PIP-boxes. Importantly, although Red1 dimerization involves a similar region, the Red1 mutant variant defective in Ddc1 binding (I⁷⁴³A) was still proficient in Red1-Red1 binding (**Fig. 16D**), demonstrating that this mutant is only defective in 9-1-1 interaction. Interestingly, the C-terminal region of Red1 (aa 735-795) including aa I⁷⁴³ in *S. cerevisiae* shares high homology with other yeasts (Lorenz et al., 2004).

III.3.2 Function of Red1 interaction with the 9-1-1 complex

To study the functional significance of the observed Red1 interaction with 9-1-1 during meiosis, we expressed the Red1 variants defective in either Mec3 binding (Q⁵³⁷A, V⁵⁴⁰A; termed Red1^{-Mec3}) or Ddc1 binding (I⁷⁴³A; termed Red1^{-Ddc1}) as the only source of Red1 from the diploid genome. First, we tested spore survival of cells having the mutated form of Red1 as the only source in the diploid genome. Surprisingly, we detected a very mild phenotype in *red1^{-Mec3}* strains while the *red1^{-Ddc1}* single or *red1^{-Mec3-Ddc1}* double mutant led to severely defective spores (**Fig. 17A**). These defects are in the range of the phenotypes observed in 9-1-1 deletions (**Fig. 17A**).

As a more specific assay and in order to test whether these *red1* mutants are still capable in 9-1-1-dependent pachytene checkpoint signalling, we additionally deleted the gene for the meiotic recombinase Dmc1. Cells deficient in Dmc1 accumulate resected DSBs and recombination intermediates, which normally (when wild-type Red1 is expressed) activate the pachytene checkpoint (Bishop et al., 1992; Sacher et al., 2006). When we assayed for checkpoint activation by monitoring histone H2A serine-129 phosphorylation (equivalent to mammalian γ -H2AX) and Rad52 SUMOylation (Sacher et al., 2006), we found no significant defect with mutants expressing the Red1 variant deficient in Mec3 binding (*red1^{-Mec3}*) (data not shown). By

contrast, *red1^{-Ddc1}* mutants completely fail to induce the pachytene checkpoint (**Fig. 17B**) reminiscent of 9-1-1-deficient mutants (Lydall et al., 1996), indicating that interaction of Red1 with the Ddc1 subunit of 9-1-1 is essential for this activity.

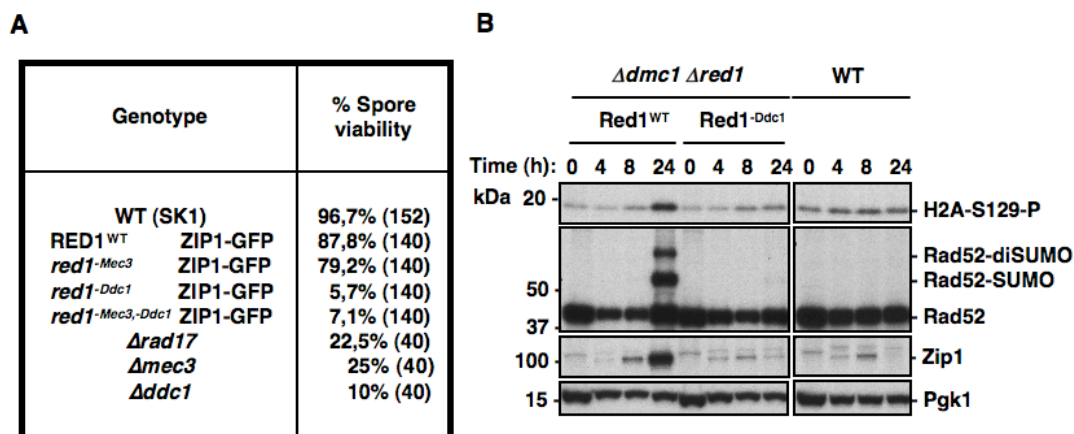


Figure 17: Red1 mutants deficient in Ddc1 binding show phenotypes in checkpoint activation. A: Spore viabilities of mutants. WT cells (SK1 strain) were compared with GFP-Zip1-expressing cells that express Red1 WT or 9-1-1 binding-deficient Red1 variants (*red1^{-Mec3}*, *red1^{-Ddc1}*, *red1^{-Mec3,-Ddc1}*). Also shown are spore viabilities of 9-1-1 mutants ($\Delta rad17$, $\Delta mec3$, $\Delta ddc1$). Strains were released into sporulation in 1,5% potassium acetate solution for 3 days before tetrad dissection, and spore viability was scored on YPD plates after 3 days. Indicated are the percentages of viable spores and the total number of spores counted (brackets). **B:** Ddc1-binding-deficient Red1 variant (Red1^{-Ddc1}) reverts pachytene checkpoint arrest of *dmc1* deletion strains. Extracts of synchronously sporulating cells were made at the indicated times and probed by Western analysis for Zip1, and Pgk1 expression, and in parallel for phosphorylated H2A (equivalent to mammalian γ H2AX) and Rad52 SUMOylation as measures for checkpoint activation.

Pachytene arrested cells also accumulate SCs and thus SC proteins like Zip1 because they do not progress further in the meiotic cell cycle (Roeder and Bailis, 2000). In $\Delta dmc1$ strains, Red1 expression is normally induced, but accumulates until at least 24 hours in sporulation media (**Fig. 17B**), while in wild-type cells, Red1 expression reaches a maximum at around 6 hours and is hardly detectable after 24 hours. The accumulation of Red1 probably reflects the arrested state due to an active pachytene checkpoint and is observed in a number of other background strains arresting at certain points during early meiosis I (**Fig. 21**). We further observed that Zip1 is similarly expressed like Red1 in $\Delta dmc1$ strains. The accumulation of both Red1 and Zip1 in a $\Delta dmc1$ background was abolished when we integrated the *red1^{-Ddc1}* mutant as the

only source of Red1 into $\Delta dmc1 \Delta red1$ strains (**Fig. 17B** and data not shown). $\Delta dmc1$ strains with Red1 mutated in the Mec3 binding domain show no severe defects in all phenotypes tested, except a very mild defects in spore viability and a slightly delayed onset of Rad52 SUMOylation (data not shown). Altogether, these phenotypes argue for a crucial role of the Red1-Ddc1 interaction in pachytene checkpoint signalling.

Because the $red1^{-Ddc1}$ mutation has a very strong effect on spore viability (Figure 17A) and since Red1 is a structural component of the SC, we speculated that the mutant might also show deficiencies in SC formation. Indeed, when we assayed for SC formation utilizing GFP-tagged Zip1, we noticed a moderate defect in $red1^{-Mec3}$ mutants, but a virtually complete loss of normal SCs in $red1^{-Ddc1}$ mutants and $red1$ mutants defective in interaction with both 9-1-1 subunits ($red1^{-Mec3,-Ddc1}$) (**Fig. 18A**). Interestingly, although pre-assemblies of SCs were detectable, fully formed SCs were not formed if Red1 fails to bind 9-1-1 (Ddc1). Notably, the degree of SC formation defects of these $red1$ mutants was mirrored by their deficiencies in spore viability (**Fig. 17A**). The expression profile of Red1^{-Ddc1} during the meiotic time-course still shows a similar induction and decrease as in wild-type cells (**Fig. 18B**). The slightly reduced overall expression of mutated Red1^{-Ddc1} protein results from the inability to form mature SCs, but is not the reason for the observed phenotype in SC formation as cell with several Red1^{-Ddc1} integrations and therefore higher expression levels still show the very same defect in both pachytene checkpoint activation and SC maturation (data not shown). In contrast, $red1^{-Mec3}$ mutants (and the $red1^{-Mec3,-Ddc1}$ mutant) do show changes in the profile which can however not be connected to significant phenotypes in spore viability or SC formation assays (**Fig. 17A; 18A,B**). It is interesting to speculate that the unique profile of Red1 expression is triggered by its binding to the Mec3 subunit of 9-1-1. Moreover, Red1 expression seems to have direct influence on the levels of the central element protein Zip1 suggesting that Zip1 is stabilized by its interaction with Red1 (**Fig. 18B**).

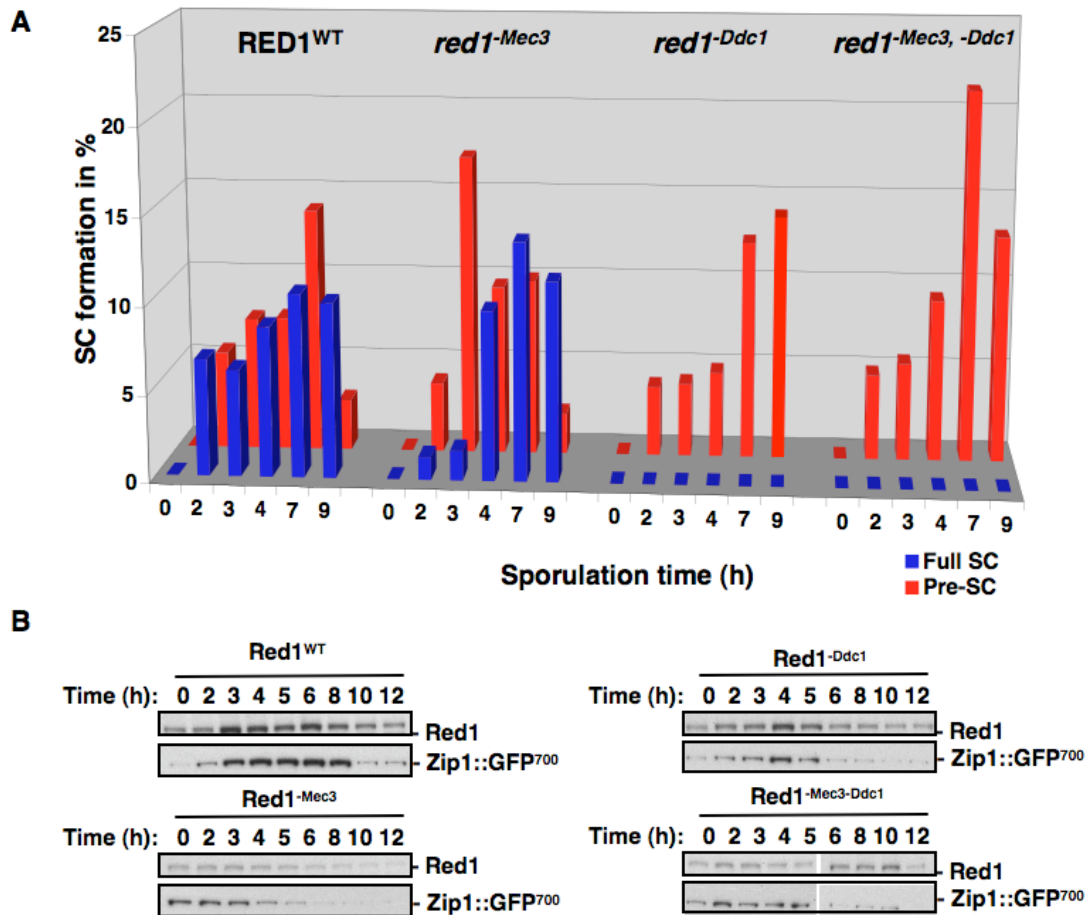


Figure 18: Red1 mutants deficient in 9-1-1 binding show phenotypes in SC formation. A: SC formation in WT and *red1* mutants (9-1-1-binding mutants). SCs were visualized using GFP-tagged Zip1 and spinning disk microscopy as in Fig. 14C. Maturation of SCs was categorized in the indicated classes (early stage, diffuse, dot-like, pre-SCs and full SCs). In the quantified assay only pre-SCs and full SCs were distinguished. Cells were released into synchronous sporulation and samples observed after the indicated times. For each time-point more than 100 cells were analyzed. **B:** Red1 expression levels (from the identical experiment as in A).

III.4 Regulation of Red1 SUMOylation and expression

III.4.1 Regulation of Red1 SUMOylation

We next wanted to know how Red1 SUMOylation is regulated, thereby also addressing the question which factors influence the timing of SC initiation. For this, we integrated ^{His}SUMO under an *ADH1* promoter in the *URA3* locus in different background strains. Equal ^{His}SUMO expression levels in each strain were confirmed by Western blot analysis. To monitor Red1 SUMOylation, Ni-NTA pull-downs were carried out and the samples analyzed by Western blot using an anti-Red1 antibody.

Considering our finding that Red1 SUMOylation is involved in the initiation of SC formation, we first tested the influence of the SUMO E3 ligase Zip3, which is known to associate with sites where SC formation initiates (Agarwal and Roeder, 2000). In support of the model that SUMO-modification of Red1 secures timely SC assembly we found that Zip3 is indeed responsible for the bulk of Red1 SUMOylation *in vivo* (**Fig. 19A**). Moreover, Zip3 binds the SC protein Zip1 (Agarwal and Roeder, 2000) and also associates with the heterotrimeric MRX (Mre11-Red50-Xrs2) complex (Agarwal and Roeder, 2000) involved in meiotic recombination. Together with the finding that Zip3 auto-SUMOylation seems to depend on the Spo11 nuclease (Cheng et al., 2006), which catalyzes meiotic DSBs (Keeney et. al., 1997), Zip3 activity and therefore Red1 SUMOylation might be closely linked to the induction, processing and monitoring of DSB. In line with this notion is the finding, that Red1 SUMOylation seems to be reduced in *spo11* deletion strains (**Fig. 19A**). Interfering with later factors in the meiotic recombination pathway by deleting the recombinase Dmc1, does however not show significant effects on Red1 SUMOylation as compared to wild-type cells until 8 hours in sporulation media (**Fig. 19B**).

Given the strong interaction between Red1 and two subunits of the 9-1-1 checkpoint complex, we decided to take a closer look at the dependency of Red1 SUMOylation on 9-1-1. In detail, we asked whether the pachytene checkpoint in general and more specifically the Red1—9-1-1 interaction (by

using Red1 alleles deficient in Mec3 or Ddc1 interaction) directly regulates Red1 SUMOylation.

The deletion of the 9-1-1 subunits Rad17, Mec3 or Ddc1 did not show reproducible effects on Red1 SUMOylation and expression (data not shown). The reduction of SUMO-modified species in some experiments was most likely due to reduced Red1 expression rather than a specific effect on the Red1 SUMOylation efficiency. Moreover, the additional deletion of Rad17 in *Δdmc1* strains did not significantly reduce the levels of SUMO-modified Red1 (data not shown), again suggesting that the 9-1-1 complex is not an essential prerequisite for Red1 SUMOylation.

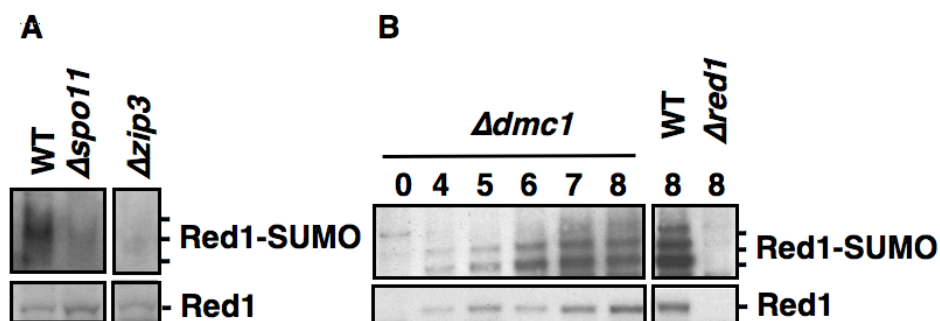


Figure 19: Red1 SUMOylation in different checkpoint mutant backgrounds. **A:** Endogenous Red1 SUMOylation is regulated by Spo11 and depends on the E3 SUMO ligase Zip3. Homozygous SK1 diploid strains with the indicated gene deleted were released into synchronous sporulation. Red1 SUMO-conjugates of cells extracts harvested at the indicated times were isolated by Ni-NTA pull-down and detected by western blotting using anti-Red1 antibodies (lower panel: Red1 input levels). **B:** Red1 SUMOylation is not significantly influenced in a *dmc1* deletion strain as compared to WT. Ni-NTA pull-down experiments were done as in A.

However, we expected a clearer answer on the connection between the 9-1-1-dependent checkpoint and Red1 SUMOylation using Red1 alleles deficient in 9-1-1 binding. In order to approach the question whether the direct interaction of Red1 with Mec3 or Ddc1 would directly influence the SUMOylation of Red1, we expressed the respective Red1 mutants (as well as the double mutant) under the endogenous *RED1* promoter in *Δred1* strain and additionally integrated ^{His}SUMO under an *ADH1* promoter. Using Ni-NTA pull-down assays, we captured SUMO-modified Red1 in these cells and found that *red1*^{-Mec3-Ddc1} mutants (as well as single mutants) did not show significant

changes in the SUMOylation status (**Fig. 20**). This finding suggests that while 9-1-1 might be necessary for inducing Red1 expression, the direct interaction of Red1 with 9-1-1 does not directly influence the SUMOylation (and therefore SC initiation) but rather pachytene checkpoint signalling (and therefore SC formation in general).

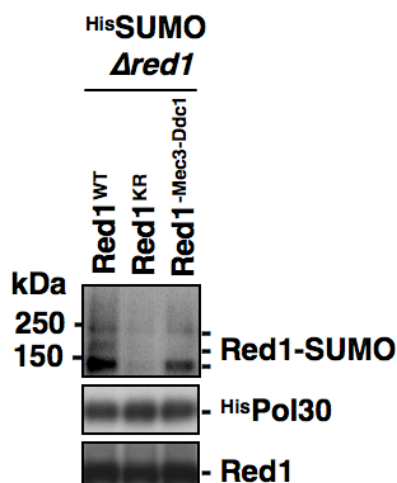


Figure 20: SUMOylation of a Red1 variant deficient in 9-1-1 binding. 9-1-1 binding to Red1 has no significant influence on Red1 SUMOylation. Diploid homozygous SK1 $\Delta red1$ deletion strains with integrated genes encoding ^{His}SUMO (expression by *ADH1* promoter) and a Red1 variant deficient in 9-1-1 binding (Red1^{-Mec3,-Ddc1}) were released into synchronous sporulation. SUMO-conjugates were isolated by Ni-NTA pull-down after 8 hours and detected by Western blotting using an anti-Red1 antibody. Samples from separate ^{His}Pol30-expressing cultures were added to control for pull-down efficiency. The SUMOylation-deficient Red1^{KR} variant was used as a negative control (lower panel: Red1 input levels).

9-1-1-dependent checkpoint activation is directly connected to the action of the Mec1 kinase, which, among other substrates, phosphorylates histone 2A on serine 129 (the mammalian γ -H2AX) as a hallmark of an activated checkpoint. 9-1-1 and Mec1 are recruited independently to DNA damage sites, but tightly work together to trigger a robust checkpoint answer. Namely, Mec1 directly phosphorylates the 9-1-1 subunits Mec3 and Ddc1 and is itself only fully activated in the presence of the trimeric complex (Majka et al., 2006b). Interestingly, it has been shown recently, that the axial element protein Hop1 is phosphorylated by Mec1 at several specific consensus sites thereby ensuring interhomolog recombination (Carballo et al., 2008). Given

these data and the fact that Red1 tightly binds two 9-1-1 subunits, we speculated whether Red1 is also a substrate for Mec1 kinase. Indeed, sequence analysis revealed exactly one consensus site within Red1, which interestingly lies in direct proximity to the K-rich region and close to the Mec3 interaction domain. Towards a function for this potential phosphorylation site, we directly generated mutants that would either prevent or mimic Red1 phosphorylation at serine 597 (*red1^{S597A}*, *red1^{S597D}*). Although both mutants did not show any effects on spore viability of these strains, the phospho-mimicking mutant showed an increase in its SUMO-modification (data not shown). This finding suggests a model, in which checkpoint signalling via Mec1 leads to increased Red1 SUMOylation within the K-rich region by either stimulating its modification through the recruitment of Ubc9 and Zip3 or by preventing Ulp2-mediated SUMO de-conjugation.

III.4.2 Regulation of Red1 expression

Using an anti-Red1 peptide antibody developed in this study, Red1 expression levels could be visualized during meiotic time-course in different deletion strains. In a SK1 WT strain, Red1 is expressed rapidly after induction of sporulation, peaking after 5 hours and then declining to very low expression levels after 10 hours. In contrast, Red1 is still fully expressed and accumulates until 24 hours after induction of sporulation in strains where the pachytene checkpoint is constitutively active (e.g. in *Δdmc1* strains) or where meiotic progression is delayed by blocking either the APC/C complex (*Δmnd2* strains) or the expression of mid- to late-sporulation genes (*Δndt80* strains). In a simplified view, one can sort the mutants into two groups (**Fig. 21**): strains in which Red1's expression profile is similar to wild-type and strains in which Red1 protein expression levels accumulate due to a meiotic arrest. These data give a hint how the specific expression profile of Red1 is maintained and which factors are potentially involved in its degradation (e.g. APC/C complex). In addition, Red1 expression serves as a tool to test for meiotic progression in different deletion background strains.

Strain background (diploid)	Function of the deleted gene
Red1 expression similar to wild-type	
$\Delta spo11$	Initiates meiotic recombination by induction of DSBs
$\Delta dmc1 \Delta rad17$	Dmc1 is a meiosis-specific Rad51 homologue essential for pairing of homologue chromosomes Rad17 is a subunit of the 9-1-1 checkpoint complex
$\Delta rad50$	Subunit of the MRX complex involved in processing DSBs
$\Delta spo13$	Meiosis-specific protein involved in maintaining sister chromatid cohesion during meiosis I and promoting proper attachment of kinetochores to spindle during meiosis I and II
$\Delta sgs1$	Nucleolar RecQ DNA helicase involved in maintenance of genome integrity, regulation of chromosome synapsis and meiotic crossing over
$\Delta pch2$	Nucleolar component of the pachytene checkpoint
Red1 accumulation during meiotic time-course	
$\Delta dmc1$	Meiosis-specific Rad51 homologue essential for pairing of homologue chromosomes
$\Delta sae2$	Accurate meiotic and mitotic DSB repair, exonuclease activity
$\Delta zip1$	Transverse filament protein of the synaptonemal complex
$\Delta ndt80$	Meiosis-specific transcription factor required for exit from pachytene and full meiotic recombination, activates mid- sporulation genes
$\Delta hop2$	Meiosis-specific protein that prevents synapsis between nonhomologous chromosomes, in complex with Mnd1
$\Delta mnd1$	In complex with Hop2
$\Delta mnd2$	Subunit of the anaphase-promoting complex (APC), needed for meiotic nuclear division

Figure 21: Red1 expression profile as a marker for meiotic progression. Shown is a table of SK1 deletions which either result in wild-type Red1 expression profiles (upper part) or in an accumulation of Red1 until 24 hours after induction of synchronous sporulation. The function of the deleted gene is described in the right column.

III.5 SUMOylation of the 9-1-1 complex

III.5.1 Each 9-1-1 subunit is modified with SUMO

Given the fact that the homotrimeric complex PCNA is subject to different types of modifications (**Fig. 3**), we speculated that also functions of the 9-1-1 checkpoint complex might be regulated by SUMO and ubiquitin. Following a protocol for isolating SUMO-modified species, we found that each subunit of the 9-1-1 complex is modified by several SUMO moieties (**Fig. 22A** and data not shown). Interestingly, the modification specifically occurred upon DNA damage (**Fig. 22A**). In order to rule out the possibility that the modifications are artificial and arise from SUMO overexpression, yeast strains expressing His⁶SUMO under the endogenous *SUMO* (*SMT3*) promoter were constructed and Ni-NTA pull-down assays carried out. The 9-1-1 subunits Rad17, Mec3 and Ddc1, were fused to protein A at the endogenous locus and could therefore be detected by Western blot analysis using antibodies against the tag. Compared to systems in which the His-tagged version is expressed in much higher levels under an *ADH1* promoter, SUMOylation of each subunit was detectable in similar amounts.

By using His-tagged ubiquitin in a similar approach, polyubiquitylated forms of Rad17 and Mec3 (Ddc1 has not been tested) were detected (data not shown). To reveal the role of 9-1-1 ubiquitylation, the exact conditions under which this modification occurs as well as the chain linkages remain to be examined. This will reveal whether ubiquitylation signals proteasome-dependent degradation, or plays other yet unknown roles. As a very recent study reports that the 9-1-1 subunit Rad17 is mono-ubiquitinated after DNA damage (Fu et al., 2008), the signal in the TCA preparations has to be taken with care. Although we could not detect a specific induction of mono-ubiquitinated 9-1-1 upon DNA damage, it is possible that the signals for ubiquitin and SUMO are overlapping.

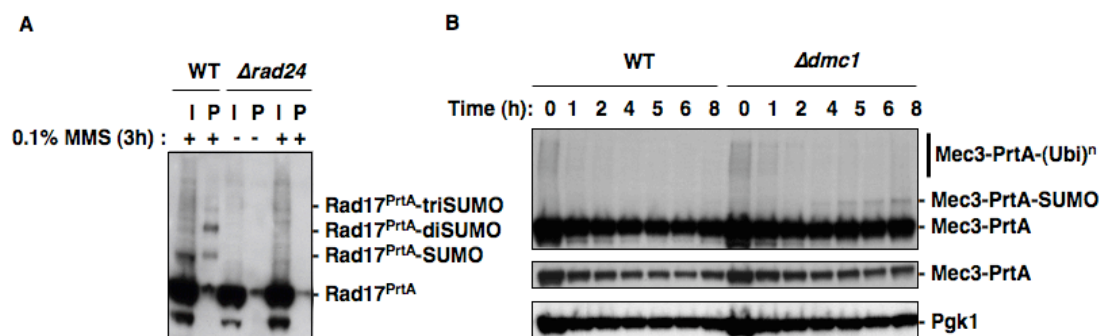


Figure 22: SUMOylation of each 9-1-1 subunit is induced in the presence of damaged DNA. **A:** Rad17 is modified with SUMO upon DNA damage. ^{His}SUMO pull-downs are carried out in the presence and absence of the DNA alkylating agent MMS (methyl-methane sulfonate) in WT and $\Delta rad24$ cells. **B:** Mec3 modification in pachytene-arrested $\Delta dmc1$ cells. “I” indicates the input, “P” presents Ni-NTA pull-down samples.

In order to identify SUMO acceptor sites within each 9-1-1 subunit, we carried out site-directed mutagenesis. Replacement of any single lysine to arginine (as well as several combinations) within the 9-1-1 subunit Mec3 and subsequent ^{His}SUMO pull-down did not show reduced SUMO modification, thus indicating that the SUMO conjugation can occur on several lysines redundantly. As an internal control for the pull-down experiments, separate yeast cultures expressing ^{His}PCNA were added to the cultures before harvesting and pull-down analysis. In order to find the acceptor lysines within each subunit of the 9-1-1-complex, biochemical approaches to purify SUMO-modified 9-1-1 subunits *in vivo* from yeast were established. In a one-step purification approach using IgG beads for capturing protein A-tagged 9-1-1, SUMOylated species were clearly visible after Western blotting. Therefore, samples from coomassie gels were analyzed by mass spectrometry in order to identify the SUMO acceptor lysines (collaboration with the laboratory of Prof. Matthias Mann, MPI of Biochemistry). Due to low expression levels of 9-1-1 in yeast and the fact that the complex is only transiently conjugated with SUMO, sufficient amounts of the modified form could not be obtained so far.

III.5.2 Regulation of 9-1-1 SUMOylation

As mentioned before, 9-1-1 SUMOylation was only visible after treating cells with DNA damage inducing agents (**Fig. 22A**) like ionizing radiation (UV), 4-nitroquinoline N-oxide (4NQO) or methylmethanesulphonate (MMS). Interestingly 9-1-1-modified species also occur during meiosis when the pachytene checkpoint is activated in a *Δdmc1* strain, where unresolved recombination structures accumulate (**Fig. 22B**) but is absent in a *Δdmc1 Δspo11* strain, which is unable to induce DSBs and thus meiotic recombination (data not shown). 9-1-1 SUMOylation further depends on the clamp-loader Rad24 as well as on the SUMO E2 conjugating enzyme Ubc9. Interestingly, however, it apparently does not depend on the three so far known E3 ligases Siz1, Siz2 and Mms21 in mitotic cells.

SUMOylation of each subunit was strictly dependent on DNA damage caused by e.g. methylmethanesulphonate (MMS) upon which the amounts of modified protein peaked around 3 hours after treatment. This is rather late compared to PCNA modifications, which either means that the modification marks a later function in the DNA damage response (e.g. in the unloading of the complex) or that extra time elapses for full expression of the modification (e.g. because the 9-1-1 complex binds to chromatin late after MMS treatment). Interestingly, increasing amounts of 4NQO do not seem to trigger earlier onsets of the SUMO modification, but led to a reduced SUMOylation pattern, which would suggest a role e.g. in inactivating the checkpoint response.

In order to enrich chromatin-associated 9-1-1, we carried out chromatin-binding assays and detected modified Rad17 species in concentrated chromatin fractions. As expected, we found that the clamp-loader Rad24 is strictly required for loading 9-1-1 on damaged DNA. Interestingly, however, virtually absent 9-1-1 SUMOylation in a *ubc9-1ts* allele did not disturb the loading process, but seems to result in a prolonged association of Rad17 on chromatin (**Fig. 23**).

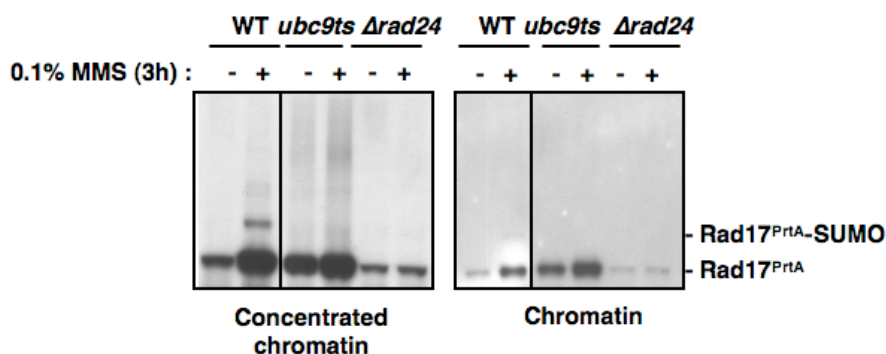


Figure 23: Rad17 SUMOylation is enriched in the chromatin fraction. Chromatin fractions were isolated from Protein A-tagged Rad17^{PrtA}-expressing WT, *ubc9ts* or $\Delta rad24$ cells. Logarithmically growing cultures were treated with or without 0,1% MMS for 3 hours and harvested. Concentrated chromatin reflects a pool of chromatin samples combined during TCA preparation.

III.5.3 Towards a function for the SUMOylation of 9-1-1

As we found SUMO-modified 9-1-1 enriched on chromatin and given the fact that loading of the complex is essential (but not sufficient) for the modification, 9-1-1 SUMOylation apparently plays a role after loading of the clamp. The strict dependency of 9-1-1 SUMOylation on DNA damage treatment further argues for modification of those 9-1-1 molecules that are recruited to damage sites. In analogy to PCNA, a more specific role of SUMO-modified 9-1-1 could be to stimulate or inhibit the recruitment of binding partners. PCNA recruits the helicase Srs2 (which contains a SIM) via its SUMO modification at lysine K164 and inhibits the association of the PIP-containing protein Eco1 by its SUMOylation at lysine K127. Indeed, 9-1-1 serves as a recruitment platform for a number of DNA repair and checkpoint proteins and one can assume that these have to be distinguished and regulated by different 9-1-1 modification states.

There is accumulating evidence in the literature that 9-1-1 plays an important role in the base excision repair pathway (BER; Boiteux and Guillet, 2004; Helt et al., 2005). SUMO modification of 9-1-1 might therefore stimulate or inhibit components of the BER pathway like the *S. pombe* MutY homolog (MUH), human polymerase beta (Pol beta), flap endonuclease (FEN1) or DNA ligase I. Structural data from the archaea *Sulfolobus* are very interesting in

that respect as this thermophilic organism possesses a heterotrimeric PCNA (PCNA1, 2 and 3), which binds different components of the BER pathway, namely Fen1, DNA polymerase and DNA ligase I (Dionne et al., 2003). From an evolutionary point of view, it is very likely that both PCNA and 9-1-1 have evolved from such a clamp. It is thus tempting to speculate that also each of the three 9-1-1 subunits of *S. cerevisiae* binds a specific BER member. So far, it has been shown that Fen1 binds 9-1-1, specificities for single subunits (and their modification states) have however not been addressed so far.

In summary, PCNA and 9-1-1 are loaded differently on 3`-DNA junctions to carry out DNA replication or 5`-DNA junctions, which are specific marks of DNA damages, respectively. The DNA nicks and damages are therefore critical for the clamp that is recruited and thus for the subsequent cellular response. After loading, each of the clamps is probably modified for selective recruitment of the appropriate set of proteins to the platform.

III.6 Psy2 links the SC to pachytene checkpoint exit

Several observations point towards a very close connection between the pachytene checkpoint and the formation of SCs. Earlier in this thesis, we could show an interaction between the axial element protein Red1 and two subunits of the 9-1-1 complex and found that this association directly influences pachytene checkpoint activation and SC formation. In addition, other studies showed more indirectly that SCs are defective in strains deleted for the clamp-loader subunit Rad24 and the 9-1-1 subunit Rad17 as well as in *mec1-1* alleles (Grushcow et al., 1999). Moreover, phosphorylation of the axial element protein Hop1 by the checkpoint kinase Mec1 at specific consensus sites is necessary for correct SC maturation (Carballo et al., 2008). Red1 is also phosphorylated in dependency of 9-1-1 and the meiosis-specific protein Mek1 (Hong and Roeder, 2002). Its de-phosphorylation is supposed to be critical for pachytene checkpoint exit and Glc7 has been discussed to be the respective phosphatase (Bailis and Roeder, 2000). Moreover, several reports discuss the presence of (at least) two genetically separable checkpoints during pachytene (**Fig. 9**), one triggered by the presence of DNA damage or recombination intermediates, another one depending on the integrity of SCs. Given these results, we can assume that structural assembly of SCs as well as DNA and chromatin metabolism are highly connected by processes of largely unknown molecular mechanisms.

III.6.1 Interaction between Zip1 and Psy2

Zip1 has two major functions during meiosis. It acts as the major transverse filament protein of the SC and also monitors meiotic recombination within the *zip1* checkpoint. However, the mechanism of how Zip1 mediates checkpoint recovery during yeast meiosis is still unclear. Recently, a physical interaction between Zip1 and the protein Psy2 was reported in the context of a large-scale two-hybrid analysis in *S. cerevisiae* (Ito et al., 2001). Psy2 (platinum sensitivity 2) was identified in a screen for genes conferring resistance to the DNA damage-inducing anticancer drug cisplatin (Wu et al., 2004). Moreover, it

is a regulatory component of a phosphatase complex required for dephosphorylation of Mec1 consensus sites in histone H2A (phosphorylated at serine 129) and Rad53, thereby playing a role in replication fork restart and DNA damage checkpoint recovery (Keogh et al., 2006; O'Neill et al., 2007). We speculated that perhaps SC establishment and checkpoint recovery are directly linked and thus we wanted to confirm the possible interaction between Zip1 and Psy2 and identify domains within these two proteins that mediate the binding.

Proteins that form transverse filaments along chromosomes and built up the proteinaceous structure of SC have been identified in several species. As a common feature, these proteins contain an extended coiled-coil domain located in the central region of the respective protein and flanked by large globular domains (Page and Hawley, 2004). The predicted secondary structure of the 875 aa protein Zip1 contains two central α -helical coiled-coil domains flanked by two terminal globular domains. As mentioned before, the C-terminal region of Zip1 is orientated towards the lateral elements and contains a SIM, which mediates its interaction with SUMOylated substrates, while the N-terminal non-helical domain faces towards the center of the SC (**Fig. 5 and 24C**).

In order to map Zip1 regions that mediate Psy2 binding, we tested the interaction of fragments of Zip1 with full-length Psy2 in yeast two-hybrid assays (**Fig. 24**). We observed a very strong physical binding between the full-length versions of Zip1 and Psy2 as well as dimerization of full-length Zip1 proteins. Truncations of Zip1 lacking the N-terminus were not capable of binding Psy2, indicating an important role of the N-terminal part of the protein. To further characterize the Psy2-interacting region of Zip1, fragments containing the N-terminal domain of Zip1 were expressed as N-terminal AD-fusions and revealed the necessity of an extended segment of Zip1 comprising the N-terminal globular domain as well as the first coiled-coil domain for proper Psy2 binding. In addition, we tested the dimerization of Zip1 truncations by expressing identical fragments as AD- and BD-fusion proteins and made the intriguing observation that both, Psy2 binding and Zip1

dimerization occur exclusively with full-length Zip1 and Zip1¹⁻⁴⁵¹. This observation suggests a direct correlation between Zip1 dimerization and its capability to bind Psy2.

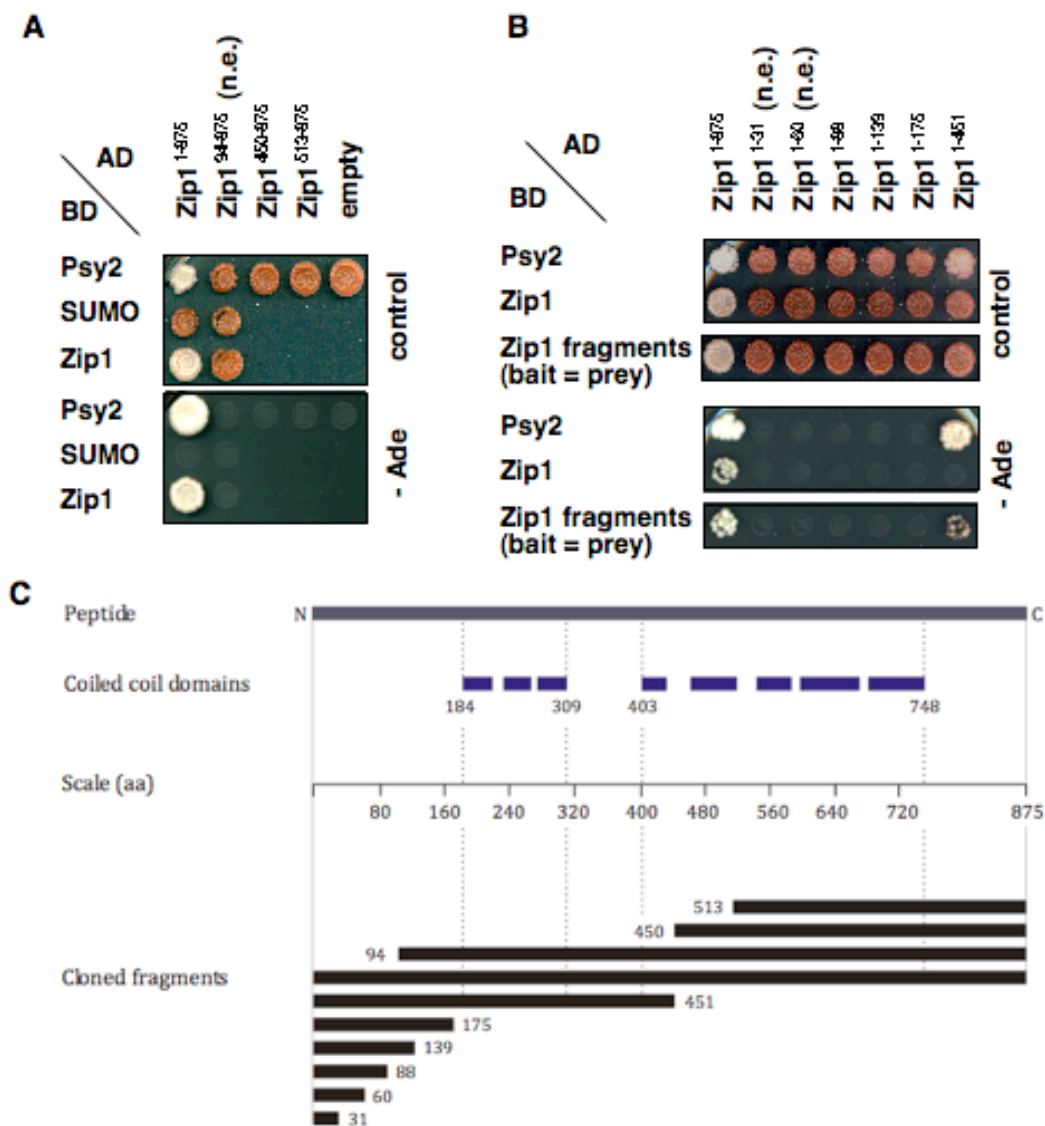


Figure 24: Psy2 binding requires the N-terminal domain of Zip1 and an extended N-terminal coiled-coil region. Yeast two-hybrid assay showing the interaction between Zip1 and Psy2. **A:** Zip1 fragments lacking the N-terminal domain were not capable of interacting with Psy2. **B:** Mapping of the Psy2-binding region of Zip1, using truncations containing the N-terminus. Dimerization and Psy2 binding was observed for full-length Zip1 and Zip1¹⁻⁴⁵¹. Expression of AD-fusion proteins as indicated above was tested by immunoblotting, using anti-AD antibodies (data not shown). **C:** Schematic representation of the predicted secondary structure of Zip1 (Figure by Florian Paasch). The protein contains two extended coiled-coil domains ranging from aa 184-309 and aa 403-748. The coiled-coil regions are flanked by largely globular domains. A set of C- and N-terminal Zip1 truncations were cloned into pGAD-C1 and pGBD-C1 to generate N-terminal AD and BD fusions for yeast two-hybrid experiments. “n.e.” indicates fusion proteins that are not expressed (as tested by Western blot analysis).

Therefore, we generated a $\Delta psy2$ strain, induced synchronous sporulation and assayed for several meiotic phenotypes. First evidence that Psy2 is necessary for faithful spore production was obtained from tetrad analysis. Besides $\Delta psy2$, WT and $\Delta zip1$ cells were tested as controls. Consistent with previous results (i.e. Mitra and Roeder, 2007), the $\Delta zip1$ mutant showed severely reduced spore viability compared to wild-type cells. Interestingly, the viability of $\Delta psy2$ spores was also significantly lower than wild-type spores, clearly demonstrating that Psy2 is essential for faithful spore production and plays an important role during meiosis (**Fig. 26A**).

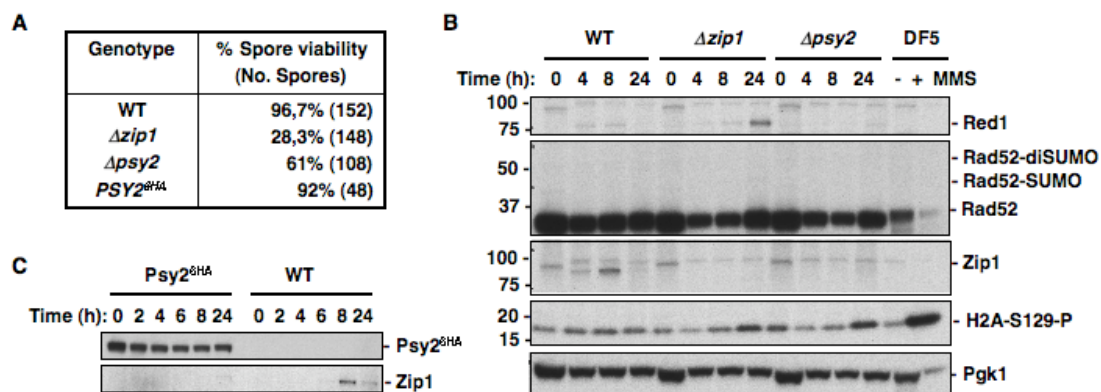


Figure 26: Psy2 plays a crucial role during meiosis. **A:** Spore viabilities of SK1 WT, $\Delta zip1$, $\Delta psy2$ and $PSY2^{6HA}$ strains. **B:** Analysis of meiotic markers in WT, $\Delta zip1$ and $\Delta psy2$ cells. Wild-type cells showed typical expression profiles of the meiosis-specific proteins Red1 and Zip1. Protein levels peaked with the establishment and stabilization of SC and declined with the disassembly of SC after meiotic recombination is completed. Rad52 SUMOylation was not induced in wild-type cells and H2A phosphorylation was observed at approximately constant levels during meiosis. Mutants deficient in Zip1 arrested in pachytene with the accumulation of Red1 and phosphorylated H2A. As $\Delta zip1$ cells do not accumulate hyperresected DSBs during meiotic recombination, Rad52 SUMOylation was not induced. Results obtained from the $\Delta psy2$ strain indicate that mutants deficient in the phosphatase subunit Psy2 delay in pachytene with accumulated Red1 and phosphorylated H2A. Notably, Zip1 protein levels were significantly reduced in $\Delta psy2$ cells. “P” indicates phosphorylation. DF5 cells treated with the DNA alkylating agent methyl-methanesulfonate (MMS) were used as a control for H2A phosphorylation. Pgk1 (3-phosphoglycerate kinase) was used as loading control. **C:** Psy2 is constantly expressed during meiosis. Psy2 and Zip1 expression during meiosis was monitored by immunoblotting in a strain carrying a 6HA-tagged version of Psy2. For the detection of 6HA-tagged Psy2, anti-HA antibodies were used. Protein samples from an isogenic strain lacking the 6HA-epitope were used as control.

Next, in order to gain more detailed insights into Psy2 functions, we specifically addressed the question whether Psy2 has an influence on the meiotic checkpoint system. As described earlier in this study, we monitored several meiotic markers in wild type, $\Delta zip1$ and $\Delta psy2$ cells by Western blot analysis (**Fig. 26B**): a) Red1/Zip1 expression as markers for meiotic progression, b) Rad52 SUMOylation indicating ongoing recombination and c) Mec1-dependent histone H2A serine 129 phosphorylation (equivalent to the mammalian γ -H2AX) showing the activity of this major checkpoint kinase (homolog to mammalian ATR).

a) First, the major lateral and central SC elements, Red1 and Zip1, show meiosis-specific expression profiles in wild-type cells, with protein levels peaking within a time range of four to eight hours after triggering synchronous sporulation. Their expression profiles correlate with SC assembly in meiotic zygotene and the disassembly in diplotene after meiotic recombination is completed. As mentioned above (**Fig. 21**), Red1 expression accumulates in strains that arrest at certain stages during meiosis, e.g. by inducing the pachytene checkpoint. In $\Delta zip1$ cells, Red1 accumulates in the course of meiosis, suggesting the persistence of axial elements as a result of defective SC assembly and/or incomplete recombination. This is consistent with the finding that chromosome synapsis does not occur in $\Delta zip1$ mutants and cells arrest in pachytene with incomplete recombination (Sym et al., 1993). Interestingly, the $\Delta psy2$ mutant exhibited significantly reduced Zip1 protein levels and Red1 protein levels accumulating over the meiotic time-course. In particular, the accumulation of Red1 shows similarity to $\Delta zip1$ cells indicating a delay of $\Delta psy2$ cells in pachytene.

b) Second, Rad52 SUMOylation was probed as a marker for ongoing recombination. Rad52 is a recombination factor of the Rad52 epistasis group (*RAD50*, *RAD51*, *RAD52*, *RAD54*, *RDH54*, *RAD55*, *RAD57*, *RAD59*, *MRE11*, *XRS2*) and was shown to be involved in all types of homologous recombination in *S. cerevisiae*. A former study identified Rad52 as SUMO substrate in *S. cerevisiae* and mammals and reported the induction of Rad52 SUMOylation by DNA DSBs, principally when recognized by the MRX

complex (Sacher et al., 2006). Notably, Rad52 SUMOylation is strongly induced in *S. cerevisiae* mutants deficient in the RecA-like strand invasion factors Dmc1 and Rad51. These mutants were previously shown to arrest in meiotic pachytene in the presence of accumulated hyperresected DSBs (Bishop et al., 1992). Consistent with previous findings, Rad52 SUMOylation was not induced in $\Delta zip1$ mutants (Sacher et al., 2006) that arrest in pachytene without the accumulation of hyperresected DSBs. Probed for Rad52, cells deficient in Psy2 did not show significant levels of Rad52 SUMOylation during meiosis. This finding provides evidence that Psy2 deficiency does not lead to the accumulation of hyperresected recombination intermediates during meiosis.

c) Phosphorylation of the budding yeast histone H2A at Ser129 by the checkpoint kinases Mec1 and Tel1 is one of the earliest marks of DNA DSBs (Downs et al., 2000). As Psy2 is a component of the three protein HTP-C phosphatase complex (histone H2A phosphatase complex; contains the phosphatase Pph3 and the regulatory subunits Psy2 and Psy4) that was reported to dephosphorylate H2A at Ser129 during recovery from DNA damage checkpoint (Keogh et al., 2006), we asked whether Psy2 is also involved in the dephosphorylation of H2A during recovery from pachytene checkpoint. Interestingly, although cells deficient in Zip1 arrest in the absence of accumulated hyperresected DSBs, an accumulation of phosphorylated H2A was observed after triggering synchronous sporulation in this strain. In contrast, wild-type cells showed approximately constant levels of phospho-H2A during the entire meiotic time-course. If Psy2 functions as a component of the HTP-C phosphatase complex and regulates H2A phosphorylation also during meiosis, phosphorylated H2A should accumulate in a corresponding deletion strain in the course of meiotic recombination. In fact, Psy2 deficiency led to an accumulation of phosphorylated H2A during sporulation, indicating a role for Psy2 in H2A dephosphorylation and checkpoint recovery during yeast meiosis.

As many meiosis-specific proteins like Red1 and Zip1 show specific profiles during synchronous sporulation, we wanted to test whether this also holds true for Psy2. Therefore, we generated an SK1-derived strain with a Psy2^{6HA} fusion protein expressed at endogenous levels by the *PSY2* promoter (**Fig. 26C**). After inducing synchronous sporulation, cells were harvested after different time-points. Subsequent Western blot analysis demonstrated that Psy2 is constantly expressed during meiosis without any meiosis-specific fluctuations. Notably, the expression levels of Zip1 peaked in the wild-type strain after 8 hours, but were significantly reduced at early time-points in the strain carrying the C-terminally 6HA-tagged version of Psy2. Based on this finding, we considered the possibility that the (untagged) C-terminus of Psy2 is required for the interaction between Zip1 and Psy2 and that this interaction might be involved in stabilizing Zip1 during meiosis I.

To further analyze if the C-terminal Psy2 segment was required for the interaction between Zip1 and Psy2, yeast two-hybrid assays were performed using C-terminal fragments of Psy2 expressed as BD-fusion proteins. In fact, yeast two-hybrid analysis demonstrated that C-terminal fragments of Psy2 were capable of interacting with Zip1 (**Fig. 27**). However, the binding capability of the expressed Psy2 truncations was slightly weaker compared with full-length Psy2, indicating that the entire protein is required for maximal interaction.

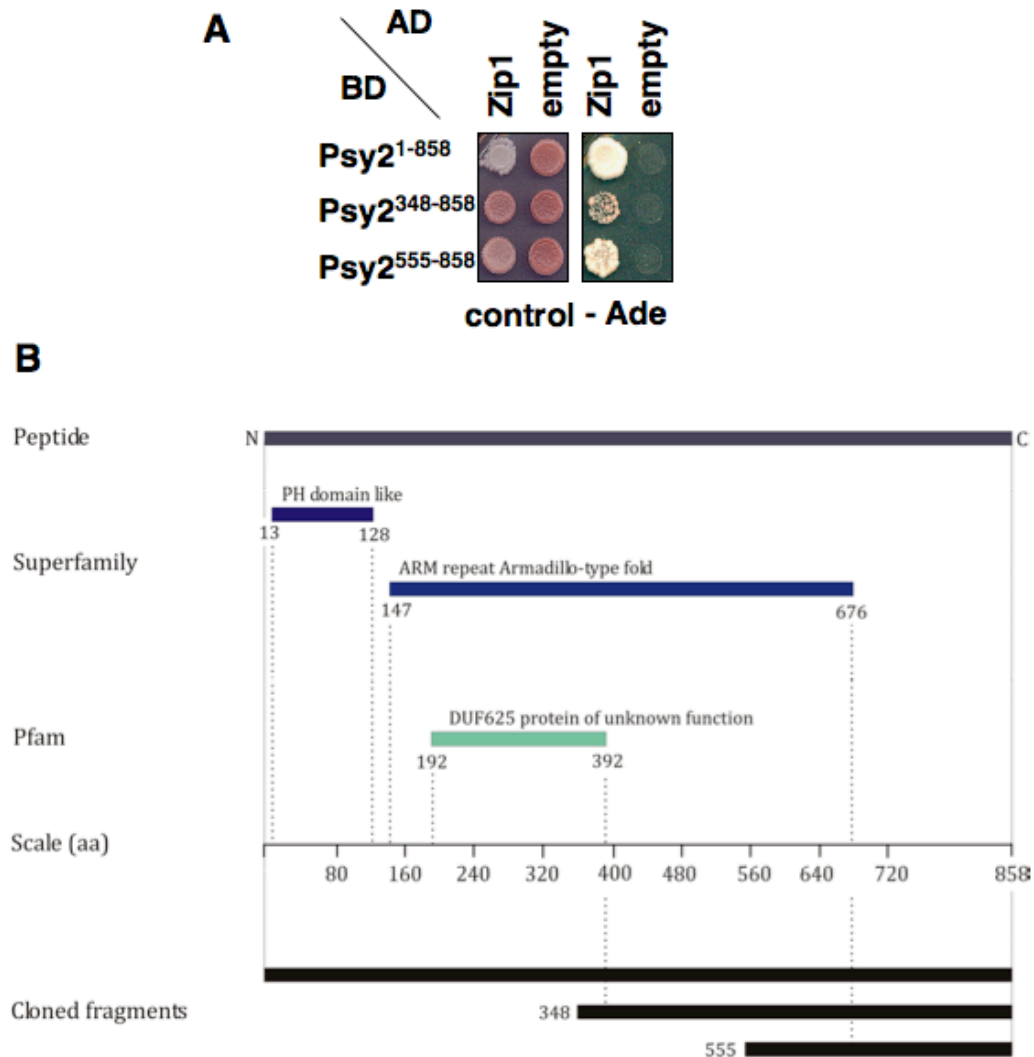


Figure 27: Zip1 interacts with a C-terminal fragment of Psy2. **A:** Zip1 interacts with the C-terminal segment of Psy2. Yeast two-hybrid assay showing the interaction of Zip1 with C-terminal fragments of Psy2 (Psy2³⁴⁸⁻⁸⁵⁸ and Psy2⁵⁵⁵⁻⁸⁵⁸). Indicated Psy2 truncations were expressed as N-terminal BD fusion proteins. Full-length Zip1 was expressed as N-terminal AD-fusion protein. **B:** Schematic representation of the predicted protein structure of Psy2. The protein contains segments with sequence similarity to the PH domain like superfamily and the Armadillo-type fold superfamily. Indicated truncations were cloned into pGBD-C1 for yeast two-hybrid analyses (Figure by Florian Paasch).

IV DISCUSSION

In this study, we found detailed molecular mechanisms for two major functions of the axial element protein Red1. First, Red is modified at a lysine-rich (K-rich) region with SUMO during early meiosis and thereby stimulates the initiation of SC formation. Second, Red1 binds two subunits of the PCNA-like 9-1-1 complex, a heterotrimeric ring with central functions in the DNA damage checkpoint response. This interaction is essential for pachytene checkpoint activation and normal SC formation. In addition, we found that each 9-1-1 subunit is SUMOylated and this occurs specifically in the presence of damaged DNA (either upon treatment with DNA damage or upon Spo11-induced DSBs during meiosis). Finally, this study describes a physical link between the central SC element Zip1 and the Psy2-containing phosphatase complex HTP-C involved in checkpoint exit. These findings will be further discussed in this section and are summarized in **Figs. 28-31**.

IV.1 Red1 SUMOylation is important for timely zipping

The role of SUMO in SC formation

Red1 plays a central role in meiosis. It is implicated in the zipping of homologous chromosomes and is linked to the pachytene checkpoint by its 9-1-1-dependent phosphorylation. Moreover, several meiotic proteins are apparently SUMOylated during meiosis either in a Zip3-dependent or – independent manner (Cheng et al., 2006). Interestingly, SUMO seems to be directly involved in the maturation of SCs, as SC formation is delayed in *ubc9*-allelic strains and defective when Zip1 is mutated in its C-terminal SUMO-interacting motif (SIM, Cheng et al., 2006; Hooker and Roeder, 2006).

Here, we show that the axial element protein Red1 is SUMOylated during early meiosis and at time-points, which correlate with the appearance of SCs. The major region of SUMO acceptor sites is a K-rich domain at aa 560 to 590 (**Fig. 28**). When lysines within this stretch are replaced with arginine, SUMOylation of both overexpressed and endogenous Red1 is

significantly reduced to less than 10%. Interestingly, a SIM-containing C-terminal fragment of the central element protein Zip1 specifically interacts with the SUMO-modified form of Red1. This finding clearly suggests that Red1-Zip1 interact in a SUMO-regulated manner and similar to the recruitment of Srs2 by SUMOylated PCNA (Pfander et al., 2005). As a consequence of less Zip1 recruitment we found that the zipping process in the *red1^{KR}* mutant is delayed by several hours resulting in a reduced viability of spores. Regarding the exact role of SUMO in the formation of mature SCs, the question remains whether SUMO-modified Red1 recruits Zip1 along the whole chromosomes or whether it rather mediates the first initiation seed and thereby promotes the initiation of zipping. The staining of whole chromosomes with anti-SUMO antibodies suggests a quantitative role for SUMO (Hooker and Roeder, 2006), whereas the rather low ratio of modified versus unmodified Red1 argues for a more specific function of SUMO-modified Red1 in triggering timely zipping at the initiation sites. Along this line, it is known that other proteins like e.g. the SUMO ligase Zip3 itself are as well SUMOylated at the time of SC formation (Cheng et al., 2006) and we show that also the second major axial element protein Hop1 interacts with SUMO. SUMOylation of several of these proteins might therefore reflect the massive recruitment of SUMO to pachytene chromosomes. The presence of further SUMO substrates might also explain the specific but rather mild phenotype of *red1^{KR}* mutants compared to *zip1-SIM* alleles (*zip1-SIM^{βN}*, *zip1-SIM^{βR}*) that show very severe phenotypes and a total loss of zipping. The finding, that Zip1 is unstable at later time-points in the *red^{KR}* mutant suggests a secondary function of SUMO-modified Red1 in stabilizing bound Zip1.

The two major components of yeast SCs, Red1 and Zip1, have functional analogues in humans, Sycp2/Sycp3 and Sycp1, respectively (Offenberg et al., 1998; Schalk et al., 1998). Moreover, it has been shown that mammalian SCs can be stained with Ubc9 antibodies and that SUMO might play a role in XY bodies of pachytene spermatocytes (Kovalenko et al., 1996; Rogers et al., 2004). Interestingly, our results show that human Sycp3

strongly binds to human Ubc9 as well as another Sycp3 and is significantly modified with SUMO upon overexpression in mammalian HEK cells.

Altogether, these observations suggest a critical role of Red1 SUMOylation in the recruitment of the central element protein Zip1. Although Red1 SUMOylation is not essential for SC formation, it is required for timely zipping - a mechanism that might very well be conserved in higher eukaryotes.

Regulation of Red1 SUMOylation and the involvement of poly-SUMO chains

It has been discussed that poly-SUMO chains play a critical role during meiosis and seem to be recognized by Zip1 *in vitro* (Cheng et al., 2006). In this study, we found that Red1 is modified with at least three SUMO moieties and that these species do not appear in strains deleted for the SUMO E3 ligase Zip3. The ladder-like SUMO pattern of endogenous Red1 suggests chain formation and indeed, in an overexpression system, we could show that Red1 SUMOylation involves SUMO linkages. Given the fact that Zip3 is essential for SC formation and as SUMO chains accumulate in a $\Delta zip3$ strain (Cheng et al., 2006), it is possible that Zip3 conjugates preformed SUMO chains to its substrate Red1, which would otherwise aggregate in poly-complexes together with the SIM-containing central element protein Zip1. Interestingly, Red1 SUMOylation seems to be stabilized in an *ulp2* deletion strain (Cheng et al., 2006) and Ulp2 was indeed reported to prevent the accumulation of poly-SUMO chains (Bylebyl et al., 2003). In order to clarify the exact nature of the Red1-SUMO-SIM-Zip1 binding interface and whether one or several SUMO moieties on Red1 are involved in this interaction, it would be interesting to carry out structural studies.

We also found that Red1 contains a SIM at aa 455-473 (**Fig. 28**). The respective mutants did not show apparent defects, possibly suggesting a role in the fine-regulation of a process, e.g. in strengthening the recruitment of SUMO-modified Zip3 to its substrate Red1. Moreover, we could show that a Red1 phospho-mimicking mutant of the only Mec1 consensus site in Red1 (which is located in close proximity to the K-rich region, **Fig. 28**) seems to be a better substrate for SUMO modification. Although the detailed mechanism is

not clear, it is tempting to speculate that Mec1-dependent pachytene checkpoint signalling via this site regulates the SUMOylation state by either stimulating Ubc9/Zip3 recruitment or inhibiting the association of Ulp2 (Fig. 28).

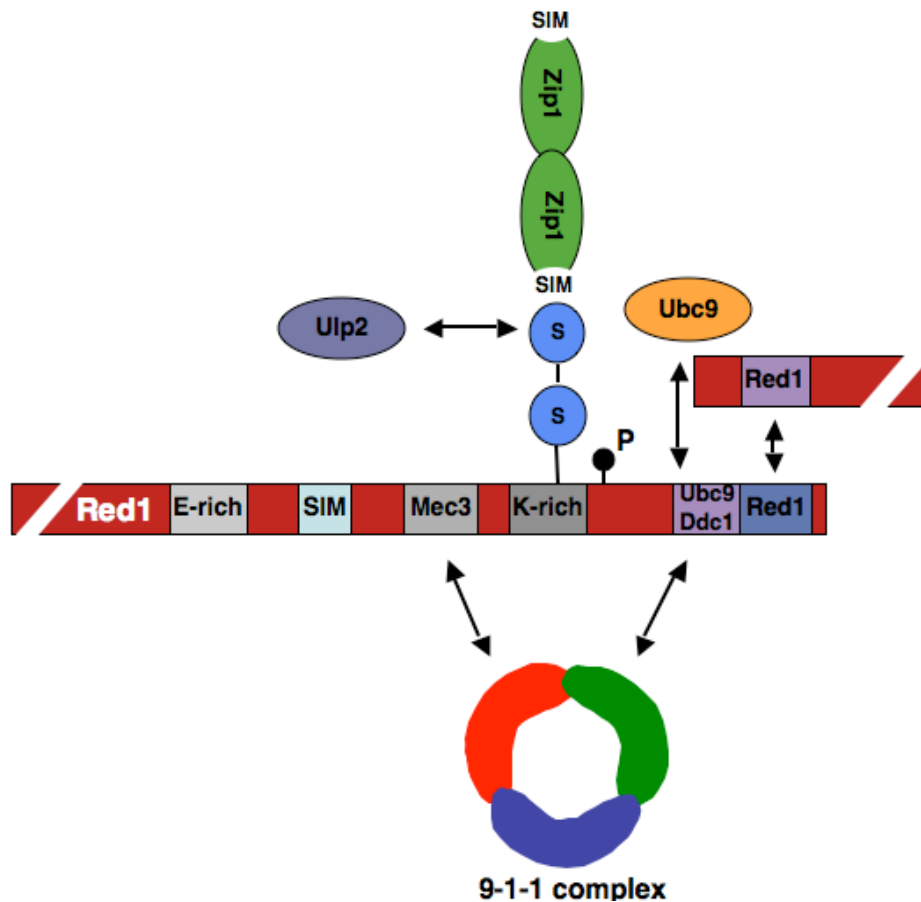


Figure 28: Summary of hypothetic and proven Red1 domains and modifications. Red1 functions at the crossroad of multiple pathways. Yeast-two hybrid analysis revealed Red1 interaction with two 9-1-1 complex components, Mec3 and Ddc1, components of the SUMO machinery including SUMO itself (via a SIM), the SUMO E2 enzyme Ubc9 and the SUMO de-conjugating enzyme Ulp2 as well as a SUMO-dependent association with the central element protein Zip1 and strong Red1-Red1 dimerization. Red1 is SUMO-modified at a lysine-rich (K-rich) domain. A glutamate-rich (E-rich) domain might mediate early (and unspecific) association of Red1 with chromatin. “P” indicates a potential Mec1 phosphorylation site.

Red1 SUMOylation and the HR pathway

We found in this study that Red1 SUMOylation depends on the SUMO E3 ligase Zip3. Interestingly, Zip3 associates with Mre11 and is found at the early sites of Spo11-induced and processed DSBs (Agarwal and Roeder, 2000). Interestingly, these sites can also be stained with SUMO antibodies (Hooker

and Roeder, 2006). The MRX complex and a set of enzymes further process DSBs, thereby generating 5' junctions for efficient loading of the 9-1-1-complex (Majka et al., 2006a) as well as long stretches of single-stranded DNA which are soon covered by Rad51 and Dmc1. As shown in this study and discussed later in this section, 9-1-1 recruits the axial element protein Red1 via two domains thereby allowing full pachytene checkpoint signalling (**Fig. 29**). While the interaction of Red1 with Ddc1 is essential for this process, Red1-Mec3 association has no significant function in signalling, but might be important for stabilizing Red1 molecules (perhaps by covering degrons) and induce Red1's meiosis-specific expression profile.

Interestingly, the 9-1-1 subunit Ddc1 co-localizes with Rad51 (Hong and Roeder, 2002) and this might explain its function in stabilizing Rad51-Dmc1 co-localization (which does not seem to occur in 9-1-1 deletion strains (Shinohara et al., 2003)). Rad51-Dmc1 filaments are supposed to trigger the homology search by which the homologous sequence of the homologous chromosome is recognized and pairing and crossover formation is induced. Notably, Rad51 also interacts with Zip3 (Agarwal and Roeder, 2000) which again explains the presence of the SUMO E3 ligase at the sites where COs are initiated.

Having recruited Red1 and Zip3 to first recombination nodules by major components of the HR pathway, Red1 might be SUMOylated by the Zip3 SUMO ligase, thereby generating an ideal trigger for the recruitment of the SIM-containing central element protein Zip1 (**Fig. 29**). In accordance with this assumption, Zip3 binds Zip2 and Zip1 (Agarwal and Roeder, 2000), and these proteins together with SUMO first localize to recombination sites before Zip1 and SUMO are subsequently found along the whole chromosome (Hooker and Roeder, 2006). Zip2 is essential for synapsis, but not the initial pairing of homologous chromosomes (Chua and Roeder, 1998).

The exact mechanism of the transition of early nodules to chromosome-wide zipping still remains to be clarified. However, it is interesting to speculate that SUMO-modified Red1 stimulates this process. As the SUMO ligase Zip3 interacts with Rad51, it might be guided to the

homologous chromosome (via the homology search) and initiate SUMOylation of Red1 and Zip1 recruitment at the recipient homologous chromosome. Such a mechanism can be postulated for three reasons: first, zipping has to be initiated from each side of a pair of homologous chromosomes; second, zipping has to be triggered specifically at sites of homologous sequences (which can only be assured via the homology search); and third, recruitment of Zip3, Zip2 and Zip1 at the recipient chromosome cannot depend on DSB processing (as DSBs are very unlikely to occur accidentally at homologous sequences of two different chromosomes). In summary, Zip3 might transfer the information for timely zipping from one chromosome to its homologue, thereby tightening initial interactions between homologous chromosomes for subsequent chromosome-wide zipping. Such a mechanism would also further explain the major function of zipping in crossover versus non-crossover decision. Namely, while single-strand annealing (leading to non-crossovers) results from unstable associations between homologous chromosomes, the tying-together of homologous sequences by zipping might ensure second-end capturing and therefore high crossover frequencies. Reduced crossovers in SC-defective mutants are very likely caused by diminished second-end capturing. Red1 SUMOylation and SC formation in $\Delta dmc1$ strains might result from zipping between non-homologous chromosomes and sister chromatids.

Assembly of axial elements

Apart from Red1's interaction with the SUMO pathway, we also found the second major axial element protein Hop1 interacting with SUMO and Ubc9. Although the significance is currently unclear, one can speculate that Hop1's interaction with SUMO may either assist in SC formation similar to the SUMOylation of Red1 or more specifically in the assembly of axial elements (AE). Generally, AE assembly occurs in a highly ordered manner (Page and Hawley, 2004). Apparently, meiotic cohesion and condensin are prerequisites for the sequential recruitment of the three crucial axial element proteins, Red1, followed by Hop1 and finally Mek1. This order is postulated because of the severity of each deletion phenotype. While $\Delta red1$ strains fail to form any SCs

or AEs, $\Delta hop1$ strains form AEs that do not synapse and $\Delta mek1$ strains do form extensive SCs.

In detail, Red1 and Hop1 localization to chromatin is dependent on condensin. Hop1 further needs Red1 for its recruitment, which can be abolished by a specific point mutation in Red1 (Woltering et al., 2000). It is further interesting to note, that Hop1 preferentially binds to regions with low concentrations of Zip1 suggesting Red1 to be the critical protein for mediating the binding to the central element. Mek1, a protein kinase, is the most downstream component of these three proteins. It is very likely that it triggers the cellular response to DSBs or unresolved recombination events by phosphorylating a group of checkpoint effectors similar to the function of Rad53 in the checkpoint response of mitotic cells. Its localization to meiotic chromosomes depends on Red1 and Hop1 and also requires Ddc1 and Mec3. It further colocalizes with DSB on meiotic chromosomes upon activation of the pachytene checkpoint (e.g. caused by the deletion of Hop2).

The meiosis-specific protein Hop1 is involved in the pairing of homologous chromosomes and the establishment of the SC. Whether Hop1's interaction with SUMO reflects Hop1 binding to SUMOylated substrates or rather SUMO-conjugation of Hop1 is still unclear. It is tempting to speculate, however, that the phenotype of described Hop1 mutants can be explained by Hop1's connection with the SUMO pathway. Namely, two lysine mutants, $hop1^{K590A}$ and $hop1^{K593A}$, result in 42-59% or 21% spore viability, respectively. In addition, $hop1^{K593A}$ shows defective chromosome synapsis and may fail to prevent Dmc1-independent DSB repair (Niu et al., 2005).

Axial elements are highly stained with Hop1 and Red1 antibodies suggesting that they are the major proteins. So far, a Red1 mutant ($red1^{K348E}$) has been described that is apparently deficient in Hop1 binding (Woltering et al., 2000). We see however also a binding of Hop1 to the C-terminus of Red1. This can be due to Hop1's binding to the SUMOylated C-terminus of Red1, as Hop1 interacts with SUMO in a two-hybrid assay and as C-terminal fragments of Red1 are SUMOylated in this system. The question of the exact binding therefore still remains and it will be interesting to test whether SUMO plays a

direct role in Red1-Hop1 interaction and axial element formation. Assuming that Red1 oligomerizes and interacts with Hop1 via more than one binding site, several models for the order of axial element assembly can be postulated. In the first model, the proteins assemble in the following order: Hop-Hop-Red-Red-Hop-Hop-Red-Red. In the second, interaction occurs via Red1-SUMO and a potential SIM in Hop1. In the third model, the order is: Red-Red-Hop-Red-Red-Hop (reflecting the possibility of two Hop1 binding domains within Red1). Notably, Red1 and Hop1 are also crucially involved in pachytene checkpoint signaling, which might work independent of their role in axial element formation.

IV.2 Red1 binds 9-1-1 for pachytene checkpoint activation and normal SC formation

Red1—9-1-1 interaction within the pachytene checkpoint pathway

Apart from its function in SC formation, Red1 plays a major role in pachytene checkpoint signalling, although the exact mechanism was not understood so far. Towards a clearer picture, we found in this study that Red1 interacts with two subunits of the 9-1-1 complex (Mec3, Ddc1), suggesting a direct role of Red1 as a checkpoint protein. Indeed, Red1 mutants that do not interact with the 9-1-1 subunit Ddc1 are incapable to activate the pachytene checkpoint. In a $\Delta dmc1$ deletion background where the pachytene checkpoint is active, signalling can be totally blocked by introducing a single point mutation in Red1, which abolishes the interaction with Ddc1. The pachytene checkpoint arrest was characterized by monitoring Rad52 SUMOylation (as a marker for ongoing recombination), phosphorylation of histone H2A at serine 129 (the mammalian γ -H2AX equivalent, a marker for sites of damaged DNA and Mec1 kinase activity), spore viability (as a measure for meiotic competence) as well as expression of the SC component Zip1.

A key finding of this work is that Red1-Ddc1 interaction is essential for pachytene checkpoint activation and provides a “missing link” in the signalling

pathway (**Fig. 29**). In detail, 9-1-1 loading is the first factor in sensing sites of DNA damage. This checkpoint platform guides Red1 to damaged sites, which further allows Hop1 association (and probably Hop1's Mec1-dependent phosphorylation) as well as recruitment (and activation) of the kinase Mek1 via a FHA domain that recognizes phosphorylated Red1 and/or Hop1. Mek1 has several downstream targets and plays a major role in assuring Dmc1-dependent interhomolog recombination rather than intersister recombination (Niu et al., 2007). In summary, the checkpoint pathway involving 9-1-1, Red1, Hop1 and Mek1 establish a so-called barrier to sister-chromatid recombination (BSCR) and therefore lead to high crossover rates and high spore viabilities.

Interfering with the Red1-Mec3 interaction leads to very mild or no phenotypes in regard to spore viability, checkpoint signalling and SC formation. However, this interaction triggers Red1 protein levels and seems to be necessary for Red1's unique expression pattern during meiotic progression. While the expression of early meiotic proteins (including Red1) is mainly regulated by specific promoter sequences that are activated stepwise during meiosis (Chu et al., 1998; Clancy, 1998; Primig et al., 2000), meiotic proteins might generally be short-lived and protected from degran-mediated degradation by their interaction partners. This phenomenon seems relevant for Red1-Mec3 interaction, but possibly also for Red1-Zip1 binding as well as Red1-Red1 dimerization. Together, these mechanisms could explain the meiosis-specific expression profiles of Red1, Zip1 and other proteins and suggest that proteolysis may play a so far unrecognized role in early meiosis.

Pachytene checkpoint signalling is essential for SC formation

Checkpoint activation is essential for normal SC maturation. Namely, SC maturation is disturbed in $\Delta rad24$, $\Delta rad17$, and $mec1-1$ strains, in cells that express Hop1 variants that cannot be phosphorylated by Mec1 as well as in Mek1-defective mutants (Bailis and Roeder, 1998; Carballo et al., 2008; Grushcow et al., 1999). Therefore, a major function of the pachytene checkpoint pathway is the regulation of processes that assure normal SC

formation. The exact mechanisms are not known so far, but the central player might be the downstream effector kinase Mek1, which either has a direct effect on SC proteins or indirectly ensures Dmc1-dependent inter-homolog crossovers (and thereby SC formation).

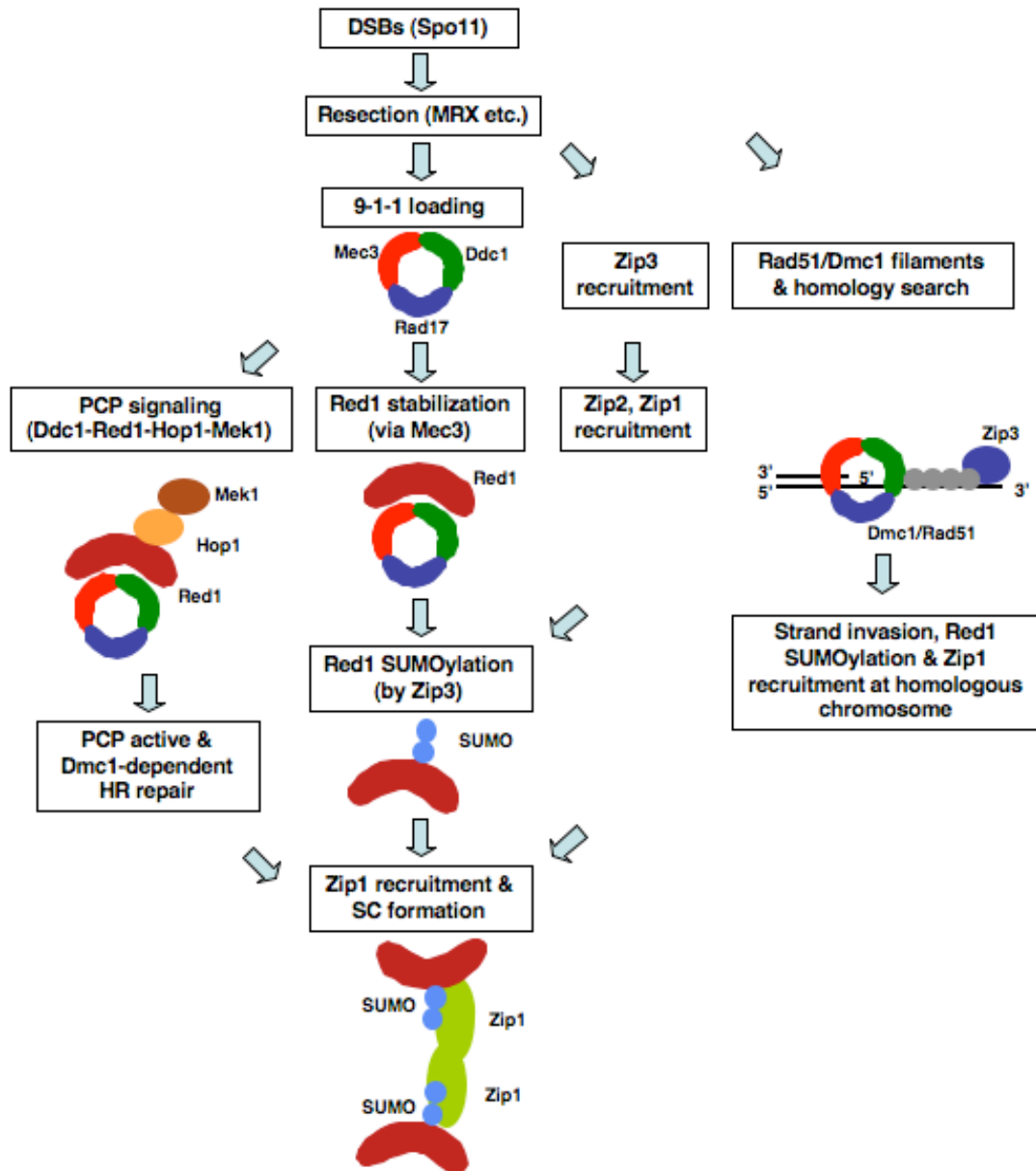


Figure 29: Mechanisms leading to mature SC formation. Spo11-induced DSBs are processed by the MRX complex (and other enzymes). Zip3 (and then Zip2 and Zip1) are recruited by the MRX complex and probably by Rad51/Dmc1 filaments. Processed DSBs are recognized by 9-1-1 which serves as a platform for Red1 recruitment via two domains. Red1's interaction with Mec3 seems to protect degradation and thereby stabilizes Red1, while the interaction with Ddc1 is essential for checkpoint signalling via a pathway that involves Hop1 and Mek1 and finally ensures DSB repair by Dmc1-dependent homologous recombination. Zip3 modifies Red1 with SUMO thereby fostering the interaction with Zip1 and ensuring timely SC formation.

IV.3 Intimate connection between pachytene checkpoint and SC formation

Several studies report an intimate connection between pachytene checkpoint signalling and the establishment of SCs. First, as discussed in the previous paragraph, the axial element protein Red1 directly interacts with two 9-1-1 subunits, thereby suggesting a direct link between the DNA damage checkpoint and SC formation. Second, phosphorylation of the two major axial element proteins Hop1 and Red1 by the checkpoint kinases Mec1 and (the meiosis-specific) Mek1, respectively, further provide evidence for a role of SC proteins in pachytene checkpoint signalling (Carballo and Cha, 2007; Carballo et al., 2008; Niu et al., 2007). In paragraph III.6 of this study, we report a first link between SC maturation and the exit of checkpoint arrest.

Cell cycle checkpoints during meiosis are indispensable for the surveillance of meiotic recombination and faithful gamete production. Meiotic checkpoints involve a complex network of signals, signal sensors and signal transduction pathways that correlate meiotic recombination and cell cycle progression. Function of all checkpoints monitoring genomic integrity requires 9-1-1, the clamp-loader subunit Rad24 and the major checkpoint kinase Mec1. As a broad range of checkpoint targets are posttranslationally modified by phosphorylation, checkpoint recovery is dependent on the action of specific phosphatases. A factor apparently involved in recovery from the pachytene checkpoint is protein phosphatase 1 (PP1) that contains the catalytic subunit Glc7. Overexpression of Glc7 was shown to shorten the G2/prophase delay of a set of mutants defective in completing meiotic recombination. Moreover, Glc7 apparently functions in the reversal of Mek1-dependent phosphorylation and recovery from pachytene checkpoint by de-phosphorylation of potential Mek1 substrates such as Red1 (Bailis and Roeder, 2000; Hochwagen et al., 2005). This study presents evidence that Psy2, a regulatory subunit of the Pph3-phosphatase complex (HTP-C), is required for faithful spore production and for de-phosphorylation of histone H2A at serine 129 during recovery from a checkpoint monitoring meiotic recombination.

Interaction between Psy2 and Zip1 seems to require Zip1 dimerization. First evidence that Psy2 is involved in meiosis was provided by a large-scale study that reported a potential physical interaction with the meiosis-specific central element protein Zip1 (Ito et al., 2001). Here, yeast two-hybrid analyses using different Zip1 truncations revealed that the interaction between Zip1 and Psy2 is mediated by the C-terminal region of Psy2 and requires an extended fragment of Zip1 comprising the N-terminal globular domain as well as the first coiled-coil domain (aa 184-309). Importantly, Psy2 binding by Zip1 fragments correlates with the capability of these fragments to form dimers. This observation suggests that Psy2 may specifically recognize only Zip1 dimers (or oligomers) in the physiological context of a fully assembled SC. The observation that Psy2 binding to Zip1 was not affected by the amino acid replacements in the *zip1^{L657A}* and *zip1^{L664}* mutants strongly suggests that the domain from aa 643-664 is not required for Psy2 binding. Moreover, our finding that Zip1 dimerization is functional in the mutants, is consistent with the observation, that the *zip1^{4LA}* mutant is capable of assembling apparently normal SCs with wild type kinetics (Mitra and Roeder, 2007).

Psy2 regulates H2A phosphorylation during meiosis. As a component of the Pph3-phosphatase complex, Psy2 regulates histone H2A and Rad53 de-phosphorylation during recovery from DNA damage (Keogh et al., 2006; O'Neill et al., 2007). Results obtained from Δ *psy2* cells generated during this study indicate, that Psy2 is also required for the de-phosphorylation of H2A during meiosis and may regulate recovery from the meiotic recombination checkpoint. Moreover, the observation that Psy2 deficiency as well as C-terminal modification (using a 6HA-tag) of Psy2 seems to alter the typical early-meiotic protein expression profile of Zip1, raises the possibility that Psy2 may be involved in stabilizing Zip1 filaments or perhaps more likely in sensing the status of the SC. In particular, the accumulation of Red1 and Zip1 at late time-points (24h) of synchronously sporulating Δ *psy2* cells indicates delays or arrests in the pachytene stage of meiosis I. However, it is unknown whether this delay is a direct consequence of Psy2 deficiency or rather caused by changed Zip1 protein expression levels (at early time-points; 4-8 hours after

sporulation) that lead to activation of the *zip1* checkpoint. An attractive model and new concept in the field would be that the “activation“ of the so-called *zip1* checkpoint rather results from an inability to turn off the Mec1/9-1-1-dependent meiotic recombination checkpoint (by Psy2-dependent de-phosphorylation of H2A at serine 129; **Fig. 30**).

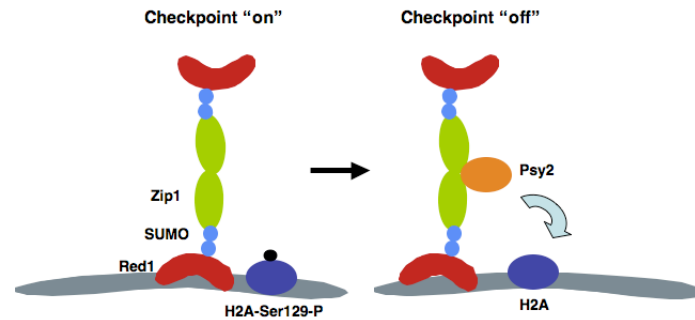


Figure 30: Hypothetic model for Psy2 function in triggering pachytene checkpoint exit. The phosphatase subunit Psy2 might recognize Zip1 dimers/oligomers (within a functional SC) and subsequently trigger checkpoint exit upon Pph3-dependent de-phosphorylation of histone H2A serine 129. This phosphorylation mark corresponds to mammalian γ -H2AX and is crucial for recruiting checkpoint proteins to damaged sites.

Furthermore, expressing a Psy2^{6HA} fusion protein and subsequent immunoblotting demonstrated that Psy2 is expressed at approximately constant levels throughout meiosis. In this context it would be interesting to test whether Psy2 expression is specifically induced in the course of recovery from DNA damage. Another testable idea is whether high levels of Psy2 shorten the delay of mutants defective in completing meiotic recombination. As such an effect has already been reported for Glc7 (Bailis and Roeder, 2000), this would provide further evidence that Psy2 is involved in meiotic checkpoint recovery. To further prove this model (**Fig. 30**), fluorescence microscopy experiments should tell whether Psy2 is directly an incorporated or rather transiently associated SC protein. As both Zip1 and a GST-tagged C-terminal part of Psy2 are currently purified, pull-down experiments will show whether Psy2 specifically interacts with Zip1 dimers or oligomers (using an improved protocol adapted from Dong and Roeder, 2000). Lastly, it will be interesting to get specific point mutations interfering with Zip1-Psy2 binding to further uncover detailed functions of this protein-protein interaction.

Succinct model

In conclusion, our major findings suggest a model in which Red1, a structural component of the lateral element of the SC, connects key steps of meiosis through direct physical interactions (**Fig. 31**). Red1 appears to locally restrict Spo11-induced DSB formation to specific sites (Prieler et al., 2005). After loading of 9-1-1 and its association with Red1, SCs are formed, which by its architecture are thought to facilitate interhomolog, but repress sister chromatid recombination (Page and Hawley, 2004). Interaction of 9-1-1 (Ddc1) and Red1 is essential for the pachytene checkpoint pathway, which governs meiotic surveillance and repression of sister chromatid recombination partially through Hop1 and Red1 phosphorylation (Carballo et al., 2008; Niu et al., 2007), as well as for normal SC formation. In parallel, Zip3-dependent Red1 SUMOylation stimulates the association of Red1 to the central element Zip1, thereby securing timely SC formation. Interestingly, another surveillance pathway involving the chaperone-like ATPase Pch2 seems to monitor correct Zip1-Red1-mediated SC assembly (Wu and Burgess, 2006), corroborating that Red1 lies at the heart of meiotic control.

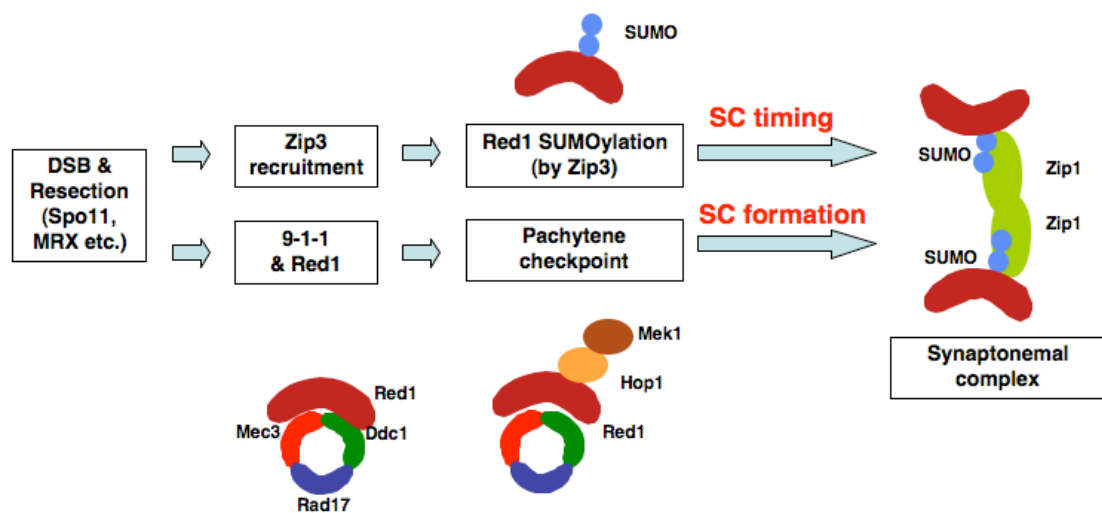


Figure 31: Hypothetical model for early meiotic functions. Induced and processed (by Spo11, MRX etc.) double-strand breaks (DSBs) recruit 9-1-1 (tri-colored ring), which binds Red1 (red) via two Red1 domains. Red1—9-1-1-interaction is needed for the activation of the pachytene checkpoint, which is further essential for normal SC formation (probably by assuring DSB repair via Dmc1-dependent homologous recombination). In parallel, Zip3 (SUMO ligase) might be recruited to DSBs by binding the MRX complex. Zip3’s SUMOylation (blue) of Red1 controls SC formation timing, but not SC formation itself.

V MATERIAL AND METHODS

The following microbiological, molecular biological and biochemical methods are based on standard techniques (Ausubel et al., 1994; Sambrook et al., 1989) or on the manufacturers' instructions.

Unless otherwise mentioned, chemicals and reagents were purchased from Amersham-Pharmacia, Applied Biosystems, Biomol, Biorad, Difco, Fluka, Invitrogen, Kodak, Merck, New England Biolabs, Promega, Roth, Roche, Riedel de Haen, Serva or Sigma. For all methods described, de-ionized sterile water, sterile solutions and sterile flasks were used.

V.1 Computational analyses

For database searches (sequence search and comparison) electronic services were used provided by the *Saccharomyces Genome Database* (<http://www.yeastgenome.org/>) and the *National Center for Biotechnology Information* (<http://www.ncbi.nlm.nih.gov/>). Most of the protein sequence analyses were done with software programs from *ExpASY Proteomics Server* (<http://www.expasy.org/>) or from *Pole Bioinformatique lyonnais* (<http://npsa-pbil.ibcp.fr>). For assessment of protein domain composition and protein folding, the program *SMART* (<http://www.smart.embl-heidelberg.de>) was used. DNA sequence analyses (DNA restriction enzyme maps, DNA sequencing analyses, DNA primer design) were done with DNA-Star (DNA Star Inc.).

Western blots were digitalized using an AGFA scanner (Arcus II) and further processed using Adobe Photoshop (Adobe Systems Inc.). Alternatively chemiluminescence signals of immunoblots were detected by a CCD camera (LAS 3000, Fujifilm), quantified with the software program Image Gauge V4.1 (Fujifilm) and processed with Adobe Photoshop (Adobe Systems Inc.). For the presentation of text, tables, graphs and figures, software programs of the Microsoft Office package (Microsoft Corp.) were used.

V.2 Microbiological and genetic techniques

V.2.1 *Escherichia coli* techniques

E. coli strains

Strain	Genotype	Company
XL1-Blue	hsdR17 recA1 endA1 gyrA46 thi-1 supE44 relA1 lac [F' proAB lacI q ZΔM15 Tn10 (Tet r)]	Stratagene
BL21(DE3)/RIL	B F ompT hsdS(rB mB) dcm Tet gal (DE3) EndA Hte [argU ileY leuW Camr]	Stratagene

E. coli vectors

Vector	Purpose	Company
pQE32	Expression with His-tag	Qiagen
pGEX-4T	Expression with GST-tag	Amersham
pET28M	Expression with His-SUMO1-tag	Core facility, MPIB
pETM14	Expression with His-tag	Core facility, MPIB
pETM33	Expression with His-GST-tag	Core facility, MPIB

***E. coli* plasmids**

pGEX- and pQE32-versions of Red1, Zip1, and Zip3 (full-length and fragments) were created by PCR from DF5 yeast genomic DNA extracts. 9-1-1 subunits (Rad17, Mec3, Ddc1) were cloned into pET28M-Sumo1-ccdB (N-His-Sumo1 tagging) plasmids by SLIC (seamless ligation independent cloning). pETM14-ccdB (N-His)-Zip1¹⁻⁸⁷⁵, Zip1¹⁻⁴⁵¹, and Zip1²⁰⁻⁷⁰⁰ as well as pETM33-ccdB (N-His-GST)-Psy2¹⁻⁸⁵⁸ and Psy2⁵⁵⁵⁻⁸⁵⁸ fragments were also constructed by SLIC.

***E. coli* media:**

LB-medium (and plates)

- 1% (w/v) tryptone (Difco)
- 0.5% (w/v) yeast extract (Difco)
- 1% (w/v) NaCl
- 1.5% (w/v) agar (plates)
- sterilized by autoclaving

Cultivation and storage of *E. coli* cells

Liquid cultures were grown in LB media at 37°C (or 23°C and 30°C for expression experiments). Cultures on agar plates were incubated at 37°C. For the selection of transformed bacteria, ampicillin (50µg/ml) was used. The culture density was determined by measuring the absorbance at a wavelength of 600nm (OD₆₀₀). Cultures on solid media were stored at 4°C for maximal 3 days. For long-term storages, stationary cultures were frozen in 15% (v/v) glycerol solutions at -80°C.

Preparation of electro-competent *E. coli* cells

DNA plasmids were transformed into *E. coli* competent cells by electroporation. For the preparation of electro-competent cells, 1l liquid LB medium was inoculated with 10ml of an overnight culture derived from a single *E. coli* colony and grown to an OD₆₀₀ of 0.8 at 37°C. After cooling the culture flask on ice for 30min, cells were harvested by centrifugation (10min, 5000g, 4°C). All following steps were performed with pre-cooled sterile materials and solutions at 4°C. The pellets were washed once with 1l ice-cold water and once with 0.5l ice-cold 10% (v/v) glycerol. Finally, the cells were resuspended in 3ml 10% (v/v) glycerol and stored as 100µl aliquots at -80 °C.

Transformation of plasmid DNA into *E. coli* cells

Electro-competent cells were thawed on ice. For the electroporation, 40µl electro-competent cells were mixed with 2µl of dialysed ligation samples. The suspension was electroporated in a pre-cooled 0.1cm Gene pulser cuvette (Biorad) with a pulse of 1.8kV and 25µF at a resistance of 200Ω. After addition of 1ml pre-warmed LB medium (without antibiotics), the suspension was incubated for 1h on a shaker at 37°C. Selection of transformants was carried out on ampicillin-containing LB agar plates over night at 37°C.

Expression of proteins in *E. coli* cells

For the expression of recombinant proteins, the *E. coli* strain BL21 (DE3)/RIL was used. Liquid LB medium was inoculated at a 1:100-dilution of an overnight culture of a freshly transformed colony. Generally, cultures were incubated at 30°C until they reach an OD₆₀₀ of 0.6 and protein expression was induced by addition of IPTG to 1mM final concentration. Cells were harvested 3-12h after IPTG addition by centrifugation (10min, 5000g, 4°C), washed in ice-cold PBS and stored at -80°C after shock freezing in liquid nitrogen. Expression of the protein of interest was confirmed by analyzing samples taken before and after IPTG-induction using SDS-PAGE and coomassie staining.

V.2.2 *Saccharomyces cerevisiae* techniques

S. cerevisiae strains

All deletion mutants and tagging strains were constructed by a PCR-based strategy (Janke et al., 2004; Knop et al., 1999) and confirmed by PCR using specific primers.

Strain	Genotype	Reference
DF5	<i>his3Δ200, leu2-3,11, lys2-801, trp1-1, ura3-52,</i>	(Finley et al., 1987)
Y1094*	<i>SMT3::pYI-ADH1p^{-His}SMT3::URA3</i>	this study
Y1083 (SK1)	<i>ho::hisG/ ho::hisG, lys2/lys2, ura3/ura3, leu2/ leu2,</i> <i>his3/ his3, trp1-ΔFA/trp1-ΔFA</i>	(Gasior et al., 1998; Huang et al., 2005)
CE382	<i>URA3::pYI-ADH1p^{-His}SMT3</i>	this study
CE387	<i>red1::kanMX6/red1::kanMX6,</i> <i>URA3::pYI-ADH1p^{-His}SMT3</i>	this study
CE659	<i>red1::kanMX6/red1::kanMX6,</i> <i>URA3::pYI-ADH1p^{-His}SMT3,</i> <i>LEU2::pYI-RED1^{WT}/LEU2::pYI-RED1^{WT}</i>	this study
CE662	<i>red1::kanMX6/red1::kanMX6,</i> <i>URA3::pYI-ADH1p^{-His}SMT3,</i> <i>LEU2::pYI-RED1^{KR}/LEU2::pYI-red1^{KR}</i>	this study
CE663	<i>red1::kanMX6/red1::kanMX6,</i> <i>URA3::pYI-ADH1p^{-His}SMT3,</i> <i>LEU2::pYI-RED1^{-Mec3,-Ddc1}/LEU2::pYI-red1^{-Mec3,-Ddc1}</i>	this study
CE 774	<i>red1::kanMX6/red1::kanMX6,</i> <i>zip1::natNT2/zip1::natNT2,</i> <i>URA3::pYI-ZIP1::GFP⁷⁰⁰, LEU2::pYI-RED1^{WT}</i>	this study
CE 775	<i>red1::kanMX6/red1::kanMX6,</i> <i>zip1::natNT2/zip1::natNT2,</i> <i>URA3::pYI-ZIP1::GFP⁷⁰⁰, LEU2::pYI-red1^{-Mec3}</i>	this study
CE 776	<i>red1::kanMX6/red1::kanMX6,</i> <i>zip1::natNT2/zip1::natNT2,</i> <i>URA3::pYI-ZIP1::GFP⁷⁰⁰, LEU2::pYI-red1^{-Ddc1}</i>	this study
CE 777	<i>red1::kanMX6/red1::kanMX6,</i> <i>zip1::natNT2/zip1::natNT2,</i> <i>URA3::pYI-ZIP1::GFP⁷⁰⁰, LEU2::pYI-red1^{-Mec3,-Ddc1}</i>	this study

Strain	Genotype	Reference
CE 778	<i>red1::kanMX6/red1::kanMX6</i> , <i>zip1::natNT2/zip1::natNT2</i> , <i>URA3::pYI-ZIP1::GFP⁷⁰⁰</i> , <i>LEU2::pYI-red1^{KR}</i>	this study
CE 525	<i>rad17::natNT2/rad17::natNT2</i>	this study
CE 528	<i>mec3::natNT2/mec3::natNT2</i>	this study
CE 531	<i>ddc1::natNT2/ddc1::natNT2</i>	this study
CE 522	<i>zip3::natNT2/zip3::natNT2</i>	this study
Y2109	<i>zip1::kanMX6/zip1::kanMX6</i>	this study
CE 834	<i>spo11::hisG-URA3-hisG/spo11::hisG-URA3-hisG</i> , <i>LEU2::pYI-ADH1p^{-His}SMT3</i>	this study
CE 566	<i>zip3::natNT2/zip3::natNT2</i> <i>URA3::pYI-ADH1p^{-His}SMT3</i>	this study
CE 384	<i>dmc1::HIS3MX6/dmc1::HIS3MX6</i> <i>URA3::pYI-ADH1p^{-His}SMT3</i>	this study
CE 571	<i>dmc1::HIS3MX6/dmc1::HIS3MX6</i> , <i>red1::kanMX6/red1::kanMX6</i> , <i>LEU2::pYI-RED1^{WT}</i>	this study
CE 579	<i>dmc1::HIS3MX6/dmc1::HIS3MX6</i> , <i>red1::kanMX6/red1::kanMX6</i> , <i>LEU2::pYI-red1^{-Ddc1}</i>	this study
CE001a*	<i>smt3::HIS3MX6</i> , <i>SMT3::pYI-SMT3p^{-His}SMT3^{WT}::URA3</i>	this study
YMIS043	<i>smt3::HIS3MX6</i> , <i>SMT3::pYI-SMT3p^{-His}SMT3^{KKK}::URA3</i>	Michael Schwarz
YBP122*	<i>RAD17^{PrtA}::kanMX6</i> , <i>SMT3::pYI-ADH1p^{-His}SMT3::URA3</i>	Boris Pfander
YBP123*	<i>MEC3^{PrtA}::kanMX6</i> , <i>SMT3::pYI-ADH1p^{-His}SMT3::URA3</i>	Boris Pfander
YBP124*	<i>DDC1^{PrtA}::kanMX6</i> , <i>SMT3::pYI-ADH1p^{-His}SMT3::URA3</i>	Boris Pfander
YMAS9*	<i>rad24::HIS3MX6</i> , <i>RAD17^{PrtA}::kanMX6</i> , <i>SMT3::pYI-ADH1p^{-His}SMT3::URA3</i>	Maria Schmid
YMAS10*	<i>ubc9-1::TRP1</i> , <i>ubc9-1::LEU2</i> , <i>bar1::HIS3MX6</i> , <i>RAD17^{PrtA}::kanMX6</i> , <i>SMT3::pYI-ADH1p^{-His}SMT3::URA3</i>	Maria Schmid
CE002*	<i>RAD17^{PrtA}::kanMX6</i> , <i>smt3::HIS3MX6</i> <i>SMT3::pYI-SMT3p^{-His}SMT3::URA3</i>	this study
CE004*	<i>MEC3^{PrtA}::kanMX6</i> , <i>smt3::HIS3MX6</i> <i>SMT3::pYI-SMT3p^{-His}SMT3::URA3</i>	this study
CE008*	<i>DDC1^{PrtA}::kanMX6</i> , <i>smt3::HIS3MX6</i> <i>SMT3::pYI-SMT3p^{-His}SMT3::URA3</i>	this study
YMAS28	<i>MEC3^{PrtA}::kanMX6/MEC3^{PrtA}::kanMX6</i>	Maria Schmid
YMAS30	<i>dmc1::HIS3MX6/dmc1::HIS3MX6</i> , <i>MEC3^{PrtA}::kanMX6/MEC3^{PrtA}::kanMX6</i>	Maria Schmid
CE683	<i>psy2::HIS3MX6/psy2::HIS3MX6</i>	this study
CE689	<i>PSY2^{6HA}::natNT2/PSY2^{6HA}::natNT2</i>	this study
PJ69-7A**	<i>trp901-</i> , <i>leu2-3,112</i> , <i>ura3-53</i> , <i>his3-200</i> , <i>gal4</i> , <i>gal80</i> , <i>GAL1::HIS3</i> , <i>GAL2-ADE2</i> , <i>met2::GAL7-lacZ</i>	(James et al., 1996)

All strains are isogenic SK1 background except:

* DF5 or derivatives of DF5 strains described in (Finley et al., 1987).

** Two-hybrid strain described in (James et al., 1996).

***S. cerevisiae* vectors**

Vector	Purpose	Reference
pYCplac33, pYCplac22, pYCplac111	CEN plasmids	(Gietz and Sugino, 1988)
pYEplac195, pYEplac112, pYEplac181	2 μ plasmids	(Gietz and Sugino, 1988)
pYIplac211, pYIplac204, pYIplac128	INT plasmids	(Gietz and Sugino, 1988)
pGAD-C1, pGBD-C1	Two-Hybrid	(James et al., 1996)

***S. cerevisiae* plasmids**

All two-hybrid constructs generated in this study were based on pGAD-C1 vectors for AD fusions and pGBD-C1 vectors for BD fusions. The respective ORFs (full-length or fragments) were amplified by PCR from genomic DNA of DF5 yeast extracts using specific primer and compatible restriction enzyme sites. Mutations (in Red1, Zip1, and Ulp2) were introduced by mutagenesis PCR using specific primer.

Integration plasmids were based on the YIplac vector series. For the expression of *RED1* with endogenous levels, the full-length *RED1* ORF plus 641 bp of the upstream promoter and 514 bp of the terminator were cloned into an integrative plasmid. All *red1* mutant plasmids were constructed by mutagenesis-PCR using specific primer. To accurately compare the phenotypes of different Red1-expressing strains, plasmids expressing *RED1* WT and mutants were cut by *AflIII* and integrated directly into the *LEU2* locus of the same diploid parental strain. Only diploid strains expressing *RED1* WT and mutants from two copies (confirmed by real-time PCR in comparison to a control locus; expression levels were further confirmed by Western blot analysis) were used for phenotypic analysis. The internally GFP-tagged Zip1 construct (obtained from D. Kaback and described previously in Scherthan et al., 2007) was cut by *ApaI* and integrated into the *URA3* locus.

^{His}SUMO constructs under the *ADH1* promoter were used in previous studies in the Jentsch laboratory, the constructs for expression under the endogenous *SMT3* promoter were generated in this study. A ^{His}SUMO^{KKK} construct mutated in the first three lysines was obtained from Michael Schwarz. All ^{His}SUMO constructs were integrated into the *URA3* locus by cutting with *EcoRV* and expression levels were tested by Western blot analysis.

S. cerevisiae* media and solutions*YPD:**

- 1% (10 g/l) yeast extract (Difco)
- 2% (20 g/l) bacto-peptone (Difco)
- 2% (20 g/l) D-(+)-glucose
- 2% (20 g/l) agar (for plates)
- sterilized by autoclaving

YPD G418/NAT plates:

- YPD medium with 2% agar was autoclaved and cooled to 50°C
- G418 (geneticine disulfate; Sigma) or NAT (noursethricin, HKI Jena) were added to 200mg/l or 100mg/l, respectively

YP acetate media

- 1% (10 g/l) yeast extract (Difco)
- 2% (20 g/l) bacto-peptone (Difco)
- 2% (w/v) potassium acetate

SC-media/plates:

- 0.67% (6,7 g/l) yeast nitrogen base (Difco)
- 0.2% (2 g/l) drop out amino acid mix
- 2% (20 g/l) glucose, raffinose, or galactose
- 2% (20 g/l) agar (for plates)
- sterilized by autoclaving

Drop out amino acid mix:

- 20 mg Ade, Ura, Trp, His
- 30 mg Arg, Tyr, Leu, Lys
- 50 mg Phe
- 100 mg Glu, Asp
- 150 mg Val
- 200 mg Thr
- 400 mg Ser

Sporulation media:

- 1,5% (w/v) potassium acetate (Sporulation for tetrad dissection)
- 0,4% or 2% (w/v) potassium acetate (Synchronous sporulation)

SORB:

- 100 mM CH₃COOLi
- 10 mM Tris-HCl, pH 8.0
- 1 mM EDTA, pH 8.0
- 1 M sorbitol
- sterilized by filtration

PEG:

- 100 mM CH₃COOLi
- 10 mM Tris-HCl, pH 8.0
- 1 mM EDTA, pH 8.0
- 40% (w/v) PEG-3350
- sterilized by filtration

Zymolase 20T solution:

- 0.9 M sorbitol
- 0.1 M Tris-HCl, pH 8.0
- 0.2 M EDTA, pH 8.0
- 50 mM DTT
- 0.5 mg/ml zymolase 20T (ICN Biochemicals)

Cultivation and storage of *S. cerevisiae*

Liquid pre-cultures were inoculated with a single yeast colony from freshly streaked plates and grown over night at 30°C with shaking. The culture density was determined by measuring the absorbance at a wavelength of

600nm (OD_{600}), with $OD_{600}=1$ corresponding to 1.5×10^7 cells/ml. In general, main cultures were inoculated with overnight cultures resulting in an OD_{600} of 0.2 and incubated at 30°C with shaking at 150-200rpm until the culture reaches the mid-log phase of growth ($1-5 \times 10^7$ cells/ml). Cultures on solid media were stored at 4°C up to 1-2 months. For long-term storages, stationary (overnight) cultures were frozen in 15% (v/v) glycerol solutions at -80°C.

Preparation of competent yeast cells

A 50ml-culture of yeast cells from mid-log phase was harvested by centrifugation (500g, 5min, RT), washed once with 20ml sterile water, once with 10ml SORB solution and resuspended in 360µl SORB solution. After addition of 40µl carrier DNA (salmon sperm DNA, 10mg/ml, Invitrogen), competent cells were stored in 50µl aliquots at -80°C.

Transformation of yeast cells

For yeast transformation, 0.2µg of circular or 2µg of linearized plasmid DNA (or PCR product) was mixed with 10µl or 50µl competent cells, respectively. After adding 6 volumes of PEG solution, the cell suspension was roughly vortexed and incubated at RT for 30 min. Subsequently, DMSO was added to a final concentration of 10% and a heat shock was performed at 42°C for 15min. Cells were pelleted by centrifugation (2000rpm, 2 min, RT), resuspended in 100µl sterile water and plated on the respective SC medium plates. After 3 days of incubation at 30°C, transformants were used for further analysis. When using the antibiotics G418 or NAT for selection, transformed cells were incubated with shaking in YPD medium for 3h or 5 h, respectively, before they were streaked out onto plates containing G418 or NAT. Generally, if necessary, transformants were replica-plated on selection plates to remove the background of false-positive colonies.

Genomic integration by homologous recombination

The YIplac vector series (Gietz and Sugino, 1988) was used for stable integration of DNA into the yeast genome. As these plasmids do not contain autonomous replication elements, only stably integrated vectors are propagated in yeast. The ORF of the respective gene was cloned into YIplac vectors including the endogenous or a constitutive promoter (e.g. the *ADH1* promoter for overexpression) and a terminator element. Before transformation, vectors were linearized by a restriction enzyme that specifically cuts within the auxotrophy marker gene. These linearized plasmids can then be integrated into the genome by homologous recombination with the endogenous locus of the marker gene.

A similar approach was used in order to delete genes or tag endogenous genes with an epitope (Knop et al., 1999; Longtine et al., 1998). For this method, PCR products were used to transform competent yeast cells. To allow homologous recombination with the endogenous locus of a gene, PCR products were generated using primers that contain sequences for amplification of special cassettes (including the marker gene) as well as sequences complementary to the gene of interest. For gene deletions, the forward primer contains 55bp of the promoter sequence 5' of the start codon

(ATG) of the respective gene, while the reverse primer includes 55bp of the terminator sequence 3' of the stop codon. For C-terminal epitope tagging of a gene, a forward primer containing 55bp 5' of the stop codon were used instead. Generally, PCR products were purified and concentrated after amplification using ethanol precipitation, and competent yeast cells transformed and plated on selection plates. The correct recombination was confirmed by PCR analysis for gene deletions and Western blot for epitope tagging.

Mating type analysis of haploid strains

The tester strains RC634a and RC75-7 α were used for identification of yeast mating types. These strains are hypersensitive to the pheromone secreted by yeast strains of the opposite mating type. 500 μ l of a suspension of a tester strain was mixed with 50ml of molten agar (1% w/v water, cooled to 45°C) and 8ml were poured over each YPD plate. Plates containing cultures to be analyzed were either replica plated on the a- and α -tester plate. Alternatively, single colonies can be streaked on each tester plate. The principle of this test is the fact, that tester strains cannot grow in proximity of colonies of different mating type, thereby generating a so-called "halo" of clear agar. Therefore, after 1-2 days of incubation at 30°C, a halo appears around a haploid colony, if the mating type of the strain is different, while diploid cells do not secrete any mating type pheromones and therefore do not give halos on each mating tester plates.

Mating of haploid *S. cerevisiae* strains

Haploid strains of opposite mating types (MATa, MAT α) were grown to mid-log growth phase and mixed by spotting 10 μ l of each strain on YPD plates overnight at 30°C. Cells were streaked on YPD or selection plates and diploids were identified by their colony shape after growth on YP glycerol plates (only in case of SK1 strains) and by mating type analysis.

Sporulation and tetrad analysis of diploid *S. cerevisiae* strains

500 μ l of diploid stationary phase yeast cells were harvested by centrifugation (500g, 3min), washed 3 times with sterile water and resuspended in 4ml sporulation medium (1,5% potassium acetate). After incubation on a shaker at RT for 3 days, 10 μ l of the culture was mixed with 10 μ l zymolase-20T solution and incubated at RT for 10min. The spores were dissected in tetrads with a micromanipulator (Singer MSM Systems) and grown on YPD plates for 2-3 days. Subsequently, tetrads were replica plated and analyzed genotypically on selection plates for specific markers or by their phenotypes.

Synchronous sporulation and spore viability assay

Strains were inoculated in YPD and cultured overnight at 30°C, diluted 1:50 in pre-warmed YP acetate media and again cultured overnight at 30°C. Cells were then harvested (2000g, 5min, RT), washed twice with pre-warmed water, resuspended in 2% pre-warmed potassium acetate media, and cultured under rigorous shaking at 30°C. For spore viability assay, overnight cultures in YPD media were washed four times with pre-warmed

water, and released into sporulation in 1,5% potassium acetate solution for 3 days at RT. Samples were digested for 5min with zymolase, and tetrads were dissected. Survival of spores on YPD plates was scored after 3 days.

Analyses of protein-protein interactions using the two-hybrid system

All full-length ORFs, fragments and mutant variants of proteins used for yeast-two hybrid assays in this study (Red1, Zip1, etc.) were fused to the C-terminus of the DNA-binding domain (BD) or activation domain (AD) of the Gal4 protein by cloning them into pGBD-C1 or pGAD-C1 vectors, respectively. The expression constructs were used to transform PJ69-7A cells (James et. al., 1996) and spotted on –His plates (SC^{-leu-trp-his}) plates for selection or control plates (SC^{-leu-trp}). Physical interaction between BD- and AD-fusion proteins leads to reconstitution of the Gal4 transcription factor, which induces expression of *HIS3* and *ADE2* reporter genes and allows cell growth on the respective selection plates. White colony colour is indicative of better growth. Images were usually taken after growth for 3 days at 30°C.

V.3 Cell biological techniques

V.3.1 Tissue culture

Mammalian cell lines and expression vectors

Cell lines	Origin
HEK 293T	human embryonic kidney cells
U2OS	human osteosarcoma cells
Expression vector	Source
pCI	Stefan Müller, MPIB

Plasmid constructs for tissue culture

For mammalian studies, human Sycp3 was cloned into a pCI vector (T7 promoter, HA-tag). All other constructs used for mammalian SUMO studies were kindly provided by the group of Dr. Stefan Müller (MPIB).

Cultivation of mammalian cell lines

In this study, all mammalian cells were cultured at 37°C with 7,5% CO₂ and 96% humidity using special culture dishes (Falcon). Dulbecco's Modified Eagle Medium (GIBCO-BRL) complemented with 10% heat-inactivated fetal bovine serum (GIBCO-BRL) and 1% Penicillin/Streptomycin mixture (GIBCO-BRL) were used as the growth medium. When cells reached a confluence of 80-100%, cultures were splitted. For this, cells were washed once with PBS, and removed from the culture dish by incubation for 5min at 37°C with 2ml/150cm² trypsin/EDTA solution (GIBCO-BRL). The cell suspension was resuspended in medium, centrifuged (4min, 400g, 23°C) and the pellet was resuspended in fresh medium and inoculated in new culture dishes at 1:5-1:10 dilutions. The number of cells was counted using an automated cell counter (Beckman).

Transfection of mammalian cell lines

Mammalian cells were transfected using the Lipofectamine Plus Transfection Kit (Invitrogen) using the manufacturer's instructions. Generally, 0.5µg plasmid DNA was used for transfection of 3×10^7 cells. GFP constructs can be used as transfection controls.

V.3.2 Live-cell microscopy

Synaptonemal complex formation was studied (Scherthan et al., 2007) by spinning disk microscopy. An ANDOR/TiLL iMIC CSU22 spinning disk confocal microscope with a 100x 1.45NA objective lens (Olympus) was used to capture image stacks of 250nm step-size. Diploid $\Delta zip1 \Delta red1$ strains with an integrated Zip1-GFP construct were transformed with exactly two copies of RED1 WT or mutant versions (as tested by real-time PCR) and released into synchronous sporulation. Samples were taken at the respective time-point, directly mounted onto Concanavalin A-coated glass bottom dishes (MatTek), and immediately observed under the microscope. After taking a bright-field picture to count the total number of cells in the respective field, several stacks of the Zip1-GFP fusion signal were monitored. For data analysis, maturation of SCs was categorized into five classes: early stage, diffuse, dot-like, pre-SCs and full SCs. For quantification, only pre-SCs and full SCs were distinguished. For each time-point more than 100 cells were analyzed.

V.4 Molecular biology techniques

General buffers and solutions

Breaking buffer

- 2% (v/v) Triton X-100
- 1% (w/v) SDS
- 100 mM NaCl
- 10 mM Tris-HCl, pH 8.0
- 1 mM EDTA, pH 8.0

TE buffer

- 10 mM Tris-HCl, pH 8.0
- 1 mM EDTA
- sterilized by autoclaving

TBE buffer (5x)

- 90 mM Tris
- 90 mM boric acid
- 2.5 mM EDTA, pH 8.0
- sterilized by autoclaving

DNA loading buffer (6x)

- 0.5% (w/v) SDS
- 0.25% (w/v) bromophenol blue or orange G
- 0.25% (v/v) glycerol
- 25 mM EDTA, pH 8.0

*V.4.1 Isolation of DNA***Isolation of plasmid DNA from *E. coli***

LB medium (5 ml) containing the appropriate antibiotic was inoculated with a single *E. coli* colony harbouring the DNA plasmid of interest and incubated with shaking overnight at 37°C. Plasmids were isolated using commercially available kits from either Qiagen (Plasmid Mini Kit) or Bioneer (AccuPrep Plasmid Mini Extraction Kit) according to the manufacturer's instructions.

Isolation of chromosomal DNA from *S. cerevisiae*

Chromosomal yeast DNA was isolated as a template for the amplification of yeast genes via PCR. Therefore, cells from a saturated yeast culture (10ml) were sedimented by centrifugation (1500g, 5min, 23°C), washed once in 0.5ml water and resuspended in 200µl breaking buffer. Next, 200µl phenol/chloroform/isoamyl alcohol (24:24:1 v/v/v; Roth) and 0.3g glass beads (ø 425-600µm; Sigma) were added and cells lysed by vortexing for 3min. The lysate was mixed with 200µl TE buffer and centrifuged (13000rpm, 5min, 23°C). The aqueous layer was transferred to a fresh microcentrifuge tube and the DNA was precipitated by adding 1ml of 100% ethanol and by subsequent centrifugation (13000rpm, 5min, 23°C). The pellet was resuspended in 0.4ml TE buffer and in order to degrade RNA contamination, 30µl of DNase-free RNase A (1mg/ml; Sigma) was added for 5min at 37°C. DNA was again precipitated with 1ml of 100% ethanol and 10µl of 4M ammonium acetate, briefly centrifuged and the pellet resuspended in 100µl TE buffer. The yield of the isolated DNA was estimated photometrically.

Precipitation of DNA

For ethanol precipitation, 1/10 volume sodium acetate (3M, pH 4.8) and 2.5 volumes ethanol were added to the DNA solution and incubated at -20 °C for 30min. The mixture was centrifuged (13000rpm, 20min, 4°C) and the pellet was washed once with 0.5ml of 70% ethanol. Finally, the DNA pellet was air-dried and resuspended in TE buffer or sterile water.

Determination of DNA concentration

The DNA concentration was photometrically determined by measuring the absorbance at a wavelength of 260nm (OD₂₆₀) using the NanoDrop ND-1000 spectrophotometer (PeqLab). An OD₂₆₀ of 1 equals a concentration of 50µg/ml double-stranded DNA.

V.4.2 Polymerase chain reaction (PCR)

In order to specifically amplify DNA fragments from small amounts of DNA templates PCR techniques were used. This technique was applied for amplification of DNA fragments for subsequent cloning, amplification of targeting cassettes (for chromosomal gene disruptions and epitope tagging), PCR screening of genomic recombination events (“colony-PCR”), site-directed mutagenesis and quantitative real-time PCR. Except for real-time PCR, all PCR reactions were prepared in 0.2ml tubes (Biozym) on ice, in a volume of 25-50µl for preparative PCR.

Amplification of genomic DNA fragments

For the construction of genomic DNA fragments for subsequent cloning, full-length ORFs or selected truncations were amplified from genomic DNA using the highly accurate *Phusion*TM DNA polymerase (Finnzymes). The PCR reactions were prepared as indicated and cycling parameters used as listed in the following:

PCR reaction mix:

- 0.2 µg genomic DNA
- 10 µl 5x HF buffer
- 1.0 µl dNTP-Mix (10 mM each; New England Biolabs)
- 2.5 µl forward primer (10 µM)
- 2.5 µl reverse primer (10 µM)
- 0.5 µl *Phusion* DNA polymerase
- 31.5 µl dH₂O

Cycling parameters for genomic PCR (32 amplification cycles):

PCR step	T (°C)	Time
Initial denaturation	98	3 min
Denaturation	98	45 s
Annealing	48-55	45 s
Elongation	72	2-4 min
Final elongation	72	10 min
Cooling	4	∞

Amplification of targeting cassettes

Chromosomal gene deletions and epitope tagging of genes was performed by a PCR strategy based on the targeted introduction of heterologous DNA into genomic locations (Janke et al., 2004). Targeting cassettes were amplified by PCR using primers containing homology to the genomic target locus. The PCR reactions were prepared as indicated in the following, cycling conditions are described previously (Janke et al., 2004). After amplification, PCR products were concentrated by ethanol precipitation, solved in an appropriate volume of sterile water and directly used for the transformation of competent yeast cells.

PCR reaction mix:

- 50 ng plasmid DNA
- 5 µl 10x Thermopol buffer (New England Biolabs)
- 1.0 µl dNTP-Mix (10 mM each; New England Biolabs)
- 3.2 µl forward primer (10 µM)
- 3.2 µl reverse primer (10 µM)
- 0.4 µl *Taq* DNA polymerase (New England Biolabs)
- 0.5 µl *Vent* DNA polymerase (New England Biolabs)
- 31.25 µl dH₂O

PCR screening of genomic recombination events (“colony-PCR”)

For the verification of chromosomal gene disruptions, correct recombination events were identified by “colony-PCR”. The screening strategy is based on oligonucleotide probes, which anneal in the promoter region of the respective gene (forward primer) or in the marker gene (reverse primer). Prior to the PCR, a single yeast colony from a selective plate was resuspended in 20µl and incubated at 95°C for 5min with rigorous shaking (1400rpm). Next, the solution was briefly centrifuged (1300rpm, RT) and 4.0µl of the supernatant were directly used as a template for PCR. The PCR reactions were prepared as indicated below and cycling conditions are listed in the following table.

PCR reaction mix:

- 4.0 µl template DNA
- 5 µl 10x Thermopol buffer (New England Biolabs)
- 1.0 µl dNTP-Mix (10 mM each; New England Biolabs)
- 3.2 µl forward primer (10 µM)
- 3.2 µl reverse primer (10 µM)
- 0.8 µl MgSO₄ (100 mM; New England Biolabs)
- 0.4 µl *Taq* DNA polymerase (New England Biolabs)
- 31.6 µl dH₂O

Cycling parameters for “colony PCR” (32 amplification cycles):

PCR step	T (°C)	Time
Initial denaturation	94	5 min
Denaturation	94	30 s
Annealing	50	30 s
Elongation	68	1 min/kb
Final elongation	68	4 min
Cooling	4	∞

Site-directed mutagenesis

To introduce specific point mutations or deletions in DNA sequences, a PCR-based strategy was developed according to the Quick-change protocol (Stratagene). This method uses two complementary oligonucleotide primers with the codon to be mutated in the middle of the sequence flanked by at least 15 additional base pairs, each corresponding to the target sequence. The

PCR was prepared in a volume of 25 μ l as shown below and cycling conditions were chosen as indicated in the following table.

PCR reaction mix:

- 0.5 μ l plasmid DNA (Mini preparation)
- 2.5 μ l 10x Pfu Buffer (Stratagene)
- 0.6 μ l dNTP-Mix (10mM each; New England Biolabs)
- 0.5 μ l mutagenesis primer #1 (100 μ M)
- 0.5 μ l mutagenesis primer #2 (100 μ M)
- 0.5 μ l *Pfu Turbo* DNA polymerase (Stratagene)
- 20 μ l dH₂O

Cycling parameters for site-directed mutagenesis PCR (19 amplification cycles):

PCR step	T (°C)	Time
Initial denaturation	94	3 min
Denaturation	94	30 s
Annealing	49	45 s
Elongation	68	16 min
Final elongation	68	16 min
Cooling	4	∞

In order to eliminate template DNA (which does not harbor the mutation), 17 μ l of the PCR products were treated with 1 μ l *DpnI* endonuclease (and 2 μ l of the respective buffer) for 2-3 hours at 37°C. *DpnI* endonuclease is specific for methylated and hemimethylated DNA and as most plasmid DNA from *E. coli* is methylated, *DpnI* treatment of the PCR product leads to the selective digestion of the parental DNA template. After dialysis, the PCR product was directly used for transformation and mutated plasmids were identified by DNA sequencing.

Real-time PCR

The real-time PCR method was used to quantify the integration events of Red1 WT and mutants on an integrative vector. For this, a primer pair specific for the Red1 ORF were used for the reaction and compared to control primers annealing at a unrelated locus in the genome. For analysis by real-time PCR, chromosomal yeast DNA was isolated from yeast overnight cultures (5 OD cells) as described earlier in this section and resuspended in TE buffer for subsequent real-time PCR analysis. Samples for real-time PCR were prepared as shown in the following using the cycling parameters indicated below. The PCR reaction mix is based on the Light Cycler 480 SYBR Green I Master system (Roche), the PCR reactions were run in a Light Cycler 480 (Roche).

Real-time PCR reaction mix:

- 2 μ l genomic DNA (from chromosomal DNA preparation)
- 10 μ l Taq-Mix (Roche)
- 0.12 μ l 100 μ M forward primer
- 0.12 μ l 100 μ M reverse primer
- 7.76 μ l dH₂O

Cycling parameters for real-time PCR (45 amplification cycles)

PCR step	T (°C)	Time
Initial denaturation	95	10 min
Denaturation	95	10 s
Annealing	55	10 s
Elongation	72	16 s
Denaturation	95	30 s
Annealing	65	30s
Stepwise denaturation	65-95	(ramp rate 0.11 °C/s)
Cooling	40	30s

*V.4.3 Cloning of plasmid constructs***Digestion of DNA with restriction enzymes**

The sequence-specific cleavage of DNA with restriction enzymes was performed according to standard protocols (Sambrook et al., 1989) and the instructions of the manufacturer (New England Biolabs). In general, 5 to 10 units of the respective restriction enzyme were used for digesting 1µg DNA. Reaction samples were incubated in the appropriate buffers (New England Biolabs) at the recommended temperature. Usually, circular vectors were digested for 1-2 hours, while PCR products were digested overnight. In order to avoid re-circulation of linearized vectors (without the insert fragment), the 5' end of the vector DNA was dephosphorylated by incubation at 37°C for 1h with 1µl of the calf intestinal phosphatase (CIP; New England Biolabs).

Separation of DNA by gel electrophoresis

To isolate DNA fragments, DNA samples were mixed with 6x DNA loading buffer and subjected to electrophoresis using 1.5% agarose gels containing 0.5µg/ml ethidium bromide at 120V in TBE buffer. Separated DNA fragments could be visualized by using an UV transilluminator (324 nm), due to intercalation of ethidium bromide into DNA. The size of the fragments was estimated using standard size markers (1kb DNA ladder, Invitrogen).

Isolation of DNA fragments from agarose gels

After separation by gel electrophoresis, DNA fragments were excised from the agarose gel using a sterile razor blade. DNA was then extracted from the agarose block using kits from Qiagen (QIAquick Gel Extraction Kit) or Bioneer (AccuPrep Gel Purification Kit) according to manufacturer's instructions and eluted with an appropriate volume of sterile water.

Ligation of DNA fragment

The amounts of linearized vector and insert fragments were estimated by electrophoresis in an agarose gel containing ethidium bromide. Typically, a vector to insert ratio of around 1:7 – 1:10 was used for the ligation reaction, which was carried out by the T4 DNA ligase (10 units per 100ng DNA; New England Biolabs). Religation of the linearized vector was controlled using samples containing sterile water instead of insert DNA. The ligation reactions were incubated overnight at 16°C, then dialyzed against water for 15min

on a nitrocellulose filter (pore size 0.05 μ m; Millipore) and were directly used for the transformation of electro-competent *E. coli* bacteria.

DNA sequencing

DNA sequencing was carried out at the Microchemistry Core Facility (Max Planck Institute of Biochemistry) using an ABI 3730 sequencing machine. The sample usually contained 0.5 μ g of plasmid DNA and 5pmol primer. Sample preparation and sequencing reactions were performed with the DYEnamic ET terminator cycle sequencing kit (Amersham-Pharmacia) according to manufacturer's instructions.

V.5 Biochemical techniques

Antibodies

Antibodies were used in this study for detection of proteins by immunoblotting, for studying protein-protein interactions by immunoprecipitation and for observing intracellular localization of proteins by immunofluorescence microscopy.

Primary antibodies	Source
Red1 (polyclonal)	this study
Rad52 (polyclonal)	(Sacher et al., 2006)
Zip1 (polyclonal)	Michael Knop (EMBL)
PCNA (polyclonal)	Carsten Höge
Pgk1 (monoclonal)	Molecular Probes
GAL-TA (C-10) AD (monoclonal)	Santa Cruz
GAL4 (DBD) BD (monoclonal)	Santa Cruz
SUMO (yeast Smt3; polyclonal)	Carsten Höge
p53 (DO-1; monoclonal)	Santa Cruz
HA (Clone 16B12; monoclonal)	Convance
H2A-serine 129-phospho (polyclonal)	Upstate
Secondary antibodies	Source
HRP-coupled anti-rabbit IgG	Dianova
HRP-coupled anti-mouse IgG	Dianova
HRP-coupled anti-Protein A IgG	DAKO

V.5.1 Gel electrophoresis and immunoblot techniques

General buffers and solutions

HU sample buffer:

- 200 mM Tris, pH 6.8
- 8 M urea
- 5% (w/v) SDS
- 1 mM EDTA
- 1.5% (w/v) DTT
- 0.1% (w/v) bromophenol blue

Laemmli sample buffer:

- 2% (w/v) SDS
- 20% (v/v) glycerol
- 100 mM Tris base
- 60 mM EDTA
- 0.1% (w/v) bromophenol blue

MOPS running buffer:

- 50 mM MOPS
- 50 mM Tris base
- 3.5 mM SDS
- 1 mM EDTA

Coomassie brilliant blue solution:

- 20% (v/v) methanol
- 10% (v/v) acetic acid
- 0.1% (w/v) Coomassie Brilliant Blue R-250

Destaining solution:

- 20% (v/v) methanol
- 10% (v/v) acetic acid

Blotting buffer:

- 250 mM Tris base
- 1.92 M glycine
- 0.1% (w/v) SDS
- 20% (v/v) methanol

TBST:

- 25 mM Tris-HCl, pH 7.5
- 137 mM NaCl
- 2.6 mM KCl
- 0.1% (v/v) Tween 20

Stripping buffer:

- 4 % (w/v) SDS
- 100 mM β -mercaptoethanol
- 62.5 mM Tris/HCl, pH 6.8

SDS polyacrylamide gel electrophoresis (SDS-PAGE)

For separation of proteins, SDS-PAGE was performed in Mighty Small electrophoresis chambers (Hoefer) using 4-12% gradient Bis-Tris polyacrylamide gels (Invitrogen or self-poured; see table below). These gels allow resolution of proteins over a large range of different molecular weights (10-200kDa) and do not require stacking gels. Generally, samples were prepared in Laemmli or HU sample buffer and denatured by heating for 5min at 95°C or 10min at 65 °C, respectively. Next, electrophoresis was carried out at a constant voltage of 140 V using MOPS as a running buffer. The *All Blue Precision Plus Protein Pre-stained Standard* (Bio-Rad) was used as a molecular weight marker. Subsequently the gels were subjected to coomassie staining or immunoblotting.

Solutions for pouring 4-12% Bis-Tris SDS-PAGE gradient gels:

	4% solution	12% solution
30% acrylamide/0.8% bis-acrylamide (ProtoGel; National diagnostics)	2.2 ml	6.6 ml
2.5 M Bis-Tris-HCl pH 7.5	2.4 ml	2.4 ml
65% (w/v) sucrose	---	1.2 ml
10% (w/v) SDS	82.5 μ l	82.5 μ l
10% (w/v) ammonium peroxodisulphate	82.5 μ l	82.5 μ l
TEMED (Sigma)	16.5 μ l	16.5 μ l
dH ₂ O	11.85 ml	6.2 ml

Coomassie staining of protein gels

For visualization of proteins bands after separation by electrophoresis, gels were stained for 30min in coomassie solution and the background was subsequently removed by intensive washing in destaining solution.

Western blotting

The transfer of proteins separated by gel electrophoresis onto PVDF membranes (ImmobilonTM-P, 0.45 μ m pore size; Millipore) in a wet tank blot system (Hofer). Western blotting was carried out using blotting buffer and a constant voltage of 70V for 90min at 4°C.

Immunological detection of membrane-bound proteins

Directly after protein transfer, the blotting system was disassembled and the membrane was blocked by shaking in 5 % (w/v) skim milk powder (Fluka) in TBST for 30min at RT. After addition of the primary antibody, the blots were incubated overnight at 4°C on a shaking platform. The next day, the membrane was washed 3 times for 5min in TBST and incubated for 1 h with a secondary antibody coupled to horseradish peroxidase (Dianova) dissolved 1:2000-1:5000 in 5% milk in TBST. Afterwards, the membrane was washed five times for 5min with TBST and subjected to chemiluminescence detection. For the chemiluminescence detection of specific proteins the Amersham ECLTM and the ECLTM Advance western blotting detection systems (GE Healthcare) were used according to the manufacturer's instructions. Immunoblots were then visualized by exposure of the membrane to a chemiluminescence film (Amersham Hyperfilm ECL, GE Healthcare) with variable exposure times and subsequent automated film development. Alternatively, a CCD (charged-coupled device) camera (LAS 3000, Fujifilm) was used for signal detection. Digitalized images acquired by a CCD camera were quantified with the software program Image Gauge V4.1 (Fujifilm).

Stripping of immunoblot membranes

For the sequential incubation of immunoblot membranes with different primary antibodies, bound immunoglobulins were removed by incubating the PVDF membranes in stripping buffer for 30min at 60°C. Afterwards, the membrane was washed twice for 10min with TBST and then subjected to blocking and probing with the next primary antibody.

V.5.2 Preparation of cell extracts

Preparation of denatured yeast extracts

In order to preserve post-translational modifications, yeast cells were lysed under denaturing conditions. For preparation of denatured protein extracts, 1ml of a yeast culture of $OD_{600}=1$ were pelleted by centrifugation (13000rpm, 3min, RT) and immediately frozen in liquid nitrogen. After thawing on ice, the pellets were resuspended in 1ml ice-cold sterile water and lysed by addition of 150 μ l denaturing lysis buffer (1.85M NaOH, 7.5% β -mercaptoethanol) on ice for 15min. For protein precipitation, the lysate was mixed with 150 μ l 55% (w/v) trichloroacetic acid (TCA) and further incubated on ice for 10min. The precipitated material was recovered by two centrifugation steps (13000rpm, 4°C, 15min). The thus prepared protein pellet was resuspended in 50 μ l sample buffer and stored at -20°C.

Preparation of native yeast extracts

Native protein extracts were used for immunoprecipitation and GST-pull-down experiments. For that, logarithmically growing yeast cells were harvested by centrifugation, washed once with ice-cold PBS and resuspended in an equal volume of lysis buffer (Tris-HCl, pH 7.4, 150mM NaCl) containing protease inhibitors (complete inhibitor set (Roche), Pefabloc SC (Roche), and 20mM NEM). After adding glass beads (ϕ 425-600 μ m, Sigma) the cells were lysed by vortexing 4 times for 1.5min at 4°C or using a bead beater (Retsch). To remove glass beads and cell debris, samples were briefly centrifuged (500g, 5min, 4°C). Supernatants were collected, incubated with 1% Triton and 0.05% SDS for 30min at 4°C and followed by centrifugation (14000rpm, 15min, 4°C). Next, the protein concentration of those extracts was determined using the NanoDrop ND-1000 spectrophotometer (PeqLab) and were directly used for co-immunoprecipitation or GST-pull-down experiments.

Preparation of denatured extracts from mammalian cells

HEK 293 T cells were transfected in 10cm diameter dishes as described before. For the preparation of mammalian cell extracts, HEK 293T cells were harvested 36-48 hours after transfection, washed once with PBS and lysed in 1ml lysis buffer (6M Guanidine-HCl, 0.1M NaH_2PO_4 , 0.05% Tween 20, 0.01M Tris, pH adjusted to 8.0 with NaOH). Samples were then sonicated to shear DNA, centrifuged and 100 μ l of the supernatant was used for TCA preparation, while the remaining 900 μ l were subjected to Ni-NTA pulldown. Briefly, for TCA preparation, 100 μ l of the supernatant from the step before were mixed with an equal volume of 10% TCA, vortexed and incubated on ice for 15min. After centrifugation (13000rpm, 15min, 4°C) pellets were washed with 200 μ l ice-cold ethanol, again centrifuged and the pellet dried in a SpeedVac (Eppendorf). Finally, the protein input samples were denatured by boiling for 15min at 95°C and directly used for loading on gels using SDS-PAGE.

V.5.3. Protein purification and binding experiments

Purification of recombinant proteins from *E. coli*

GST-tagged protein or His-tagged proteins were expressed in *E. coli* BL21DE3/RIL cells. In general, recombinant proteins were purified by affinity chromatography for the respective tag.

For purifying GST-fusion proteins, cells from 1l bacterial culture were resuspended in 30ml PBS (containing 0.1mM EDTA and protease inhibitors), lysed by high pressure in an Emulsiflex C5 cell disruptor (Avestin). Next, TritonX-100 was added to the lysate to a final concentration of 1%, incubated for 30min at 4°C and centrifuged (20000g, 30min, 4°C). Afterwards, the supernatant was mixed with Gluthathion Sepharose (Amersham) for 3h at 4°C. After centrifugation (500g, 2min, 4°C), the beads were washed once with PBS (containing 300mM NaCl and 1% Triton) and twice with PBS (containing 0.1% Triton). After a final wash step with PBS, the GST-tagged proteins were eluted from the beads by several incubations (5-8 times) with equal volumes of 50mM Tris pH8.0 containing 25mM reduced Glutathione and 0.1% TritonX-100. The eluted protein fractions were analyzed by gel electrophoresis and coomassie staining, pooled and dialyzed twice overnight against PBS at 4°C and frozen in liquid nitrogen.

His-tagged recombinant proteins were also purified from *E. coli* by affinity chromatography for the tag. For that, cell pellets from 1l bacterial culture were resuspended in Ni-NTA lysis buffer, lysed in an Emulsiflex C5 cell disruptor (Avestin) and sonicated for 2min using a Sonopuls HD2200 sonicator (Bandelin). After centrifugation (20000g, 30min, 4°C) the supernatant was incubated for 3h with Ni-NTA Agarose (Qiagen). Next, the agarose was washed several times with Ni-NTA washing buffer, bound proteins were eluted by repeated incubations with Ni-NTA elution buffer and further treated as described above.

Ni-NTA buffers:

- 300mM NaCl
- 50mM NaH₂PO₄, pH8.0
- 10mM Imidazole (lysis buffer),
20mM Imidazole (washing buffer)
or 250mM Imidazole (elution buffer)

Ni-NTA chromatography from yeast extracts

For isolation of ubiquitinated or SUMOylated yeast proteins, denatured extracts were prepared and Ni-NTA chromatography carried out. In general, 200ml of logarithmically growing cells (OD₆₀₀=1) were harvested by centrifugation (4000g, 5min, 4°C), washed with cold dH₂O and lysed with 6ml 1.85M NaOH/ 7.5% (v/v)-mercaptoethanol for 15min on ice. The proteins were precipitated by adding 6ml 55% TCA and another 15min incubation on ice. Next, the precipitate was pelleted by centrifugation (3500rpm, 15min, 4°C), washed twice with acetone and finally resuspended in buffer A (6M

guanidinium-hydrochloride, 0.1M NaH₂PO₄, 0.01M Tris-HCl, pH8, 20mM imidazole) containing 0.05% Tween- 20 and incubated for 1h at RT on a shaker. After removal of insoluble aggregates by centrifugation (13000g, 20min, 4°C), the protein solution was incubated overnight (4°C, rolling) with 50µl Ni-NTA magnetic agarose beads (Qiagen) or with Dynabeads TALON (Invitrogen) in the presence or absence of 20mM imidazole, respectively. The next day, the beads were washed three times with buffer A containing 0.05% Tween-20 and five times with buffer C (8M urea, 0.1M NaH₂PO₄, 0.01M Tris-HCl, pH6.3) with 0.05% Tween-20. Proteins bound to the beads were finally eluted by incubation with 20µl 1% SDS at 65°C, dried in a SpeedVac (Eppendorf) and heated in 10µl sterile water and 25µl HU sample buffer for subsequent analysis by gel electrophoresis and immunoblot. Usually, to control for pulldown efficiency, ^{His}Pol30 (PCNA)-expressing cultures were mixed with the yeast cultures before lysis and pulldown, and ^{His}Pol30 was detected by Western analysis using an anti-Pol30 antibody.

NiNTA-chromatography of mammalian cell extracts

For capturing ^{His}SUMO from mammalian cell extracts, denatured mammalian cell extracts transfected with ^{His}SUMO overexpression as well as HA-tagged human Sycp3 constructs were prepared as described before. Principally an adapted protocol described previously (Treier et al., 1994) was used for that purpose. 900µl of lysed and cleared mammalian denatured extract were incubated with 20µl magnetic Ni-Agarose beads (Quiagen) overnight on a rotating wheel. To remove the supernatant, the tubes were placed in a magnetic stand and the supernatant was aspirated with a 26G needle. Next, beads were washed 6-8 times with wash buffer A (8M Urea, 0.1M NaH₂PO₄, 0.05% Tween 20, 0.01M Tris, pH adjusted to 8.0 with NaOH) and finally, once with PBS. After removal of PBS, the beads were boiled for 5min at 95°C in 80µl Lämmli sample buffer and loaded on a gel for subsequent analysis by immunoblotting.

Co-immunoprecipitation from native yeast extracts

Protein-protein interactions from native yeast extracts were analyzed by immunoprecipitation experiments. In general, native yeast extracts (500µl of 10µg/µl) of strains expressing e.g. Rad17^{PrtA} or ^{3HA}Red1 under their endogenous promoter (or an untagged version as a control) were incubated with 25µl of the respective antibodies coupled to beads (IgG or anti-HA beads) for 3 hours at 4°C. Background binding was removed by washing 5 times with PBS containing 1% TritonX-100 and 0-0.05% SDS. Finally, proteins were eluted from the beads by boiling in HU buffer and identified by Western blot analysis.

GST-pulldowns from native yeast extracts

For GST-pulldown assays, 50µg of GST-Zip1 and GST-Red1 (full-length or fragment of either wild-type or a mutant version) as well as GST alone for control were bound to sepharose beads for 2h at 4°C. Next, the beads were incubated with 5mg of yeast native lysate for 3h at 4°C, washed four times with the respective incubation buffer, eluted in HU sample buffer and loaded

on a gel for electrophoresis and subsequent immunoblot analysis.

Affinity purification of polyclonal antibodies

In the course of this study, Red1 peptides were designed for immunization of rabbits and generation of polyclonal antibodies. The immunization of rabbits was carried out by a company (Eurogentec), all further antibody purification steps were done following the SulfoLink Coupling Gel method (Pierce) according to the instructions of the manufacturer. In principal, this method allows covalent immobilization of sulfhydryl-containing peptides (the same that were used for the immunization of the rabbit) to agarose beads, which were used for affinity purification procedures of high affinity anti-Red1 antibodies from the rabbit serum.

Chromatin binding assay

In order to enrich Protein A-tagged 9-1-1 subunits on chromatin, the chromatin fraction was purified from yeast cells as described in (Kai et al., 2001). Therefore, 25ml logarithmically growing cells ($OD_{600}=1$) cell cultures were harvested by centrifugation (4000g, 10min, 4°C), washed with SP1 buffer. Next, spheroplasts were generated by digestion with Zymolyase100T (Seikagaku) in SP1 buffer for 15min at 30°C and the reaction was stopped by addition of buffer SP2. The spheroplasts were further washed with 1.2M sorbitol and lysed with 1% Triton in lysis buffer. The chromatin was then pelleted by centrifugation (12000g, 10min, RT). After washing the pellets with lysis buffer containing 150mM NaCl (to remove background binding) and digestion with DNase (Roche, to release chromatin-bound proteins), the chromatin fraction was analyzed by immunoblotting using the respective antibodies.

SP1 buffer:

- 1.2 M sorbitol
- 50 mM $MgSO_4$
- 100 mM K_3PO_4 , pH7.4

SP2 buffer:

- 1 M sorbitol
- 5 mM $MgSO_4$
- 1 mM EDTA
- 25 mM MES, pH6.4

Lysis buffer:

- 1 M sorbitol
- 50 mM potassiumacetate
- 2 mM $MgCl_2$
- 20 mM HEPES, pH7.9
- protease inhibitors

VI REFERENCES

Agarwal, S., and Roeder, G. S. (2000). Zip3 provides a link between recombination enzymes and synaptonemal complex proteins. *Cell* *102*, 245-255.

Alani, E., Thresher, R., Griffith, J. D., and Kolodner, R. D. (1992). Characterization of DNA-binding and strand-exchange stimulation properties of γ -RPA, a yeast single-strand-DNA-binding protein. *J Mol Biol* *227*, 54-71.

Amerik, A. Y., and Hochstrasser, M. (2004). Mechanism and function of deubiquitinating enzymes. *Biochim Biophys Acta* *1695*, 189-207.

Ausubel, F. M., Brent, R., Kingston, R. E., Moore, D. D., Seidman, J. G., Smith, J.A., and Struhl, K. (1994). *Current Protocols in Molecular Biology*. Green and Wiley, New York.

Baba, D., Maita, N., Jee, J. G., Uchimura, Y., Saitoh, H., Sugasawa, K., Hanaoka, F., Tochio, H., Hiroaki, H., and Shirakawa, M. (2005). Crystal structure of thymine DNA glycosylase conjugated to SUMO-1. *Nature* *435*, 979-982.

Bachant, J., Alcasabas, A., Blat, Y., Kleckner, N., and Elledge, S. J. (2002). The SUMO-1 isopeptidase Smt4 is linked to centromeric cohesion through SUMO-1 modification of DNA topoisomerase II. *Mol Cell* *9*, 1169-1182.

Bailis, J. M., and Roeder, G. S. (1998). Synaptonemal complex morphogenesis and sister-chromatid cohesion require Mek1-dependent phosphorylation of a meiotic chromosomal protein. *Genes Dev* *12*, 3551-3563.

Bailis, J. M., and Roeder, G. S. (2000). Pachytene exit controlled by reversal of Mek1-dependent phosphorylation. *Cell* *101*, 211-221.

Barlow, J. H., Lisby, M., and Rothstein, R. (2008). Differential regulation of the cellular response to DNA double-strand breaks in G1. *Mol Cell* *30*, 73-85.

Bergink, S., Jentsch, S. (2009). Principles of ubiquitin and SUMO modifications in DNA repair. *Nature* *458*, 461-7.

Bishop, D. K., Park, D., Xu, L., and Kleckner, N. (1992). DMC1: a meiosis-specific yeast homolog of *E. coli* recA required for recombination, synaptonemal complex formation, and cell cycle progression. *Cell* *69*, 439-456.

Boiteux, S., and Guillet, M. (2004). Abasic sites in DNA: repair and biological consequences in *Saccharomyces cerevisiae*. *DNA Repair (Amst)* *3*, 1-12.

Bonilla, C. Y., Melo, J. A., and Toczyski, D. P. (2008). Colocalization of sensors is sufficient to activate the DNA damage checkpoint in the absence of damage. *Mol Cell* *30*, 267-276.

Borner, G. V., Kleckner, N., and Hunter, N. (2004). Crossover/noncrossover differentiation, synaptonemal complex formation, and regulatory surveillance at the leptotene/zygotene transition of meiosis. *Cell* *117*, 29-45.

Bowman, G. D., O'Donnell, M., and Kuriyan, J. (2004). Structural analysis of a eukaryotic sliding DNA clamp-clamp loader complex. *Nature* *429*, 724-730.

Branzei, D., Sollier, J., Liberi, G., Zhao, X., Maeda, D., Seki, M., Enomoto, T., Ohta, K., and Foiani, M. (2006). Ubc9- and mms21-mediated sumoylation counteracts recombinogenic events at damaged replication forks. *Cell* *127*, 509-522.

Branzei, D., Vanoli, F., and Foiani, M. (2008). SUMOylation regulates Rad18-mediated template switch. *Nature* *456*, 915-920.

Burgess, R. C., Rahman, S., Lisby, M., Rothstein, R., and Zhao, X. (2007). The Slx5-Slx8 complex affects sumoylation of DNA repair proteins and negatively regulates recombination. *Mol Cell Biol* *27*, 6153-6162.

Bylebyl, G. R., Belichenko, I., and Johnson, E. S. (2003). The SUMO isopeptidase Ulp2 prevents accumulation of SUMO chains in yeast. *J Biol Chem* *278*, 44113-44120.

Carballo, J. A., and Cha, R. S. (2007). Meiotic roles of Mec1, a budding yeast homolog of mammalian ATR/ATM. *Chromosome Res* *15*, 539-550.

Carballo, J. A., Johnson, A. L., Sedgwick, S. G., and Cha, R. S. (2008). Phosphorylation of the axial element protein Hop1 by Mec1/Tel1 ensures meiotic interhomolog recombination. *Cell* *132*, 758-770.

Cheng, C. H., Lo, Y. H., Liang, S. S., Ti, S. C., Lin, F. M., Yeh, C. H., Huang, H. Y., and Wang, T. F. (2006). SUMO modifications control assembly of synaptonemal complex and polycomplex in meiosis of *Saccharomyces cerevisiae*. *Genes Dev* *20*, 2067-2081.

Chu, S., DeRisi, J., Eisen, M., Mulholland, J., Botstein, D., Brown, P. O., and Herskowitz, I. (1998). The transcriptional program of sporulation in budding yeast. *Science* *282*, 699-705.

Chua, P. R., and Roeder, G. S. (1998). Zip2, a meiosis-specific protein required for the initiation of chromosome synapsis. *Cell* *93*, 349-359.

Clancy, M. J. (1998). Meiosis: step-by-step through sporulation. *Curr Biol* *8*, R461-463.

Dawlaty, M. M., Malureanu, L., Jeganathan, K. B., Kao, E., Sustmann, C., Tahk, S., Shuai, K., Grosschedl, R., and van Deursen, J. M. (2008). Resolution of sister centromeres requires RanBP2-mediated SUMOylation of topoisomerase IIalpha. *Cell* *133*, 103-115.

Denison, C., Rudner, A. D., Gerber, S. A., Bakalarski, C. E., Moazed, D., and Gygi, S. P. (2005). A proteomic strategy for gaining insights into protein sumoylation in yeast. *Mol Cell Proteomics* *4*, 246-254.

Desterro, J. M., Rodriguez, M. S., and Hay, R. T. (1998). SUMO-1 modification of I κ B α inhibits NF- κ B activation. *Mol Cell* *2*, 233-239.

- Deveraux, Q., Ustrell, V., Pickart, C., and Rechsteiner, M. (1994). A 26 S protease subunit that binds ubiquitin conjugates. *J Biol Chem* *269*, 7059-7061.
- Dionne, I., Nookala, R. K., Jackson, S. P., Doherty, A. J., and Bell, S. D. (2003). A heterotrimeric PCNA in the hyperthermophilic archaeon *Sulfolobus solfataricus*. *Mol Cell* *11*, 275-282.
- Dong, H., and Roeder, G. S. (2000). Organization of the yeast Zip1 protein within the central region of the synaptonemal complex. *J Cell Biol* *148*, 417-426.
- Downs, J. A., Lowndes, N. F., and Jackson, S. P. (2000). A role for *Saccharomyces cerevisiae* histone H2A in DNA repair. *Nature* *408*, 1001-1004.
- Eladad, S., Ye, T. Z., Hu, P., Leversha, M., Beresten, S., Matunis, M. J., and Ellis, N. A. (2005). Intra-nuclear trafficking of the BLM helicase to DNA damage-induced foci is regulated by SUMO modification. *Hum Mol Genet* *14*, 1351-1365.
- Felberbaum, R., and Hochstrasser, M. (2008). Ulp2 and the DNA damage response: desumoylation enables safe passage through mitosis. *Cell Cycle* *7*, 52-56.
- Finley, D., Ozkaynak, E., and Varshavsky, A. (1987). The yeast polyubiquitin gene is essential for resistance to high temperatures, starvation, and other stresses. *Cell* *48*, 1035-1046.
- Fu, Y., Zhu, Y., Zhang, K., Yeung, M., Durocher, D., and Xiao, W. (2008). Rad6-Rad18 mediates a eukaryotic SOS response by ubiquitinating the 9-1-1 checkpoint clamp. *Cell* *133*, 601-611.
- Garvik, B., Carson, M., and Hartwell, L. (1995). Single-stranded DNA arising at telomeres in *cdc13* mutants may constitute a specific signal for the RAD9 checkpoint. *Mol Cell Biol* *15*, 6128-6138.
- Gasior, S. L., Wong, A. K., Kora, Y., Shinohara, A., and Bishop, D. K. (1998). Rad52 associates with RPA and functions with rad55 and rad57 to assemble meiotic recombination complexes. *Genes Dev* *12*, 2208-2221.
- Gerton, J. L., and DeRisi, J. L. (2002). Mnd1p: an evolutionarily conserved protein required for meiotic recombination. *Proc Natl Acad Sci U S A* *99*, 6895-6900.
- Giannattasio, M., Lazzaro, F., Plevani, P., and Muzi-Falconi, M. (2005). The DNA damage checkpoint response requires histone H2B ubiquitination by Rad6-Bre1 and H3 methylation by Dot1. *J Biol Chem* *280*, 9879-9886.
- Gietz, R. D., and Sugino, A. (1988). New yeast-*Escherichia coli* shuttle vectors constructed with in vitro mutagenized yeast genes lacking six-base pair restriction sites. *Gene* *74*, 527-534.
- Gill, G. (2004). SUMO and ubiquitin in the nucleus: different functions, similar mechanisms? *Genes Dev* *18*, 2046-2059.

Girdwood, D., Bumpass, D., Vaughan, O. A., Thain, A., Anderson, L. A., Snowden, A. W., Garcia-Wilson, E., Perkins, N. D., and Hay, R. T. (2003). P300 transcriptional repression is mediated by SUMO modification. *Mol Cell* *11*, 1043-1054.

Gravel, S., Chapman, J. R., Magill, C., and Jackson, S. P. (2008). DNA helicases Sgs1 and BLM promote DNA double-strand break resection. *Genes Dev* *22*, 2767-2772.

Grushcow, J. M., Holzen, T. M., Park, K. J., Weinert, T., Lichten, M., and Bishop, D. K. (1999). *Saccharomyces cerevisiae* checkpoint genes MEC1, RAD17 and RAD24 are required for normal meiotic recombination partner choice. *Genetics* *153*, 607-620.

Guan, X., Bai, H., Shi, G., Theriot, C. A., Hazra, T. K., Mitra, S., and Lu, A. L. (2007). The human checkpoint sensor Rad9-Rad1-Hus1 interacts with and stimulates NEIL1 glycosylase. *Nucleic Acids Res* *35*, 2463-2472.

Guo, Z., Chavez, V., Singh, P., Finger, L. D., Hang, H., Hegde, M. L., and Shen, B. (2008). Comprehensive mapping of the C-terminus of flap endonuclease-1 reveals distinct interaction sites for five proteins that represent different DNA replication and repair pathways. *J Mol Biol* *377*, 679-690.

Haglund, K., Di Fiore, P. P., and Dikic, I. (2003). Distinct monoubiquitin signals in receptor endocytosis. *Trends Biochem Sci* *28*, 598-603.

Hannich, J. T., Lewis, A., Kroetz, M. B., Li, S. J., Heide, H., Emili, A., and Hochstrasser, M. (2005). Defining the SUMO-modified proteome by multiple approaches in *Saccharomyces cerevisiae*. *J Biol Chem* *280*, 4102-4110.

Hardeland, U., Steinacher, R., Jiricny, J., and Schar, P. (2002). Modification of the human thymine-DNA glycosylase by ubiquitin-like proteins facilitates enzymatic turnover. *Embo J* *21*, 1456-1464.

Hassold, T., and Hunt, P. (2001). To err (meiotically) is human: the genesis of human aneuploidy. *Nat Rev Genet* *2*, 280-291.

Hay, R. T. (2005). SUMO: a history of modification. *Mol Cell* *18*, 1-12.

Hay, R. T. (2007). SUMO-specific proteases: a twist in the tail. *Trends Cell Biol* *17*, 370-376.

Helt, C. E., Wang, W., Keng, P. C., and Bambara, R. A. (2005). Evidence that DNA damage detection machinery participates in DNA repair. *Cell Cycle* *4*, 529-532.

Ho, J. C., Warr, N. J., Shimizu, H., and Watts, F. Z. (2001). SUMO modification of Rad22, the *Schizosaccharomyces pombe* homologue of the recombination protein Rad52. *Nucleic Acids Res* *29*, 4179-4186.

Hochwagen, A., and Amon, A. (2006). Checking your breaks: surveillance mechanisms of meiotic recombination. *Curr Biol* *16*, R217-228.

- Hochwagen, A., Tham, W. H., Brar, G. A., and Amon, A. (2005). The FK506 binding protein Fpr3 counteracts protein phosphatase 1 to maintain meiotic recombination checkpoint activity. *Cell* *122*, 861-873.
- Hoegel, C., Pfander, B., Moldovan, G. L., Pyrowolakis, G., and Jentsch, S. (2002). RAD6-dependent DNA repair is linked to modification of PCNA by ubiquitin and SUMO. *Nature* *419*, 135-141.
- Hoeijmakers, J. H. (2001). Genome maintenance mechanisms for preventing cancer. *Nature* *411*, 366-374.
- Hollingsworth, N. M., Goetsch, L., and Byers, B. (1990). The HOP1 gene encodes a meiosis-specific component of yeast chromosomes. *Cell* *61*, 73-84.
- Hong, E. J., and Roeder, G. S. (2002). A role for Ddc1 in signaling meiotic double-strand breaks at the pachytene checkpoint. *Genes Dev* *16*, 363-376.
- Hooker, G. W., and Roeder, G. S. (2006). A Role for SUMO in meiotic chromosome synapsis. *Curr Biol* *16*, 1238-1243.
- Huang, L. S., Doherty, H. K., and Herskowitz, I. (2005). The Smk1p MAP kinase negatively regulates Gsc2p, a 1,3-beta-glucan synthase, during spore wall morphogenesis in *Saccharomyces cerevisiae*. *Proc Natl Acad Sci U S A* *102*, 12431-12436.
- Huen, M. S., Grant, R., Manke, I., Minn, K., Yu, X., Yaffe, M. B., and Chen, J. (2007). RNF8 transduces the DNA-damage signal via histone ubiquitylation and checkpoint protein assembly. *Cell* *131*, 901-914.
- Huertas, P., Cortes-Ledesma, F., Sartori, A. A., Aguilera, A., and Jackson, S. P. (2008). CDK targets Sae2 to control DNA-end resection and homologous recombination. *Nature* *455*, 689-692.
- Li, T., Fung, J., Mullen, J. R., and Brill, S. J. (2007a). The yeast Slx5-Slx8 DNA integrity complex displays ubiquitin ligase activity. *Cell Cycle* *6*, 2800-2809.
- Li, T., Mullen, J. R., Slagle, C. E., and Brill, S. J. (2007b). Stimulation of in vitro sumoylation by Slx5-Slx8: evidence for a functional interaction with the SUMO pathway. *DNA Repair (Amst)* *6*, 1679-1691.
- Ishov, A. M., Sotnikov, A. G., Negorev, D., Vladimirova, O. V., Neff, N., Kamitani, T., Yeh, E. T., Strauss, J. F., 3rd, and Maul, G. G. (1999). PML is critical for ND10 formation and recruits the PML-interacting protein daxx to this nuclear structure when modified by SUMO-1. *J Cell Biol* *147*, 221-234.
- Ito, T., Chiba, T., and Yoshida, M. (2001). Exploring the protein interactome using comprehensive two-hybrid projects. *Trends Biotechnol* *19*, S23-27.
- James, P., Halladay, J., and Craig, E. A. (1996). Genomic libraries and a host strain designed for highly efficient two-hybrid selection in yeast. *Genetics* *144*, 1425-1436.

Janke, C., Magiera, M. M., Rathfelder, N., Taxis, C., Reber, S., Maekawa, H., Moreno-Borchart, A., Doenges, G., Schwob, E., Schiebel, E., and Knop, M. (2004). A versatile toolbox for PCR-based tagging of yeast genes: new fluorescent proteins, more markers and promoter substitution cassettes. *Yeast* *21*, 947-962.

Johnson, E. S. (2004). Protein modification by SUMO. *Annu Rev Biochem* *73*, 355-382.

Johnson, E. S., and Blobel, G. (1999). Cell cycle-regulated attachment of the ubiquitin-related protein SUMO to the yeast septins. *J Cell Biol* *147*, 981-994.

Kai, M., Tanaka, H., and Wang, T. S. (2001). Fission yeast Rad17 associates with chromatin in response to aberrant genomic structures. *Mol Cell Biol* *21*, 3289-3301.

Kalocsay, M., Hiller, N. J., and Jentsch, S. (2009). Chromosome-wide Rad51 spreading and SUMO-H2A.Z-dependent chromosome fixation in response to a persistent DNA double-strand break. *Mol Cell* *33*, 335-343.

Kamitani, T., Nguyen, H. P., Kito, K., Fukuda-Kamitani, T., and Yeh, E. T. (1998). Covalent modification of PML by the sentrin family of ubiquitin-like proteins. *J Biol Chem* *273*, 3117-3120.

Kawabe, Y., Seki, M., Seki, T., Wang, W. S., Imamura, O., Furuichi, Y., Saitoh, H., and Enomoto, T. (2000). Covalent modification of the Werner's syndrome gene product with the ubiquitin-related protein, SUMO-1. *J Biol Chem* *275*, 20963-20966.

Keeney, S. (2001). Mechanism and control of meiotic recombination initiation. *Curr Top Dev Biol* *52*, 1-53.

Keogh, M. C., Kim, J. A., Downey, M., Fillingham, J., Chowdhury, D., Harrison, J. C., Onishi, M., Datta, N., Galicia, S., Emili, A., *et al.* (2006). A phosphatase complex that dephosphorylates gammaH2AX regulates DNA damage checkpoint recovery. *Nature* *439*, 497-501.

Kerscher, O. (2007). SUMO junction-what's your function? New insights through SUMO-interacting motifs. *EMBO Rep* *8*, 550-555.

Khan, M. M., Nomura, T., Kim, H., Kaul, S. C., Wadhwa, R., Shinagawa, T., Ichikawa-Iwata, E., Zhong, S., Pandolfi, P. P., and Ishii, S. (2001). Role of PML and PML-RARalpha in Mad-mediated transcriptional repression. *Mol Cell* *7*, 1233-1243.

Knop, M., Siegers, K., Pereira, G., Zachariae, W., Winsor, B., Nasmyth, K., and Schiebel, E. (1999). Epitope tagging of yeast genes using a PCR-based strategy: more tags and improved practical routines. *Yeast* *15*, 963-972.

Kolas, N. K., Chapman, J. R., Nakada, S., Ylanko, J., Chahwan, R., Sweeney, F. D., Panier, S., Mendez, M., Wildenhain, J., Thomson, T. M., *et al.* (2007). Orchestration of the DNA-damage response by the RNF8 ubiquitin ligase. *Science* *318*, 1637-1640.

Kovalenko, O. V., Plug, A. W., Haaf, T., Gonda, D. K., Ashley, T., Ward, D. C., Radding, C. M., and Golub, E. I. (1996). Mammalian ubiquitin-conjugating enzyme

Ubc9 interacts with Rad51 recombination protein and localizes in synaptonemal complexes. *Proc Natl Acad Sci U S A* *93*, 2958-2963.

Krogh, B. O., and Symington, L. S. (2004). Recombination proteins in yeast. *Annu Rev Genet* *38*, 233-271.

Leu, J. Y., Chua, P. R., and Roeder, G. S. (1998). The meiosis-specific Hop2 protein of *S. cerevisiae* ensures synapsis between homologous chromosomes. *Cell* *94*, 375-386.

Li, S. J., and Hochstrasser, M. (1999). A new protease required for cell-cycle progression in yeast. *Nature* *398*, 246-251.

Li, S. J., and Hochstrasser, M. (2000). The yeast ULP2 (SMT4) gene encodes a novel protease specific for the ubiquitin-like Smt3 protein. *Mol Cell Biol* *20*, 2367-2377.

Li, S. J., and Hochstrasser, M. (2003). The Ulp1 SUMO isopeptidase: distinct domains required for viability, nuclear envelope localization, and substrate specificity. *J Cell Biol* *160*, 1069-1081.

Li, T., Evdokimov, E., Shen, R. F., Chao, C. C., Tekle, E., Wang, T., Stadtman, E. R., Yang, D. C., and Chock, P. B. (2004). Sumoylation of heterogeneous nuclear ribonucleoproteins, zinc finger proteins, and nuclear pore complex proteins: a proteomic analysis. *Proc Natl Acad Sci U S A* *101*, 8551-8556.

Lisby, M., Barlow, J. H., Burgess, R. C., and Rothstein, R. (2004). Choreography of the DNA damage response: spatiotemporal relationships among checkpoint and repair proteins. *Cell* *118*, 699-713.

Lisby, M., and Rothstein, R. (2004). DNA damage checkpoint and repair centers. *Curr Opin Cell Biol* *16*, 328-334.

Liu, J. G., Yuan, L., Brundell, E., Bjorkroth, B., Daneholt, B., and Hoog, C. (1996). Localization of the N-terminus of SCP1 to the central element of the synaptonemal complex and evidence for direct interactions between the N-termini of SCP1 molecules organized head-to-head. *Exp Cell Res* *226*, 11-19.

Longtine, M. S., McKenzie, A., 3rd, Demarini, D. J., Shah, N. G., Wach, A., Brachat, A., Philippsen, P., and Pringle, J. R. (1998). Additional modules for versatile and economical PCR-based gene deletion and modification in *Saccharomyces cerevisiae*. *Yeast* *14*, 953-961.

Lorenz, A., Wells, J. L., Pryce, D. W., Novatchkova, M., Eisenhaber, F., McFarlane, R. J., and Loidl, J. (2004). *S. pombe* meiotic linear elements contain proteins related to synaptonemal complex components. *J Cell Sci* *117*, 3343-3351.

Lydall, D. (2003). Hiding at the ends of yeast chromosomes: telomeres, nucleases and checkpoint pathways. *J Cell Sci* *116*, 4057-4065.

- Lydall, D., Nikolsky, Y., Bishop, D. K., and Weinert, T. (1996). A meiotic recombination checkpoint controlled by mitotic checkpoint genes. *Nature* *383*, 840-843.
- Lynn, A., Soucek, R., and Borner, G. V. (2007). ZMM proteins during meiosis: crossover artists at work. *Chromosome Res* *15*, 591-605.
- Mahajan, R., Delphin, C., Guan, T., Gerace, L., and Melchior, F. (1997). A small ubiquitin-related polypeptide involved in targeting RanGAP1 to nuclear pore complex protein RanBP2. *Cell* *88*, 97-107.
- Mahajan, R., Gerace, L., and Melchior, F. (1998). Molecular characterization of the SUMO-1 modification of RanGAP1 and its role in nuclear envelope association. *J Cell Biol* *140*, 259-270.
- Mailand, N., Bekker-Jensen, S., Fastrup, H., Melander, F., Bartek, J., Lukas, C., and Lukas, J. (2007). RNF8 ubiquitylates histones at DNA double-strand breaks and promotes assembly of repair proteins. *Cell* *131*, 887-900.
- Majka, J., Binz, S. K., Wold, M. S., and Burgers, P. M. (2006a). Replication protein A directs loading of the DNA damage checkpoint clamp to 5'-DNA junctions. *J Biol Chem* *281*, 27855-27861.
- Majka, J., Niedziela-Majka, A., and Burgers, P. M. (2006b). The checkpoint clamp activates Mec1 kinase during initiation of the DNA damage checkpoint. *Mol Cell* *24*, 891-901.
- Makhnevych, T., Sydorsky, Y., Xin, X., Srikumar, T., Vizeacoumar, F. J., Jeram, S. M., Li, Z., Bahr, S., Andrews, B. J., Boone, C., and Raught, B. (2009). Global map of SUMO function revealed by protein-protein interaction and genetic networks. *Mol Cell* *33*, 124-135.
- Mao, Y., Desai, S. D., and Liu, L. F. (2000a). SUMO-1 conjugation to human DNA topoisomerase II isozymes. *J Biol Chem* *275*, 26066-26073.
- Mao, Y., Sun, M., Desai, S. D., and Liu, L. F. (2000b). SUMO-1 conjugation to topoisomerase I: A possible repair response to topoisomerase-mediated DNA damage. *Proc Natl Acad Sci U S A* *97*, 4046-4051.
- Matunis, M. J., Coutavas, E., and Blobel, G. (1996). A novel ubiquitin-like modification modulates the partitioning of the Ran-GTPase-activating protein RanGAP1 between the cytosol and the nuclear pore complex. *J Cell Biol* *135*, 1457-1470.
- Matunis, M. J., Wu, J., and Blobel, G. (1998). SUMO-1 modification and its role in targeting the Ran GTPase-activating protein, RanGAP1, to the nuclear pore complex. *J Cell Biol* *140*, 499-509.
- Melchior, F. (2000). SUMO--nonclassical ubiquitin. *Annu Rev Cell Dev Biol* *16*, 591-626.

- Mitra, N., and Roeder, G. S. (2007). A novel nonnull ZIP1 allele triggers meiotic arrest with synapsed chromosomes in *Saccharomyces cerevisiae*. *Genetics* *176*, 773-787.
- Moldovan, G. L., Pfander, B., and Jentsch, S. (2007). PCNA, the maestro of the replication fork. *Cell* *129*, 665-679.
- Mukhopadhyay, D., and Dasso, M. (2007). Modification in reverse: the SUMO proteases. *Trends Biochem Sci* *32*, 286-295.
- Mullen, J. R., and Brill, S. J. (2008). Activation of the Slx5-Slx8 ubiquitin ligase by poly-small ubiquitin-like modifier conjugates. *J Biol Chem* *283*, 19912-19921.
- Muller, S., Berger, M., Lehembre, F., Seeler, J. S., Haupt, Y., and Dejean, A. (2000). c-Jun and p53 activity is modulated by SUMO-1 modification. *J Biol Chem* *275*, 13321-13329.
- Muller, S., Hoege, C., Pyrowolakis, G., and Jentsch, S. (2001). SUMO, ubiquitin's mysterious cousin. *Nat Rev Mol Cell Biol* *2*, 202-210.
- Muller, S., Ledl, A., and Schmidt, D. (2004). SUMO: a regulator of gene expression and genome integrity. *Oncogene* *23*, 1998-2008.
- Muller, S., Matunis, M. J., and Dejean, A. (1998). Conjugation with the ubiquitin-related modifier SUMO-1 regulates the partitioning of PML within the nucleus. *Embo J* *17*, 61-70.
- Murakami, H., and Keeney, S. (2008). Regulating the formation of DNA double-strand breaks in meiosis. *Genes Dev* *22*, 286-292.
- Neale, M. J., and Keeney, S. (2006). Clarifying the mechanics of DNA strand exchange in meiotic recombination. *Nature* *442*, 153-158.
- Niu, H., Li, X., Job, E., Park, C., Moazed, D., Gygi, S. P., and Hollingsworth, N. M. (2007). Mek1 kinase is regulated to suppress double-strand break repair between sister chromatids during budding yeast meiosis. *Mol Cell Biol* *27*, 5456-5467.
- Niu, H., Wan, L., Baumgartner, B., Schaefer, D., Loidl, J., and Hollingsworth, N. M. (2005). Partner choice during meiosis is regulated by Hop1-promoted dimerization of Mek1. *Mol Biol Cell* *16*, 5804-5818.
- O'Neill, B. M., Szyjka, S. J., Lis, E. T., Bailey, A. O., Yates, J. R., 3rd, Aparicio, O. M., and Romesberg, F. E. (2007). Pph3-Psy2 is a phosphatase complex required for Rad53 dephosphorylation and replication fork restart during recovery from DNA damage. *Proc Natl Acad Sci U S A* *104*, 9290-9295.
- Offenberg, H. H., Schalk, J. A., Meuwissen, R. L., van Aalderen, M., Kester, H. A., Dietrich, A. J., and Heyting, C. (1998). SCP2: a major protein component of the axial elements of synaptonemal complexes of the rat. *Nucleic Acids Res* *26*, 2572-2579.
- Page, S. L., and Hawley, R. S. (2004). The genetics and molecular biology of the synaptonemal complex. *Annu Rev Cell Dev Biol* *20*, 525-558.

- Palvimo, J. J. (2007). PIAS proteins as regulators of small ubiquitin-related modifier (SUMO) modifications and transcription. *Biochem Soc Trans* *35*, 1405-1408.
- Panse, V. G., Hardeland, U., Werner, T., Kuster, B., and Hurt, E. (2004). A proteome-wide approach identifies sumoylated substrate proteins in yeast. *J Biol Chem* *279*, 41346-41351.
- Papouli, E., Chen, S., Davies, A. A., Huttner, D., Krejci, L., Sung, P., and Ulrich, H. D. (2005). Crosstalk between SUMO and ubiquitin on PCNA is mediated by recruitment of the helicase Srs2p. *Mol Cell* *19*, 123-133.
- Parrilla-Castellar, E. R., Arlander, S. J., and Karnitz, L. (2004). Dial 9-1-1 for DNA damage: the Rad9-Hus1-Rad1 (9-1-1) clamp complex. *DNA Repair (Amst)* *3*, 1009-1014.
- Pfander, B., Moldovan, G. L., Sacher, M., Hoegge, C., and Jentsch, S. (2005). SUMO-modified PCNA recruits Srs2 to prevent recombination during S phase. *Nature* *436*, 428-433.
- Pichler, A., Gast, A., Seeler, J. S., Dejean, A., and Melchior, F. (2002). The nucleoporin RanBP2 has SUMO1 E3 ligase activity. *Cell* *108*, 109-120.
- Pickart, C. M. (2000). Ubiquitin in chains. *Trends Biochem Sci* *25*, 544-548.
- Prieler, S., Penkner, A., Borde, V., and Klein, F. (2005). The control of Spo11's interaction with meiotic recombination hotspots. *Genes Dev* *19*, 255-269.
- Primig, M., Williams, R. M., Winzeler, E. A., Tevzadze, G. G., Conway, A. R., Hwang, S. Y., Davis, R. W., and Esposito, R. E. (2000). The core meiotic transcriptome in budding yeasts. *Nat Genet* *26*, 415-423.
- Prudden, J., Pebernard, S., Raffa, G., Slavin, D. A., Perry, J. J., Tainer, J. A., McGowan, C. H., and Boddy, M. N. (2007). SUMO-targeted ubiquitin ligases in genome stability. *Embo J* *26*, 4089-4101.
- Richly, H., Rape, M., Braun, S., Rumpf, S., Hoegge, C., and Jentsch, S. (2005). A series of ubiquitin binding factors connects CDC48/p97 to substrate multiubiquitylation and proteasomal targeting. *Cell* *120*, 73-84.
- Rodriguez, M. S., Desterro, J. M., Lain, S., Midgley, C. A., Lane, D. P., and Hay, R. T. (1999). SUMO-1 modification activates the transcriptional response of p53. *Embo J* *18*, 6455-6461.
- Roeder, G. S., and Bailis, J. M. (2000). The pachytene checkpoint. *Trends Genet* *16*, 395-403.
- Rogers, R. S., Inselman, A., Handel, M. A., and Matunis, M. J. (2004). SUMO modified proteins localize to the XY body of pachytene spermatocytes. *Chromosoma* *113*, 233-243.

- Rosas-Acosta, G., Russell, W. K., Deyrieux, A., Russell, D. H., and Wilson, V. G. (2005). A universal strategy for proteomic studies of SUMO and other ubiquitin-like modifiers. *Mol Cell Proteomics* 4, 56-72.
- Rouse, J., and Jackson, S. P. (2002). Interfaces between the detection, signaling, and repair of DNA damage. *Science* 297, 547-551.
- Sacher, M., Pfander, B., Hoege, C., and Jentsch, S. (2006). Control of Rad52 recombination activity by double-strand break-induced SUMO modification. *Nat Cell Biol* 8, 1284-1290.
- Sacher, M., Pfander, B., and Jentsch, S. (2005). Identification of SUMO-protein conjugates. *Methods Enzymol* 399, 392-404.
- Saitoh, H., Sparrow, D. B., Shiomi, T., Pu, R. T., Nishimoto, T., Mohun, T. J., and Dasso, M. (1998). Ubc9p and the conjugation of SUMO-1 to RanGAP1 and RanBP2. *Curr Biol* 8, 121-124.
- Sambrook, J., Fritsch, E. F., and Maniatis T. (1989). *Molecular cloning*. CSH Laboratory Press
- San-Segundo, P. A., and Roeder, G. S. (1999). Pch2 links chromatin silencing to meiotic checkpoint control. *Cell* 97, 313-324.
- Schalk, J. A., Dietrich, A. J., Vink, A. C., Offenberg, H. H., van Aalderen, M., and Heyting, C. (1998). Localization of SCP2 and SCP3 protein molecules within synaptonemal complexes of the rat. *Chromosoma* 107, 540-548.
- Scherthan, H., Wang, H., Adelfalk, C., White, E. J., Cowan, C., Cande, W. Z., and Kaback, D. B. (2007). Chromosome mobility during meiotic prophase in *Saccharomyces cerevisiae*. *Proc Natl Acad Sci U S A* 104, 16934-16939.
- Schmidt, D., and Muller, S. (2003). PIAS/SUMO: new partners in transcriptional regulation. *Cell Mol Life Sci* 60, 2561-2574.
- Schwacha, A., and Kleckner, N. (1997). Interhomolog bias during meiotic recombination: meiotic functions promote a highly differentiated interhomolog-only pathway. *Cell* 90, 1123-1135.
- Schwartz, D. C., and Hochstrasser, M. (2003). A superfamily of protein tags: ubiquitin, SUMO and related modifiers. *Trends Biochem Sci* 28, 321-328.
- Seeler, J. S., Marchio, A., Losson, R., Desterro, J. M., Hay, R. T., Chambon, P., and Dejean, A. (2001). Common properties of nuclear body protein SP100 and TIF1alpha chromatin factor: role of SUMO modification. *Mol Cell Biol* 21, 3314-3324.
- Shi, G., Chang, D. Y., Cheng, C. C., Guan, X., Venclovas, C., and Lu, A. L. (2006). Physical and functional interactions between MutY glycosylase homologue (MYH) and checkpoint proteins Rad9-Rad1-Hus1. *Biochem J* 400, 53-62.
- Shiloh, Y. (2003). ATM and related protein kinases: safeguarding genome integrity. *Nat Rev Cancer* 3, 155-168.

- Shinohara, A., Gasiior, S., Ogawa, T., Kleckner, N., and Bishop, D. K. (1997). *Saccharomyces cerevisiae* recA homologues RAD51 and DMC1 have both distinct and overlapping roles in meiotic recombination. *Genes Cells* 2, 615-629.
- Shinohara, M., Sakai, K., Ogawa, T., and Shinohara, A. (2003). The mitotic DNA damage checkpoint proteins Rad17 and Rad24 are required for repair of double-strand breaks during meiosis in yeast. *Genetics* 164, 855-865.
- Smith, A. V., and Roeder, G. S. (1997). The yeast Red1 protein localizes to the cores of meiotic chromosomes. *J Cell Biol* 136, 957-967.
- Stehmeier, P., and Muller, S. (2009). Phospho-regulated SUMO interaction modules connect the SUMO system to CK2 signaling. *Mol Cell* 33, 400-409.
- Steinacher, R., and Schar, P. (2005). Functionality of human thymine DNA glycosylase requires SUMO-regulated changes in protein conformation. *Curr Biol* 15, 616-623.
- Stelter, P., and Ulrich, H. D. (2003). Control of spontaneous and damage-induced mutagenesis by SUMO and ubiquitin conjugation. *Nature* 425, 188-191.
- Sternsdorf, T., Jensen, K., and Will, H. (1997). Evidence for covalent modification of the nuclear dot-associated proteins PML and Sp100 by PIC1/SUMO-1. *J Cell Biol* 139, 1621-1634.
- Sun, Z. W., and Allis, C. D. (2002). Ubiquitination of histone H2B regulates H3 methylation and gene silencing in yeast. *Nature* 418, 104-108.
- Sym, M., Engebrecht, J. A., and Roeder, G. S. (1993). ZIP1 is a synaptonemal complex protein required for meiotic chromosome synapsis. *Cell* 72, 365-378.
- Takahashi, Y., Mizoi, J., Toh, E. A., and Kikuchi, Y. (2000). Yeast Ulp1, an Smt3-specific protease, associates with nucleoporins. *J Biochem* 128, 723-725.
- Tarsounas, M., Pearlman, R. E., Gasser, P. J., Park, M. S., and Moens, P. B. (1997). Protein-protein interactions in the synaptonemal complex. *Mol Biol Cell* 8, 1405-1414.
- Tatham, M. H., Jaffray, E., Vaughan, O. A., Desterro, J. M., Botting, C. H., Naismith, J. H., and Hay, R. T. (2001). Polymeric chains of SUMO-2 and SUMO-3 are conjugated to protein substrates by SAE1/SAE2 and Ubc9. *J Biol Chem* 276, 35368-35374.
- Treier, M., Staszewski, L. M., and Bohmann, D. (1994). Ubiquitin-dependent c-Jun degradation in vivo is mediated by the delta domain. *Cell* 78, 787-798.
- Usui, T., Ogawa, H., and Petrini, J. H. (2001). A DNA damage response pathway controlled by Tel1 and the Mre11 complex. *Mol Cell* 7, 1255-1266.
- Usui, T., Petrini, J. H., and Morales, M. (2006). Rad50S alleles of the Mre11 complex: questions answered and questions raised. *Exp Cell Res* 312, 2694-2699.

- Uzunova, K., Gottsche, K., Miteva, M., Weisshaar, S. R., Glanemann, C., Schnellhardt, M., Niessen, M., Scheel, H., Hofmann, K., Johnson, E. S., *et al.* (2007). Ubiquitin-dependent proteolytic control of SUMO conjugates. *J Biol Chem* *282*, 34167-34175.
- Venclovas, C., Colvin, M. E., and Thelen, M. P. (2002). Molecular modeling-based analysis of interactions in the RFC-dependent clamp-loading process. *Protein Sci* *11*, 2403-2416.
- Venclovas, C., and Thelen, M. P. (2000). Structure-based predictions of Rad1, Rad9, Hus1 and Rad17 participation in sliding clamp and clamp-loading complexes. *Nucleic Acids Res* *28*, 2481-2493.
- Vertegaal, A. C., Ogg, S. C., Jaffray, E., Rodriguez, M. S., Hay, R. T., Andersen, J. S., Mann, M., and Lamond, A. I. (2004). A proteomic study of SUMO-2 target proteins. *J Biol Chem* *279*, 33791-33798.
- Wan, L., de los Santos, T., Zhang, C., Shokat, K., and Hollingsworth, N. M. (2004). Mek1 kinase activity functions downstream of RED1 in the regulation of meiotic double strand break repair in budding yeast. *Mol Biol Cell* *15*, 11-23.
- Welchman, R. L., Gordon, C., and Mayer, R. J. (2005). Ubiquitin and ubiquitin-like proteins as multifunctional signals. *Nat Rev Mol Cell Biol* *6*, 599-609.
- Wohlschlegel, J. A. (2009). Identification of SUMO-conjugated proteins and their SUMO attachment sites using proteomic mass spectrometry. *Methods Mol Biol* *497*, 33-49.
- Wohlschlegel, J. A., Johnson, E. S., Reed, S. I., and Yates, J. R., 3rd (2004). Global analysis of protein sumoylation in *Saccharomyces cerevisiae*. *J Biol Chem* *279*, 45662-45668.
- Woltering, D., Baumgartner, B., Bagchi, S., Larkin, B., Loidl, J., de los Santos, T., and Hollingsworth, N. M. (2000). Meiotic segregation, synapsis, and recombination checkpoint functions require physical interaction between the chromosomal proteins Red1p and Hop1p. *Mol Cell Biol* *20*, 6646-6658.
- Wu, H. I., Brown, J. A., Dorie, M. J., Lazzeroni, L., and Brown, J. M. (2004). Genome-wide identification of genes conferring resistance to the anticancer agents cisplatin, oxaliplatin, and mitomycin C. *Cancer Res* *64*, 3940-3948.
- Wu, H. Y., and Burgess, S. M. (2006). Two distinct surveillance mechanisms monitor meiotic chromosome metabolism in budding yeast. *Curr Biol* *16*, 2473-2479.
- Wykoff, D. D., and O'Shea, E. K. (2005). Identification of sumoylated proteins by systematic immunoprecipitation of the budding yeast proteome. *Mol Cell Proteomics* *4*, 73-83.
- Xie, Y., Kerscher, O., Kroetz, M. B., McConchie, H. F., Sung, P., and Hochstrasser, M. (2007). The yeast Hex3.Slx8 heterodimer is a ubiquitin ligase stimulated by substrate sumoylation. *J Biol Chem* *282*, 34176-34184.

Xu, L., Weiner, B. M., and Kleckner, N. (1997). Meiotic cells monitor the status of the interhomolog recombination complex. *Genes Dev* *11*, 106-118.

Yang, S. H., Galanis, A., Witty, J., and Sharrocks, A. D. (2006). An extended consensus motif enhances the specificity of substrate modification by SUMO. *Embo J* *25*, 5083-5093.

Yuan, L., Liu, J. G., Zhao, J., Brundell, E., Daneholt, B., and Hoog, C. (2000). The murine SCP3 gene is required for synaptonemal complex assembly, chromosome synapsis, and male fertility. *Mol Cell* *5*, 73-83.

Zhang, H., Saitoh, H., and Matunis, M. J. (2002). Enzymes of the SUMO modification pathway localize to filaments of the nuclear pore complex. *Mol Cell Biol* *22*, 6498-6508.

Zhao, X., and Blobel, G. (2005). A SUMO ligase is part of a nuclear multiprotein complex that affects DNA repair and chromosomal organization. *Proc Natl Acad Sci U S A* *102*, 4777-4782.

Zhao, Y., Kwon, S. W., Anselmo, A., Kaur, K., and White, M. A. (2004). Broad spectrum identification of cellular small ubiquitin-related modifier (SUMO) substrate proteins. *J Biol Chem* *279*, 20999-21002.

Zhou, F., Xue, Y., Lu, H., Chen, G., and Yao, X. (2005). A genome-wide analysis of sumoylation-related biological processes and functions in human nucleus. *FEBS Lett* *579*, 3369-3375.

Zhu, Z., Chung, W. H., Shim, E. Y., Lee, S. E., and Ira, G. (2008). Sgs1 helicase and two nucleases Dna2 and Exo1 resect DNA double-strand break ends. *Cell* *134*, 981-994.

Zou, L., and Elledge, S. J. (2003). Sensing DNA damage through ATRIP recognition of RPA-ssDNA complexes. *Science* *300*, 1542-1548.

Zou, L., Liu, D., and Elledge, S. J. (2003). Replication protein A-mediated recruitment and activation of Rad17 complexes. *Proc Natl Acad Sci U S A* *100*, 13827-13832.

ABBREVIATIONS

μ	micro
ψ	aliphatic amino acid
Ω	ohm
4-NQO	4-nitroquinoline-1-oxide
9-1-1	9-1-1 checkpoint complex
aa	amino acid
AD	Gal4 activation domain
ADP	adenosine 5'-diphosphate
AE	axial element
Amp	ampicillin
APC/C	anaphase promoting complex / cyclosome
APS	ammonium-peroxo-disulfate
ATP	adenosine 5'-triphosphate
BD	Gal4 DNA binding domain
BER	base excision repair
bp	base pairs
BSA	bovine serum albumin
Cdc	cell division cycle
Cdk	cyclin-dependent kinase
cDNA	complementary DNA
CE	central element
CO	crossover
C-terminal	carboxy-terminal
D-loop	displacement loop
DMSO	dimethylsulfoxide
DNA	deoxyribonucleic acid
DNAase	deoxyribonuclease
dNTP	deoxynucleoside triphosphate
DSB	double-strand break
DTT	dithiothreitol
DUB	de-ubiquitylating enzyme
E1	ubiquitin activation enzyme
E2	ubiquitin conjugation enzyme
E3	ubiquitin ligase
E4	multiubiquitylation factor
EDTA	ethylenediaminetetraacetic acid
F	farad
g	gram; gravitational constant
G418	geneticine disulfate
GFP	green fluorescent protein
GST	gluthathion S-transferase
h	hour
H2A	histone 2 A
H2AX	histone 2 A variant X
HA	hemagglutinin
HECT	homologous to E6-AP C-terminus
HR	homologous recombination
HRP	horse radish peroxidase
HU	hydroxyurea
IP	immunoprecipitation

IPTG	isopropyl- β -D-1-thiogalactopyranoside
k	kilo
kan	kanamycine
kb	kilo base pairs
kDa	kilo Daltons
l	liter
LB media	Luria-Bertani media
LE	lateral element
m	milli
M	molar
MAT	mating type
min	minute
MMR	mismatch repair
MMS	methyl-methane sulfonate
MOPS	3-N-morpholinopropane sulfonic acid
mRNA	messenger RNA
MW	molecular weight
n	nano
NAT	noursethricin
NCO	non-crossover
NEM	N-ethylmaleimide
NER	nucleotide-excision repair
NHEJ	non-homologous end-joining
N-terminal	aminoterminal
OD	optical density
ORF	open reading frame
PAGE	polyacrylamide gel electrophoresis
PBS	phosphate-buffered saline
PCNA	proliferating cell nuclear antigen
PCR	polymerase chain reaction
PEG	polyethylene glycol
PI3K	phosphoinositide 3-kinase
PIAS	protein inhibitor of activated STAT
PIP	PCNA-Interacting protein
PML bodies	promyelocytic bodies
PMSF	phenylmethanesulfonyl fluoride
PrtA	protein A
RFC	replication factor C
RING	really interesting new gene
RN	recombination nodule
RNase	ribonuclease
RPA	replication protein A
rpm	rounds per minute
RT	room temperature
s	seconds
S	sedimentation coefficient (Svedberg)
SC	synaptonemal complex
SC media	synthetic complete media
SDS	sodium dodecylsulfate
SIM	SUMO-interacting motif
ssDNA	single-stranded DNA
SUMO	small ubiquitin-like Modifier

TBS	tris-buffered saline
TCA	trichloro acetic acid
TEMED	N,N,N',N'-tetramethylethylene diamine
Tris	tris (hydroxymethyl) aminomethane
U	unit
UBA	ubiquitin-associated domain
UBC	ubiquitin-conjugating enzyme
UBL	ubiquitin-like
UIM	ubiquitin-interacting motif
UV	ultraviolet light
V	volt
v/v	volume per volume
w/v	weight per volume
WT	wild-type
YPD	yeast bactopectone dextrose

ACKNOWLEDGEMENTS

Ich möchte mit zu aller erst ganz herzlich bei Stefan Jentsch bedanken, für seine ständige Unterstützung, Hilfsbereitschaft und Diskussionsbereitschaft. Die großen Freiheiten und das Vertrauen bei der Bearbeitung meiner Arbeit haben mir sehr geholfen. Ich bin besonders dankbar für seine Faszination an der Wissenschaft und die enge Zusammenarbeit, durch die ich sehr viel gelernt habe und die meinen Wunsch in der wissenschaftlichen Forschung zu arbeiten weiter gestärkt haben.

Bei Herrn Prof. Dr. Peter Becker vom Adolf-Butenandt-Institut der Ludwig-Maximilian-Universität München möchte ich mich sehr herzlich für sein Interesse und die Begutachtung dieser Arbeit bedanken. Zudem möchte ich allen Mitgliedern der Prüfungskommission der Ludwig-Maximilian-Universität meinen Dank für Ihr Interesse und ihre Zeit aussprechen.

Bedanken möchte ich mich auch bei der Studienstiftung des deutschen Volkes, die mich neben dem Studium und meinem einjährigen Forschungsaufenthalt am RIKEN auch während meiner Doktorarbeit mit einem Promotionsstipendium unterstützte.

Bei allen Kollegen in der Abteilung möchte ich mich für die Hilfsbereitschaft und die schöne gemeinsame Zeit in- und außerhalb des Labors bedanken. Ebenso möchte ich Ajla Hrle, Florian Paasch und Jasmin Wächter für die nette Zusammenarbeit danken. Dem Labor von Tobias Walther danke ich für die Möglichkeit der zeitintensiven Benutzung des Spinning Disk Mikroskops.

Meinen Eltern und meiner Schwester möchte ich ganz herzlich dafür danken, dass sie immer hinter mir stehen.

Finally, I am incredibly thankful to my wife Rina for her understanding and for making my life so happy.

CURRICULUM VITAE

Name: Christian Stefan Eichinger
Anschrift: Implersstraße 74, 81371 München
Geburtstag: 5. März 1979
Geburtsort: Burghausen

Schule

1985 – 1989 Grundschule Mehring
1989 – 1998 Aventinus-Gymnasium Burghausen
Abschluß mit dem Abitur im Juni 1998

Studium

1998 – 2003 Universität Regensburg, Studiengang Diplom-Biologie
Vordiplom im September 2000

08/2001 – 05/2002 Auslandsstudium an der Washington University Medical School
in St. Louis, MO, USA (Prof. Lee Ratner)

Diplomarbeit am Klinikum der Universität Regensburg
Institut für Medizinische Mikrobiologie (Prof. Susanne Modrow)
Abschluß mit dem Diplom im September 2003

Wissenschaftliche Tätigkeit

10/2003 – 12/2003 Wissenschaftlicher Angestellter, Klinikum Regensburg
01/2004 – 12/2004 Forschungsaufenthalt am RIKEN Institut, Wakoshi, Japan,
Abteilung für Zellphysiologie (Prof. Fumio Hanaoka)

Doktorarbeit

Seit April 2005 Max Planck Institut für Biochemie, Martinsried/München
Abteilung für Molekulare Zellbiologie (Prof. Stefan Jentsch)

Post-Doc

ab 2009 University of Oxford, UK
Abteilung für Biochemie (Prof. Kim Nasmyth)